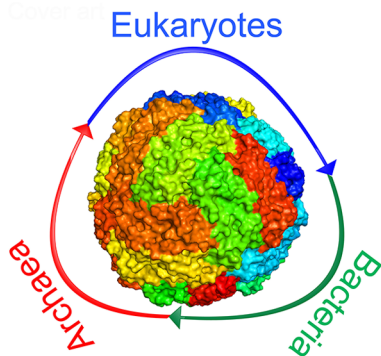


Unity in the Biochemistry of the Iron-Storage Proteins Ferritin and Bacterioferritin

Kourosh Honarmand Ebrahimi,* Peter-Leon Hagedoorn, and Wilfred R. Hagen*

Department of Biotechnology, Delft University of Technology, Julianalaan 67, 2628 BC Delft, The Netherlands



CONTENTS

1. Introduction	295
1.1. Nomenclature	297
2. How Does Ferritin Self-Assemble?	297
2.1. Mechanism of Self-Assembly	297
2.2. Application of the 24-Meric Shell of Ferritin	298
2.2.1. Synthesis of Nanoparticles Inside the Ferritin Cavity	299
2.2.2. Modification of Ferritin for Synthesis of New Materials	299
2.2.3. Application of Fe(III)-Mineral Core of Ferritin	299
3. What Is the Catalytic Center?	302
3.1. Ferritin Catalytic Site	302
3.2. Bacterioferritin Catalytic Site	304
4. How Does Fe(II) Substrate Reach the Catalytic Site?	305
4.1. Pathway of Fe(II) to Ferroxidase Center in Ferritin	305
4.2. Pathway of Fe(II) to the Ferroxidase Center in Bacterioferritin	310
5. How Is Fe(II) Oxidized?	310
5.1. What Is the Stoichiometry of the Ferroxidase Reaction?	310
5.1.1. Ferritin Ferroxidase Reaction Stoichiometry	310
5.1.2. Bacterioferritin Ferroxidase Reaction Stoichiometry	311
5.2. What Are the Intermediates of the Ferroxidase Reaction?	312
5.2.1. Blue Intermediate	312
5.2.2. Radical Intermediate	315
5.3. What Are the Fe(III) Species That Are Formed Because of Fe(II) Oxidation?	316
6. How Is the Fe(III) Product Stored after Its Formation in the Catalytic Site?	317
6.1. Mechanism of Fe(III) Storage in Ferritin	317
6.2. Mechanism of Fe(III) Storage in Bacterioferritin	320
7. How Is Iron Recovered from Ferritin?	321
7.1. Iron release in Ferritin	321
7.1.1. Spontaneous Dissolution of Fe(III)	321
7.1.2. Reduction of Fe(III) and Release of Fe(II)	321
7.1.3. Release of Fe(III) Because of Ferritin Degradation	321
7.2. Iron Release in Bacterioferritin	321
8. Concluding Remarks and Perspectives	322
Author Information	323
Corresponding Authors	323
Notes	323
Biographies	323
References	323

1. INTRODUCTION

Life on earth is dependent on the catalytic activity of a number of different metal ions in their polypeptide scaffold. Of these metals iron is widely used for catalysis of many reactions by living organisms because it can be found in all natural habitats and participate in biological transformations either as a redox center or as a Lewis acid in the catalytic site of many enzymes. Using iron in an oxygenic environment requires organisms to precisely control intracellular availability of free Fe(II) and Fe(III), which are the two most common oxidation states of iron. Free Fe(II) will donate an electron to molecular oxygen, and as a result superoxide radical, which is a reactive oxygen species (ROS), and free Fe(III) will form. ROS damage components of the cell indiscriminately, and Fe(III) is insoluble under physiological conditions (solubility 10^{-10} M)¹ and precipitates as Fe(III) oxide species. To cope with these problems the molecular machinery of living organisms has a sophisticated system to safely control cellular iron trafficking.^{2–4} A key component of this system is the ubiquitous iron-storage protein ferritin. Ferritin consists of 24 subunits, and the structure of each subunit is composed of four α -helices, helix A, B, C, and D, which together form a bundle, and a fifth C-terminal short α -helix, helix E (Figure 1a). The subunits are assembled into a spherical-shape structure with 4-3-2 symmetry (Figure 1b). Ferritin is a member of the ferritin superfamily, which encompasses proteins that have a four α -helix bundle structure⁵ such as soluble methane monooxygenase, ribonucleotide reductase, rubrerythrin, bacterioferritin, DNA binding protein from starved cells (Dps), Dps-like proteins, and the recently identified archaeoferritin.⁶ Besides ferritin, some other

Received: September 2, 2014

Published: November 24, 2014

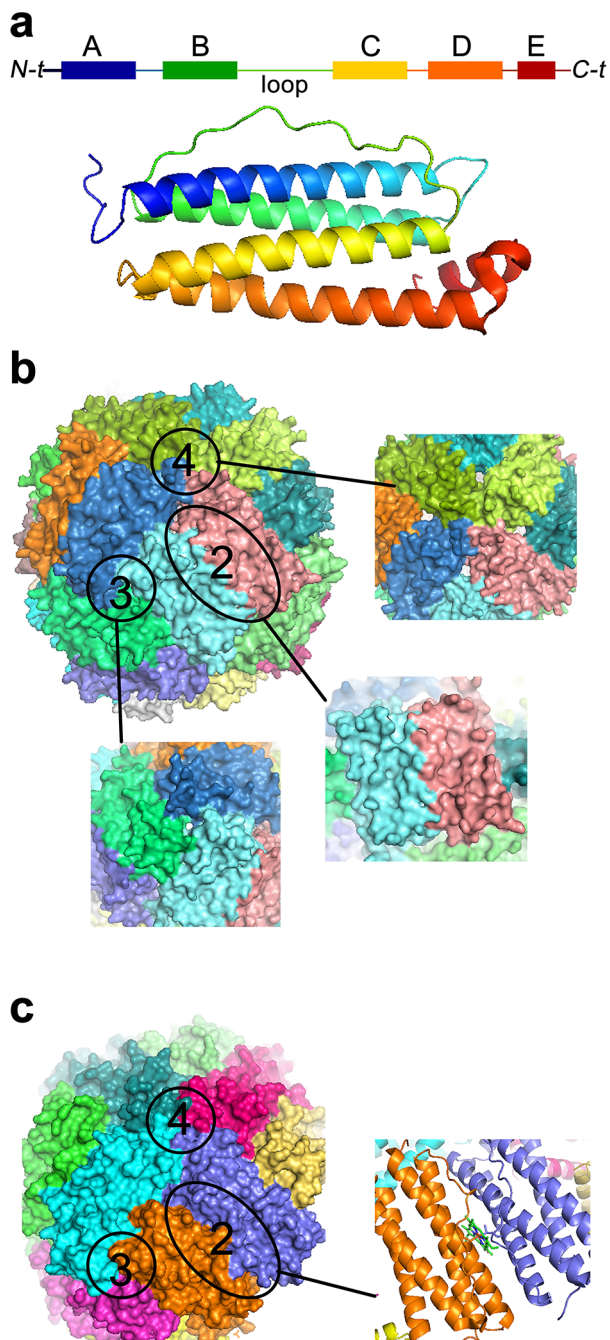


Figure 1. Structures of 24-meric nonheme ferritin and heme-containing bacterioferritin. (a) Tertiary structure of one subunit of ferritin shows four α helices forming a bundle and a short C-terminal α helix. (b) Spherical-shape quaternary structure of eukaryotic, archaeal, and bacterial ferritin is formed by self-assembly of 24 subunits into 4-3-2 symmetry. (c) Quaternary structure of heme-containing bacterioferritin is identical to that of ferritin of eukaryotes, bacteria, and archaea except that there is a heme group on the 2-fold symmetry axis between two subunits.

members of the ferritin-superfamily also possess iron-storage capacity, which are bacterioferritin,⁷ Dps and Dps-like proteins,^{8–10} and archaeoferritin.⁶ The quaternary structure of bacterioferritin is equivalent to that of ferritin, however with a heme group between pairs of subunits (Figure 1c). Dps and Dps-like proteins have a spherical-shape structure composed of 12 identical subunits; their primary function appears to be

protection of DNA against oxidative damage.^{8,11} Archaeoferritin is a monomeric protein that assembles upon aerobic addition of Fe(II); its physiological function is unknown.⁶ Because the structures of Dps and archaeoferritin are different from that of ferritin and bacterioferritin, they will not be discussed in this review: they have been discussed elsewhere.^{5,6,8,9} This review is focused on ferritin as the major iron-storage protein of all three Kingdoms of life, i.e., eukaryotes, bacteria, and archaea, and on the structurally equivalent bacterioferritin as the heme-containing iron-storage protein that is only present in bacteria.

Ferritin and bacterioferritin catalyze oxidation of Fe(II) to Fe(III) and store the Fe(III) product as a ferrihydrite-like mineral core to protect the molecular machinery of living organisms against the toxic products of spontaneous oxidation of free Fe(II): insoluble Fe(III) and ROS. In order to oxidize Fe(II) they use molecular oxygen or hydrogen peroxide. The storage cavity of the protein is separated from the solution by a protein shell with a thickness of 2 nm. In eukaryotes ferritin is the product of self-assembly of two or three types of highly homologous subunits which are named based on their relative molecular weight: L “light” (20 kDa), M “middle” (21 kDa), and H “heavy” (22.8 kDa) subunits.^{12,13} Only the H and M subunits of eukaryotic 24-meric ferritin are able to catalytically oxidize Fe(II). In bacteria and archaea ferritin is the product of self-assembly of 24 identical subunits,¹⁴ each of which is catalytically competent. The iron-storage function of ferritin has a central role in cellular iron homeostasis. Deletion of the coding gene for the H subunit in mice leads to early embryonic death¹⁵ and mutation in the gene of the L subunit in humans has been observed in neurodegenerative diseases such as neuroferritinopathy.¹⁶ It has also been observed that the ferritin expression level and amount of Fe(III) stored in the cavity of ferritin alters in response to oxidative stress and in diseases such as Parkinson’s or Alzheimer’s disease¹⁷ and acquired immunodeficiency syndrome (AIDS).¹⁸ Besides its iron-storage function recent studies have suggested other roles for ferritin¹⁹ including a role in immunity and autoimmunity²⁰ and in lipid metabolism.²¹ Thus, understanding how ferritin works is imperative, and many studies have been conducted to delineate the molecular mechanism of ferritin and bacterioferritin functioning. We will review these studies in the frame of six questions (Figure 2).

- How does ferritin self-assemble?
- What is the catalytic center?
- How does Fe(II) reach the catalytic site?
- What is the mechanism of Fe(II) oxidation?
- How is the Fe(III) product stored after its formation in the catalytic site?
- How is iron recovered from ferritin?

On the basis of the available data significant insight has been obtained regarding the mechanism of functioning of ferritin and bacterioferritin as two separate but closely related families of iron-storage proteins. Two contrasting views on the operational mechanism of ferritins or bacterioferritins have been proposed: (1) The diversity view, eukaryotic, bacterial, and archaeal ferritins have different working mechanisms^{22–25} and bacterioferritins work differently than ferritins;²⁵ (2) the unity view, eukaryotic, bacterial, and archaeal ferritins have a common working mechanism^{26,27} and the working mechanism of bacterioferritins has clear similarities to that of ferritin. In this review we discuss and re-evaluate available literature in regard

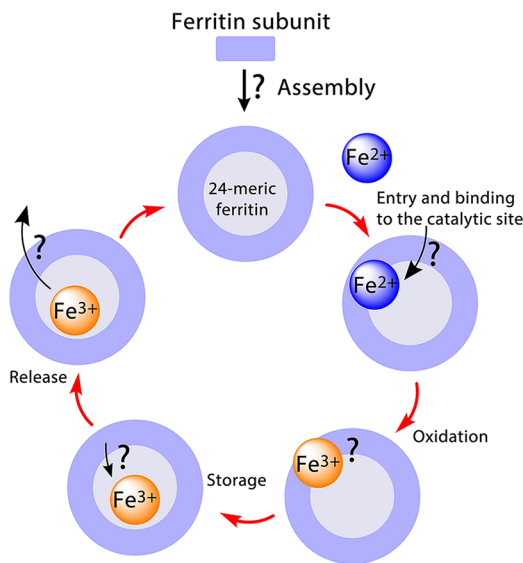


Figure 2. Mechanism of functioning of ferritin is divided into six steps: (1) Assembly of subunits to form the 24-meric shell of ferritin, (2 and 3) entry of Fe(II) to ferritin and binding to catalytic centers, (4) oxidation of Fe(II) in the catalytic center, (5) storage of the Fe(III) product inside the cavity of ferritin, and (6) release of Fe(III) from the mineral core.

to each of these views. We argue that the results and conclusion of several studies that have led to the diversity view are mutually inconsistent; these inconsistencies have not been considered in previous reviews.^{7,22–25,28,29} Our re-evaluation of these studies together with recent reports provide compelling evidence in support of the unity model. We further discuss similarities and differences between the mechanisms of bacterioferritin and ferritin and argue that bacterioferritins appear to be similar to ferritins in some of the steps described in Figure 2. We will also cover some of the applications of ferritin in different fields.

1.1. Nomenclature

We summarize the nomenclature in the literature.

- (1) Naturally occurring heteropolymeric ferritins, which have L and H subunits, of vertebrates: The first two letters for the name of the organism, the third letter for the name of the organ from which the ferritin is obtained, and the fourth letter F for ferritin, e.g., horse spleen ferritin (HoSF).
- (2) Homopolymeric ferritins of vertebrates which are heterologously expressed and consist of either L, H, or M subunit: The first two letters for the name of the organism, the third letter for the name of ferritin subunit type, i.e., H, L, or M, and the fourth letter F for ferritin, e.g., human H-type ferritin (HuHF).
- (3) Mitochondrial ferritin, which consists of H subunits only. The first letter for the name of the organism, then two letters Mt for mitochondria, and the fourth letter F for ferritin, e.g., human mitochondrial ferritin (HMtF).
- (4) Naturally occurring ferritin of invertebrates, which is a heteropolymer of H and L subunits: The first two letters for the name of the organism and the third letter F for ferritin, e.g., *Trichoplusia ni* (*Moth*) ferritin (TnF).
- (5) Naturally occurring plant, diatom, bacterial, and archaeal ferritins, which only have the H subunit: The first two letters for the name of the organism and then Ftn for

ferritin. Some organisms have more than one structural gene for ferritin, in that case a fifth letter starting from A is added for numbering, e.g., *Escherichia coli* ferritin A (EcFtnA).

- (6) Bacterioferritins. The first two letters are for the name of the bacterium and then three letters "BFR" standing for bacterioferritin, e.g., *E. coli* bacterioferritin (EcBFR).

On the basis of this nomenclature system the abbreviations of several ferritins that will be used in this review are listed in Table 1.

Table 1. List of Ferritin Abbreviations

subtype	ferritin	abbreviation	origin
1	horse spleen ferritin	HoSF	vertebrate
2	human H-type ferritin	HuHF	vertebrate
2	human L-type ferritin	HuLF	vertebrate
2	bullfrog H-type ferritin	BfHF	vertebrate
2	bullfrog M-type ferritin	BfMF	vertebrate
3	human mitochondrial ferritin	HMtF	vertebrate
4	<i>T. ni</i> (<i>Moth</i>) ferritin	TnF	invertebrate
5	soybean ferritin	SbFtn	plant
5	<i>Pseudonitzschia multiseries</i> ferritin	PmFtn	diatom
5	<i>E. coli</i> ferritin A	EcFtnA	bacterium
5	<i>Helicobacter pylori</i> ferritin	HpFtn	bacterium
5	<i>Chlorobium tepidum</i> ferritin	CtFtn	bacterium
5	<i>Pseudomonas aeruginosa</i> ferritin	PaFtn	bacterium
5	<i>Pyrococcus furiosus</i> ferritin	PfFtn	archaeon
5	<i>Archaeoglobus fulgidus</i> ferritin	AfFtn	archaeon
6	<i>Azotobacter vinelandii</i> bacterioferritin	AvBFR	bacterium
6	<i>P. aeruginosa</i> bacterioferritin	PaBFR	bacterium
6	<i>Mycobacterium smegmatis</i> bacterioferritin	MsBFR	bacterium
6	<i>Desulfovibrio desulfuricans</i> bacterioferritin	DsBFR	bacterium

2. HOW DOES FERRITIN SELF-ASSEMBLE?

Because the 24-meric quaternary structures of ferritin and bacterioferritin are equivalent (Figure 1) we discuss the assembly of these proteins together. The presence of the L subunit appears not to influence the self-assembly process in heteropolymeric eukaryotic ferritin. Moreover, the heme group present at the interface between two subunits at the 2-fold symmetry axis of bacterioferritin³⁰ (Figure 1c) appears not to be required for formation of the 24-meric shell of bacterioferritin.³¹ Studies regarding the self-assembly of 24 subunits of ferritin or bacterioferritin have been very limited until recently. Over the past few years self-assembly of these proteins has received interest because of their potential applications in nanotechnology,^{32,33} material sciences,³⁴ and biocatalysis.³⁵ Therefore, in this section, besides the mechanism of self-assembly, we briefly review a selection of technological applications of ferritin.

2.1. Mechanism of Self-Assembly

Assembly of the 24-meric shell of ferritin and bacterioferritin is assumed to occur spontaneously. In this process the first stable intermediate that leads to spontaneous formation of the 24-meric protein shell appears to be a dimer. Initial studies with horse spleen ferritin (HoSF) using sedimentation velocity centrifugation and circular dichroism spectroscopy indicated that the dimers are very stable.³⁶ Cross-linking experiments in combination with fluorescence spectroscopy suggested that not

only dimers but also trimers and tetramers of HoSF are stable species.³⁷ It was reported that the 24-meric shell could be formed from dimers or trimers with more than 80% efficiency, while tetramers alone did not efficiently assemble into a 24-meric shell.³⁷ Although these initial studies suggested that either dimers or trimers are the first stable intermediates for self-assembly of the 24-mer, recent studies have now provided compelling evidence that only dimers are the first intermediate in the self-assembly pathway. First, alanine scanning mutagenesis of *E. coli* bacterioferritin (EcBFR) was used to identify the residues at 2-fold, 3-fold, or 4-fold symmetry axes (Figure 1) that are important for formation of the 24-meric protein shell.³⁸ Two single mutations at the 3-fold symmetry axis, i.e., R61A and Y114A, and one mutation at the 2-fold symmetry axis, i.e., R30A, abolished formation of the 24-meric protein shell completely, and only dimers were formed. Second, in a more recent study³⁹ a new engineering strategy named reverse metal-templated interface redesign (rMeTIR)^{39–41} was used to study self-assembly of human H ferritin (HuHF). This study led to identification of residues that are essential for formation of dimers and assembly of the 24-meric shell in HuHF. Using rMeTIR the 2-fold symmetry axis was modified in such a way that dimers were formed from monomers only in response to the presence of Cu(II). Formation of dimers in the presence of Cu(II) then spontaneously led to formation of the 24-meric shell as determined by X-ray crystallography and transmission electron microscopy (TEM). Amino acid residues at position 56, 60, 63, and 67, which are present at the 2-fold symmetry axis, were first replaced by histidine in order to form a slightly distorted planar coordination for Cu(II). These mutations did not affect self-assembly of the 24-meric protein but successfully led to creation of Cu(II) binding sites at 2-fold symmetry axes. Subsequent mutagenesis studies to disrupt formation of dimers while not affecting the stability of monomers and the Cu(II) binding sites showed that three mutations at the 2-fold symmetry axis (Y39E, N74E, and P88A) were sufficient to form stable monomers. These monomers were able to form 24-meric structures upon addition of Cu(II), which promoted formation of dimers. Thus, this study for the first time defines a path for self-assembly of the 24-meric shell through formation of dimers. In the formation of dimers the loop between helix B and helix C of one subunit interacts with that of another subunit at 2-fold symmetry (Figure 3a). Thus, amino acid residues of this loop might also affect the self-assembly process. It has been shown that deletion of two residues of this loop in HuHF completely abolishes formation of 24-mer,⁴² and mutation of a residue, i.e., Asp80K, in the middle of this loop in BfMF reduces the solubility and stability.⁴³ Data for BfMF were interpreted to mean that the electrostatic interaction between the loops of two subunits at 2-fold symmetry modulates assembly and stability of dimers. After dimers are formed, self-assembly appears to be dependent on the amino acid residues that participate in the interaction of two, three, or four dimers (Figure 3a). Together the results obtained for ferritin and bacterioferritin suggest the following, admittedly limited, general pathway for formation of the 24-meric protein shell (Figure 3b): The very first intermediate during self-assembly of 24 subunits of ferritin or bacterioferritin is a dimer. As soon as dimers are formed self-assembly proceeds and formation of the 24-meric protein shell occurs. In eukaryotic ferritin the presence of the L subunit appears not to affect the mechanism of self-assembly because dimers were observed as the first intermediate in the self-assembly of HoSF³⁷ and

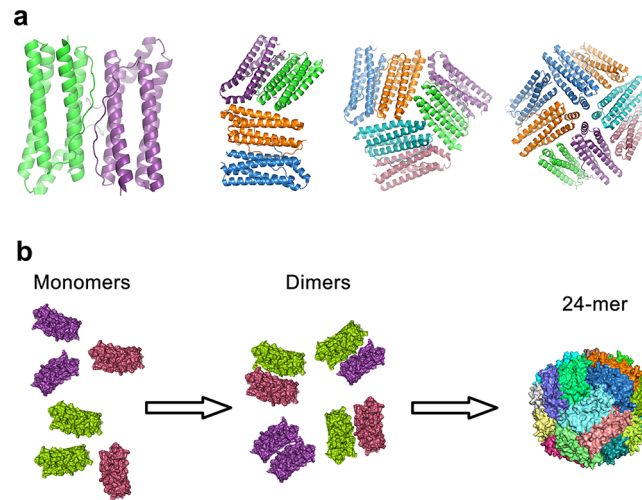


Figure 3. Pathway for self-assembly of 24 subunits of ferritin or bacterioferritin. (a) Interaction surface at 2-fold symmetry of two monomers that form a dimer, two dimers, three dimers, and four dimers is shown. Amino acid residues that participate in these interactions are possibly important for proper self-assembly of dimers. (b) First intermediate during self-assembly of 24 subunits is dimeric. Subsequently, dimers oligomerize possibly via different intermediates to form the 24-meric spherical-shape structure of the protein.

because those residues whose mutation in the H subunit were shown to impair formation of dimers, i.e., N74 and P88,³⁹ are conserved in the human L subunit.

It has been proposed that *A. fulgidus* ferritin (AfFtn), which self-assembles only at high salt concentrations⁴⁴ (>0.5 M NaCl), forms a 2-3 symmetry structure instead of 4-3-2 symmetry.⁴⁵ This suggestion is based on the observation of four large open pores in the X-ray crystal structure of AfFtn crystallized under a low ionic strength of $I = 0.15$ M only.⁴⁵ At this low salt concentration AfFtn might not have fully assembled and the 2-3 symmetry might reflect an intermediate structure. In a recent study this possibility was not considered.⁴⁶ Site-directed mutagenesis of two residues in the E-helix of AfFtn, i.e., R151 and K150, led to formation of 4-3-2 symmetry as observed by X-ray crystallography in the presence of 0.15 M salt.⁴⁶ Measurements of Fe(II) oxidation or Fe(II) reduction and release in the absence of salt were performed with WT-AfFtn and its mutants. It was observed that the rate of Fe(II) oxidation was not affected by the mutations, but the rate of Fe(III) reduction and Fe(II) release was significantly lower in the mutant compared to the WT-AfFtn. These results were interpreted as WT-AfFtn having 2-3 symmetry at high salt concentrations.⁴⁶ Because measurements of Fe(III) reduction and release were performed in the absence of salt, a condition in which both WT-AfFtn and its mutant are dimeric,^{44,46} one cannot exclude the possibility that WT-AfFtn has 4-3-2 symmetry at high salt concentrations (>0.5 M). Further experiments under appropriate experimental conditions are required to test whether WT-AfFtn has 4-3-2 symmetry or 2-3 symmetry.

2.2. Application of the 24-Meric Shell of Ferritin

Ferritin (or bacterioferritin) is relevant for various (bio)-technological applications. In this section we briefly review examples of two general methods that have been applied to the 24-meric shell of ferritin for synthesis of new materials with application in drug delivery and biocatalysis. Furthermore, we

discuss some of the applications of the natural ferrihydrite-like mineral core of ferritin.

2.2.1. Synthesis of Nanoparticles Inside the Ferritin Cavity. An advantage of using ferritin for production of nanoparticles is the narrow size distribution imposed by the protein cavity. This is essential for using nanoparticles in different fields such as drug delivery. Particles with a uniform and narrow size distribution will increase the efficiency of the drug delivery system, and nanoparticles that are covered by a protein shell could be beneficial because of their low toxicity in blood.⁴⁷ Synthesis of metallic nanoparticles inside ferritin has been achieved using two methods: (1) reduction of metal ions bound to ferritin or (2) direct assembly of ferritin subunits around metallic nanoparticles or around small molecules such as drugs. Examples of the first method include preparation of Pd nanoparticles using *P. furiosus* ferritin (PfFtn),⁴⁸ preparation of Ag nanoparticles using PfFtn,⁴⁹ or Au/Pd nanoparticles using human L-type ferritin (HuLF).⁵⁰ Pd or Ag nanoparticles inside PfFtn were prepared by incubation of PfFtn with Pd(II) or Ag(I) and subsequent chemical reduction of these metal ions using NaBH₄. The Pd nanoparticles inside ferritin were used for oxidation of various alcohols to their corresponding aldehyde using molecular oxygen as oxidant.⁴⁸ The Au/Pd core inside HuLF was prepared by incubation with [Au(III)Cl₄]⁻ ions, chemical reduction using NaBH₄, and subsequent incubation with Pd(II) ions and chemical reduction.⁵⁰ These Au/Pd nanoparticles were used as catalyst for hydrogenation of olefins.⁵⁰ Examples of the second method include salt-dependent assembly of subunits of *A. fulgidus* ferritin (Afftn) around gold nanoparticles⁴⁴ and pH-dependent dissociation and reassembly of the ferritin subunits⁵¹ to trap small molecules such as gadolinium complexes^{52,53} or doxorubicin,⁵⁴⁻⁵⁶ which is a drug in cancer treatment. Assembly of dimers of Afftn into the 24-meric shell is dependent on salt concentration, and this property was used to encapsulate gold nanoparticles inside the Afftn 24-meric protein shell.⁴⁴ The ability to dissociate subunits of ferritin at low pH,⁵¹ pH values around 2, and then to reassemble the subunits by increasing the pH to 7 to reform the 24-meric protein⁵¹ was used to encapsulate gadolinium complexes^{52,53} or doxorubicin.⁵⁴⁻⁵⁶ Gadolinium chelates encapsulated inside ferritin could be used for NMR imaging,⁵³ and doxorubicin encapsulated inside ferritin showed promising results in killing cancer tumors.⁵⁶ The ability to control assembly of the 24-meric nanocage structure of ferritin is a useful method for synthesis of nanomaterials. In this regard, the reverse metal-templated interface redesign (rMeTIR) method³⁹ that has been recently used as a tool for controlled assembly of HuHF has significant potential for synthesis of new nanomaterials using the 24-meric structure of ferritin or possibly bacterioferritin.

2.2.2. Modification of Ferritin for Synthesis of New Materials. Modification of the amino acid residues lining the inside or outside of the 24-meric shell of ferritin is another approach that has been used for development of new technological applications. For example in a recent study the influenza virus surface glycoprotein, hemagglutinin, was fused to the N terminus of *H. pylori* ferritin.⁵⁷ The resulting 24-meric ferritin had eight trimeric spikes of influenza hemagglutinin at four 3-fold symmetry axes as determined by TEM.⁵⁷ This construct was used as a vaccine and exhibited a broader and more potent immune response compared to traditional influenza vaccines.⁵⁷ Another example of ferritin modification is introduction of cysteine residues inside the cavity of L-type

ferritin or on the 3-fold symmetry axis in order to form organometallic palladium (allyl) complexes⁵⁸ or ruthenium complexes.⁵⁹ These ferritin-derived complexes were able to perform catalysis, for example, polymerization of phenylacetylene.⁶⁰

2.2.3. Application of Fe(III)-Mineral Core of Ferritin. A recent application of the ferrihydrite-like mineral core of ferritin is in removal of oxoanions such as phosphate or arsenate from surface water.⁶¹ The Fe(III) core of ferritin can bind oxoanions such as phosphate, vanadate, or arsenate.⁶² These oxoanions either incorporate into the core during oxidation of Fe(II)⁶²⁻⁶⁴ or bind to the surface of the ferrihydrite-like mineral core that is present in the cavity.⁶⁵ The amount of phosphate present in the Fe(III) core of bacterial ferritins after purification is close to one phosphate per Fe(III).⁶⁶ The potential of ferritin to store phosphate in combination with its Fe(III) mineral core has been suggested to be useful for water treatment.⁶¹ In surface water inorganic phosphate is the limiting factor for growth of aquatic plants and algae that can cause eutrophication. In most cases traditional methods are not able to decrease the level of phosphate to the ecologically desired value of 0.01 mg/L.⁶¹ Using PfFtn, which is a highly (thermo)stable protein,⁶⁷ it was possible to remove phosphate to a level of less than 0.01 mg/L.⁶¹

The property of ferritin to store Fe(III)-oxide species in a ferrihydrite-like mineral form⁶⁸ has also been used for developing new magnetic resonance imaging (MRI) contrast agents. The Fe(III)-oxide species inside the ferritin or bacterioferritin cavity have ferrihydrite-like structure and superparamagnetic properties.^{69,70} Superparamagnetic iron oxide nanoparticles (SPIONs) have potential interest in various biomedical applications.^{71,72} Several different examples exist for application of superparamagnetic properties of the ferrihydrite-like mineral core of ferritin,³⁴ and covering all of them is outside the scope of this review. Here we only review a few recent applications of ferritin as MRI contrast agent. An interesting application that was recently proposed is the use of ferritin mineral core as a reporter for visualizing recombinant protein expression of a transgene in mouse.^{73,74} In this method the genes of the L and H subunits of ferritin were included in a gene-transfer vector, i.e., a replicative-defective adenovirus (Adv) vector.⁷³ Delivery of this vector to the brain of the mouse resulted in robust expression of ferritin and sequestration of cellular Fe(II) by ferritin and its storage as ferrihydrite-like mineral core. The resulting Fe(III) core could be measured using MRI as a reporter to follow the delivery of the Adv vector.⁷³ This technology was suggested to be useful for visualizing gene delivery. Another example of using ferritin as an MRI reporter is the application of HuHF for in vivo visualization of stem cells by cardiac MRI.⁷⁵ Cardiac MRI is a method to create both still and moving pictures of the heart.⁷⁶ A lentiviral vector having the HuHF gene was used to transfect swine cardiac stem/progenitor cells.⁷⁵ Cells were subsequently cultured to obtain cardiospheres (multicellular clusters). Then the cardiospheres that contained the lentiviral vector carrying the HuHF gene were injected intramyocardially. HuHF was expressed, and it sequestered cellular Fe(II) and stored the resulting Fe(III) product. The mineral core in HuHF was detected using cardiac MRI only in heart tissue.⁷⁵ This method allowed visualization of dividing/differentiating stem cells along with cardiac morpho-functional changes in a beating heart.⁷⁵

Yet another interesting application of the ferrihydrite-like mineral core of ferritin is the use of its semiconductor

Table 2. Three Metal-Ion Binding Sites Per Subunit Are Observed in the X-ray Crystal Structure of Ferritins (except in L subunits) and Bacterioferritins

	life form	name ^a	PDB	metal	resolution (Å)	pH	metal binding sites			ref	
							A	B	C		
ferritin	eukaryotes	HuHF (Lys86Gln) ^(a)	1FHA	Tb(III)	2.40		X	X	X	81	
		HuHF (Lys86Gln)	2CEI	Zn(II)	1.80	7.5	X	X	O	82	
		HuHF (Lys86Gln and Glu27Asp)	2CIH	Zn(II)	1.50	7.5	X	X	x	82	
		HuHF (wild type)	3AJO	Mg(II)	1.52	9	X	O	X	83	
		BfMF ^(b)	1MFR	Mg(II)	2.80	5.5	X	X	O	84	
			3RBC	Fe(III)	2.70	9	X	x	O	85	
			3RGD	Fe(III)/ Fe(II)	2.89	9	X	x	x		
			3KA4	Co(II)	1.40	>7.5	X	X	x	86	
			3RE7	Cu(II)	2.82	>7.5	X	x	x	85	
		PmFtn	3E6S	Fe(III)	1.95	5.5 and 6	O	X	x	87	
			4ITT, 4IWJ, 4IWK		2.10, 1.95, 1.65	5.5	X	x	x	88	
		HMtF ^(c)	4ISM	Zn(II)	2.00	5.5	X	x	x	88	
			4ITW, 4IXK	Fe(II)	2.00, 2.10	5.5	x	O	O	88	
			1R03	Mg(II)	1.70	9	X	O	O	89	
				Mn(II)		9	X	x	x	89	
		SbFtn		Zn(II)		9	X	x	x	89	
			3A68	Ca(II)	1.80	7.8	X	O	x	90	
			1Z6O	Fe(III)	1.91	7–8	X	x	O	91	
bacteria and archaea	PfFtn	2JD7	Zn(II)	2.80	8.5	X	X	X		92	
		AfFtn ^(d)	2JD8	Fe(III)	2.80	8.5	X	x	x	92	
			1S3Q	Zn(II)	2.1	7.5	x	x	O	45	
			1SQ3	Fe(III)	2.7	7.5	X	X	X	45	
		EcFtnA ^(e)		Zn(II)	2.21	5.2	X	X	X	93,94	
			1EUM	Fe(III)	2.05	5.2	X	X	x	93,94	
		HpFtn	3BVE, 3BVI, 3BVL, 3BVK, 3BVF, 3EGM	Fe(III)	1.80, 2.00, 1.80, 1.50, 1.50, 2.10	7.5	X	X	O	95	
			4CMY	Fe(III)	2.59	9	X	X	O	96	
		PaFtn	3R2L	Fe(III)	1.85	6.5, 7.5, 10.5	X	X	X	97	
		bacterioferritin	EcBFR ^(f)	3E1P	Zn(II)/ Fe(III)	2.40	5.0	X	X	x	98
				3E1N, 3E1M	Fe(III)	2.80, 2.70	5.0	X	X	x	98
			AvBFR	2FKZ, 2FL0	Fe(II)/Fe (III)	2.00, 2.70	8	X	X	O	99
			PaBFR	3IS7, 3ISE	Fe(III)	2.10, 2.80	6.0–8.5	X	X	O	100
			MsBFR	3BKN	Zn(II)	2.72	7.5	X	X	O	101
			DdBFR	1NF4, 1NFV, 1NF6	Fe(II)/ Fe(III)	2.05, 1.95, 2.35	3.6–9	X	X	O	102,103

^aX-ray crystal structures of ferritins were solved in the presence of different metal ions. From top to bottom: human H ferritin (HuHF), bullfrog M ferritin (BfMF), bloom-forming pennate diatoms *P. multiseries* ferritin (PmFtn), human mitochondrial ferritin (HMtF), soybean ferritin (SbFtn), *T. ni* ferritin (TnFtn), *P. furiosus* ferritin (PfFtn), *Archeoglobus fulgidus* ferritin (AfFtn), *E. coli* ferritin A (EcFtnA), *H. pylori* ferritin (HpFtn), *C. tepidum* ferritin (CtFtn), *P. aeruginosa* ferritin (PaFtn), *E. coli* bacterioferritin (EcBFR), *A. vinelandii* bacterioferritin (AvBFR), *P. aeruginosa* bacterioferritin B (PaBFRB), *M. smegmatis* bacterioferritin (MsBFR), *D. desulfuricans* bacterioferritin (DdBFR). *T. ni* ferritin (TnF) consists of H and L subunits. An X means fully occupied with metal ion, an x means partially occupied, and an O means not occupied with metal ion. Site C in several ferritins shows different conformations (see text). (a) The PDB file 1FHA describes the structure of HuHF with one Fe(III) per subunit; however, the structure was solved and described in ref 81 with three Tb(III), and no coordination was deposited. (b) In the Cu(II)-loaded structure of BfMF, one Cu(II) is present in the ferroxidase center site A of each subunit, while among subunits the location of the second Cu(II) varies between sites B and C (see text). In the X-ray crystal structure of BfMF that was solved after aerobic addition of 24 Fe(II) per subunit⁸⁵ to the crystals and flash freezing crystals after 1 min, both Fe(III) and Fe(II) were possibly present (PDB 3RGD). In this structure one Fe is present in site A of the ferroxidase center of each subunit, while among the subunits the location of the second Fe varies between sites B and C (see text). (c) For HMtF there is no PDB file available for the structures solved in the presence of Mn(II) and Zn(II). In the deposited structure only one Mg(II) ion is observed in site A. (d) In the Fe(III)-loaded crystal structure of AfFtn sites A, B, and C are occupied but the occupancy of these sites was not determined. (e) For EcFtnA the structure for Fe(III)-loaded ferritin (PDB 1EUM) does not contain any Fe(III), although it has been reported in ref 88 that sites A, B, and C are

Table 2. continued

filled with Fe(III). There is no PDB file available with Zn(II) bound to EcFtnA. (f) For EcBFR crystals were prepared at pH 5.0 and subsequently soaked in Fe(II) solution at pH 7.0. In the table the resolution of each structure is obtained from the PDB file.

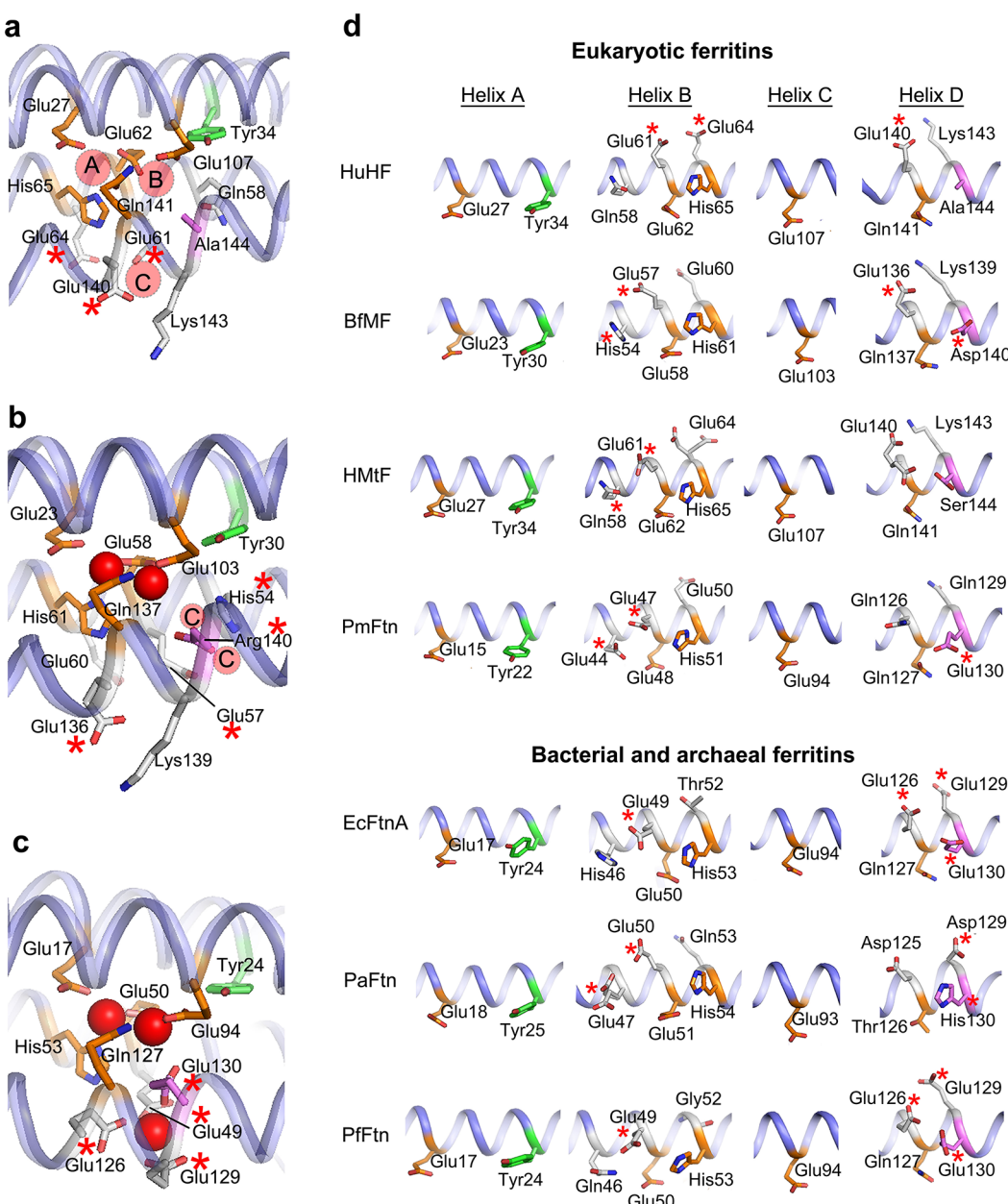


Figure 4. Metal coordination environment of the ferroxidase center and site C, or gateway site, is conserved among ferritins. (a) X-ray crystal structure of HuHF showing the possible position of metals in sites A and B of the ferroxidase center and site C (PDB 2FHA). (b) X-ray crystal structure of loaded-BfMF (loaded-BfFtn contains 2 Fe(III) per ferroxidase center) (PDB 3RBC). The structure shows the ferroxidase center filled with Fe(III), red spheres. Two conformations of site C have been observed in the crystal structure of Co(II)-loaded BfMF (PDB 3KA4), pink circles, each with an occupancy of 50%. In the Co(II)-loaded structure coordinating amino acid residues of site C, i.e., His54, Glu57, Glu136, and Asp140, show different conformations. (c) X-ray crystal structure of PfFtn showing the ferroxidase center and a site C all filled with Fe(III), red spheres. Occupancy of site B and site C is less than 70% in the crystal structure (PDB 2JD7). (d) Comparison of the motif of the ferroxidase center and site C for the X-ray crystal structure of (from top to bottom) human H ferritin (HuHF, PDB 2FHA), bullfrog M ferritin (BfMF, PDB 3RBC), bloom-forming pennate diatoms *Pseudonitzschia* ferritin (PnFtn, PDB 3E6S), *E. coli* ferritin A (EcFtnA, PDB 1EUM), *P. aeruginosa* ferritin (PaFtn, PDB 3R2R), and *P. furiosus* ferritin (PfFtn, PDB 2JD7). Asterisk marks the residues that participate in binding of metal ion to site C. Conserved residues of the ferroxidase center are shown in orange. A residue of site B or site C that is not conserved among ferritins is shown in pink. Residues of site C are shown in light gray, and a highly conserved tyrosine within 4–5 Å of the ferroxidase center is shown in green.

properties for photocatalysis.⁷⁷ Ferritin core has been used for photoreduction of different metal ions such as $[\text{Au(III)}\text{Cl}_4]^-$,⁷⁸ Cu(II) ,⁷⁹ or $[\text{Cr(VI)}\text{O}_4]^-$.⁸⁰ This method can be used for

synthesis of nanoparticles. For example, to produce gold nanoparticles HoSF containing approximately 1000 Fe(III) per 24-mer was incubated with $[\text{Au(III)}\text{Cl}_4]^-$ in the presence of a

sacrificial electron donor (citrate), and formation of gold nanoparticles was started by illumination with a mercury lamp.⁷⁸ The protein surface acted as a nucleation site for the gold nanoparticles.⁷⁸ Gold nanoparticles also formed on the inside of the protein cavity.

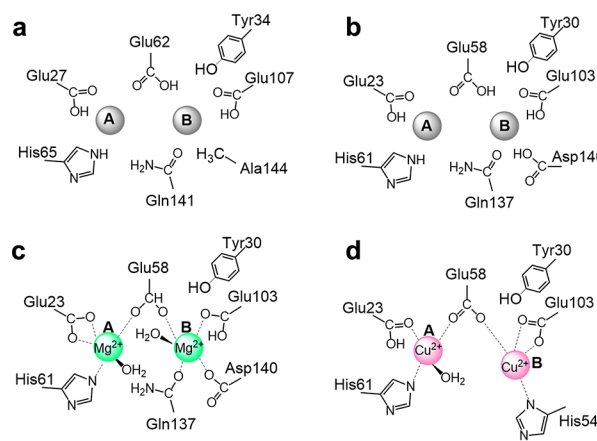
3. WHAT IS THE CATALYTIC CENTER?

A significant research effort has been concentrated on defining the catalytic site and its coordination environment in eukaryotic, archaeal, or bacterial ferritins and in bacterioferritins. Accumulating evidence (Table 2) from these studies suggest that in all ferritins, except the L subunit, and also possibly in bacterioferritin there are three metal ion binding sites in each catalytically active subunit that participate in catalysis of Fe(II) oxidation: two sites in the middle of each subunit forming a dinuclear metal ion binding site that is called the ferroxidase center and a third metal ion binding site in the vicinity of the ferroxidase center close to the inner surface of ferritin. The ferroxidase center is where oxidation of Fe(II) with molecular oxygen occurs, and the third site, which shows different conformations, is a gateway for the ferroxidase center. This view is a unification of earlier ideas that eukaryotic ferritin only has the dinuclear ferroxidase center²⁴ and that bacterial or archaeal ferritins have a trinuclear metal ion binding site as the ferroxidase center.^{22,23,25}

3.1. Ferritin Catalytic Site

The observation that the H subunit of eukaryotic ferritin can oxidize Fe(II) much faster than the L subunit¹⁰⁴ suggests that the H subunit of eukaryotic ferritin must have a catalytic site where Fe(II) can bind and subsequently be oxidized by molecular oxygen. The first evidence regarding the presence of three metal ion binding sites in the H subunit came from the X-ray crystal structure of HuHF, which was solved in the presence of Tb(III)⁸¹ (Table 2 and Figure 4a). In this structure three Tb(III) binding sites were observed: two sites in the middle of the four α -helical bundle, sites A and B, and a third site in the vicinity of these sites close to the inner surface of protein, which is commonly referred to as site C (Figure 4a). The three metal ion binding sites were also observed in the X-ray crystal structure of HuHF in the presence of Zn(II).⁸² Site C was only occupied with Zn(II) in the ferroxidase center mutants. In the L-type ferritin, which apparently oxidizes Fe(II) with a rate just above the rate of background oxidation of free Fe(II) by molecular oxygen,^{104,105} the coordination environment of sites A and B is absent.^{81,106} This observation suggests that sites A and B are essential for fast catalysis of Fe(II) oxidation by HuHF. When coordinating residues of site A or B were changed using site-directed mutagenesis, i.e., Glu62Ala or His65Ala, the rate of Fe(II) oxidation drastically diminished and became close to that of HuLF.^{104,107,108} In the presence of Mg(II) site B of the ferroxidase center was not occupied but the third site, site C, was occupied.⁸³ On the basis of the available data and for lack of X-ray crystal structures of HuHF in the presence of Fe(II)/Fe(III), a putative coordination environment of iron in the ferroxidase center of HuHF is shown in Scheme 1a. Depending on the metal ion, the conformation of site C in HuHF varies and the amino acid ligands of the metal ion in site C of HuHF are different for Tb(III), Zn(II), and Mg(II): for Tb(III),⁸¹ Glu61 and Glu64; for Zn(II),⁸² His57 and Glu61; and for Mg(II),⁸³ Glu140 (Figure 4a). Mutation of the coordinating residues of site C in HuHF decreased the rate of catalysis of Fe(II) oxidation in the ferroxidase center.⁸³

Scheme 1. Definition of Coordination of the Ferroxidase Center^a



^a(a) The coordination environment of HuHF as proposed based on available data. (b) Coordination environment of the ferroxidase center of BfMF. These coordinating residues of the ferroxidase center align with those of HuHF and other ferritins. (c) Coordinating residues of Mg(II) in the ferroxidase center of BfMF as observed by X-ray crystallography. This coordination was used in an MCD spectroscopic study to define the coordinating residues of Fe(II). (d) Definition of coordinating residues of Cu(II) in the ferroxidase center of BfMF according to Theil et al.⁸⁵ This model, which was used to define ligands of Fe(II) before oxidation in the ferroxidase center, appears to be the result of misinterpretation of the Cu(II)-loaded structure of BfMF (see text).

Therefore, site C also appears to be important for catalysis of Fe(II) oxidation (see section 4).

Another eukaryotic ferritin for which there is evidence for the presence of three metal ion binding sites is bullfrog M ferritin (BfMF) (Table 2 and Figure 4b). In the X-ray crystal structure of BfMF three Co(II) ion binding sites are observed:⁸⁶ two sites in the middle of each subunit in the same place as the ferroxidase center in HuHF and a third site with two slightly different conformations (each conformation < 50% occupancy) (Figure 4b) in a position that corresponds to that of site C in HuHF (Figure 4b). Like in HuHF mutation of the coordinating residues of site A, B, or C in BfMF also reduced the fast rate of Fe(II) oxidation.^{109,110} Subsequently, when X-ray crystals were prepared after loading and oxidation of two Fe(II) per subunit,⁸⁵ two Fe(III) were observed in sites A and B of the ferroxidase center. With these data in hand we infer that the amino acids in the coordination environment of the ferroxidase center (Scheme 1b) and site C in BfMF align with those observed in HuHF. However, attempts to define the ligands of Fe(II) (i.e., before oxidation to Fe(III)) in the ferroxidase center resulted in confusion and proposal of two mutually inconsistent models (Scheme 1c and 1d). The first model (Scheme 1c) suggested by the groups of Theil and Allewell is based on the X-ray crystal structure of BfMF in the presence of Mg(II) ions.⁸⁴ Solomon et al. used this structure to interpret magnetic circular dichroism (MCD) data for anaerobic Fe(II) binding to BfMF.¹¹¹ Comparison of MCD data for BfMF and data of the diiron cofactor site of dioxygen-activating enzymes resulted in the conclusion that each Fe(II) in sites A and B of the BfMF ferroxidase center has five coordination.¹¹¹ On the basis of the BfMF X-ray crystal structure in the presence of Mg(II) ions the coordinating ligands were then defined as site A three oxygens, one nitrogen, and a water molecule and site B

four oxygens and a water molecule. Specifically, in this model Asp140 and Gln137 provide two of the coordinating ligands to Fe(II) in site B of the ferroxidase center. The importance of Asp140 for Fe(II) binding to site B and catalysis of Fe(II) oxidation was confirmed using site-directed mutagenesis. Mutation of this residue diminished the rate of catalysis of Fe(II) oxidation¹⁰⁹ and changed the spectroscopic characteristics of Fe(II) in site B.¹¹² However, Bertini's group in collaboration with Theil's group recently proposed a different model for coordinating ligands of Fe(II) in the ferroxidase center based on what to the present reviewers appears to be a misinterpretation of the data of the X-ray crystal structure of BfMF in the presence of Cu(II) (Scheme 1d), which was used to draw Fe(II) coordination.⁸⁵ The authors reported the presence of two binding sites, i.e., sites A and B of the ferroxidase center, for Cu(II) with a distance of 4.3 ± 0.4 Å.⁸⁵ On the contrary, we observe (using the same data set as deposited in PDB file 3RE7) the presence of three binding sites for Cu(II): the first Cu(II) is present in a position that is equivalent to that of Co(II) or Mg(II) in site A of the ferroxidase center and the second Cu(II) has a different position in each of the 24 subunits with a distance between 3.7 and 5.2 Å from the Cu(II) in site A. We find that the shortest distance is between Cu(II) in site A and Cu(II) in a site that can be compared to Co(II) in site B of the ferroxidase center of BfMF.⁸⁶ The longest distance is between the Cu(II) in site A and the Cu(II) in a site that can be compared to Co(II) in site C. On the basis of these data that we obtained from the X-ray crystal structure of Cu(II)-loaded BfMF we now reinterpret the structure of BfMF solved in the presence of 24 Fe(III)/Fe(II) per subunit (PDB 3RGD). Comparison of this structure with the Cu(II) structure suggests the presence of three Fe(III)/Fe(II) binding sites: The position of the first Fe corresponds to the Cu(II) in site A of the ferroxidase center, and the position of the second Fe varies among subunits similar to that observed for Cu(II). As a result, the Fe–Fe distance is between 3.1 and 4.8 Å. Thus, the shortest distance corresponds to the distance between Fe in sites A and B of the ferroxidase center, and the longest distance corresponds to the Fe in site A and an Fe in a third site adjacent to site B, which can be compared to Cu(II) in site C. Thus, in our view the Cu(II) and Fe(III)/Fe(II) structures appear to give a snapshot of Fe(III)/Fe(II) movement in/out of the ferroxidase center that involves residues of site C in a highly conserved gateway (see section 4).

In other eukaryotic H and M, archaeal, or bacterial ferritins (Figure 4c and Table 2) three sites for metal ion binding have been observed also, i.e., sites A and B of the ferroxidase center and site C in the vicinity of the ferroxidase center. The coordination environment of these sites is highly conserved among all ferritins (Figure 4d). Like in eukaryotic ferritin mutation of the amino acid residues of sites A, B, and C in PfFtn²⁶ and EcFtnA¹¹³ was shown to reduce the fast rate of Fe(II) oxidation in the ferroxidase center. In *P. multiseries* ferritin (PmFtn) site A, B, or C is not occupied with Fe(II)/Fe(III) in the X-ray crystal structure, but in all other ferritins site A has always been found to be fully occupied with metal ion (Table 2). It appears that the occupancy of these sites with Fe(II)/Fe(III) in the X-ray crystal structure is dependent on the crystallographic conditions, e.g., pH. Full occupancy of sites A and B of the ferroxidase center has been observed for BfMF and PaFtn at neutral pH and for *C. tepidum* ferritin (CtFtn) at pH 9.0 (Table 2). In fact, from isothermal titration calorimetry experiments¹¹⁴ and steady-state kinetics studies of Fe(II)

oxidation¹⁰⁷ it is known that at pH values lower than 7, e.g., pH 6.5, binding of Fe(II) to the ferroxidase center is significantly reduced and as a consequence the rate of Fe(II) oxidation decreases. At pH 6.5, binding of Fe(II) to the ferroxidase center of HuHF is diminished and the stoichiometry of Fe(II) binding to the highest affinity binding site, i.e., site A in the ferroxidase center, drops to 0.5.¹¹⁴ This effect of pH on Fe(II) binding is possibly ascribable to the presence of histidine in the coordination environment of the ferroxidase center site A. The pK_a of histidine in proteins is approximately in the range of 5.5–8;¹¹⁵ therefore, small variation in pH may significantly affect the protonation/deprotonation of the imidazole functional group and thus its coordination to Fe(II)/Fe(III).

On the basis of the available data and a comparison of the metal ion coordinating motif of the ferroxidase center of different ferritins (Figure 4) we conclude that all ferritins, except the L subunit of eukaryotic ferritin, have two Fe(II)/Fe(III) binding sites in the ferroxidase center, i.e., sites A and B, and a third Fe(II)/Fe(III) binding site in the vicinity of the ferroxidase center, i.e., site C. This site in some ferritins shows different conformations, and in all structures it is either partially occupied with metal ion or it is vacant. Therefore, this site is possibly transient with relatively low affinity for metal ions. The precise role of site C during catalysis of Fe(II) oxidation is not known, and it has been suggested that the amino acid residues of this site act as a gateway of the ferroxidase center and are responsible for translocation of Fe(II)/Fe(III) into/out of the ferroxidase center (see section 4).²⁶ Consistent with the conclusion that all catalytically active ferritins have three metal ion binding sites is the data obtained from anaerobic Fe(II) binding to EcFtnA¹¹⁶ monitored by isothermal titration calorimetry (ITC) or to apo-HuHF and apo-PfFtn monitored by UV-vis spectroscopy and ITC.²⁶ Binding experiments under *anaerobic* conditions showed that apo-PfFtn and apo-HuHF ferritins have three Fe(II) binding sites: one high-affinity binding and two sites of lower affinity (Table 3). On the basis

Table 3. Comparison of Thermodynamic Properties of Fe(II) Binding to Eukaryotic, Archaeal, and Bacterial apo-Ferritins Measured by Isothermal Titration Calorimetry

parameters	apo-PfFtn 50 °C pH 7.0	apo-HuHF at 25 °C pH 7.0	apo-EcFtnA At 25 °C pH 7.0
N_1	1	1.0 ± 0.1	0.88 ± 0.02
K_1	$(1.2 \pm 0.2) \times 10^6$	$(5.4 \pm 0.8) \times 10^5$	$(3.5 \pm 0.8) \times 10^6$
ΔH_1	-22.4 ± 0.4	3.8 ± 0.2	3.4 ± 0.2
N_2	1	1.8 ± 0.1	0.88 ± 0.03
K_2	$(7.2 \pm 1.4) \times 10^4$	$(1.5 \pm 0.3) \times 10^3$	$(1.8 \pm 0.4) \times 10^5$
ΔH_2	29 ± 2.5	15.3 ± 0.3	9.9 ± 0.3
N_3	1		$(8.5 \pm 1.61) \times 10^5$
K_3	$(3.1 \pm 0.4) \times 10^3$		
ΔH_3	27.3 ± 2.3		
ref	26	26	116

of site-directed mutagenesis studies the higher affinity site was assigned to site A, and the two lower affinity sites were assigned to sites B and C.²⁶ It appears that the coordination environment of the ferroxidase center is related to the affinity for Fe(II): site A in PfFtn has the same coordination environment as that of site A in HuHF, and its association constant is very close in these ferritins, while site B in PfFtn has a different coordination environment than that of site B in

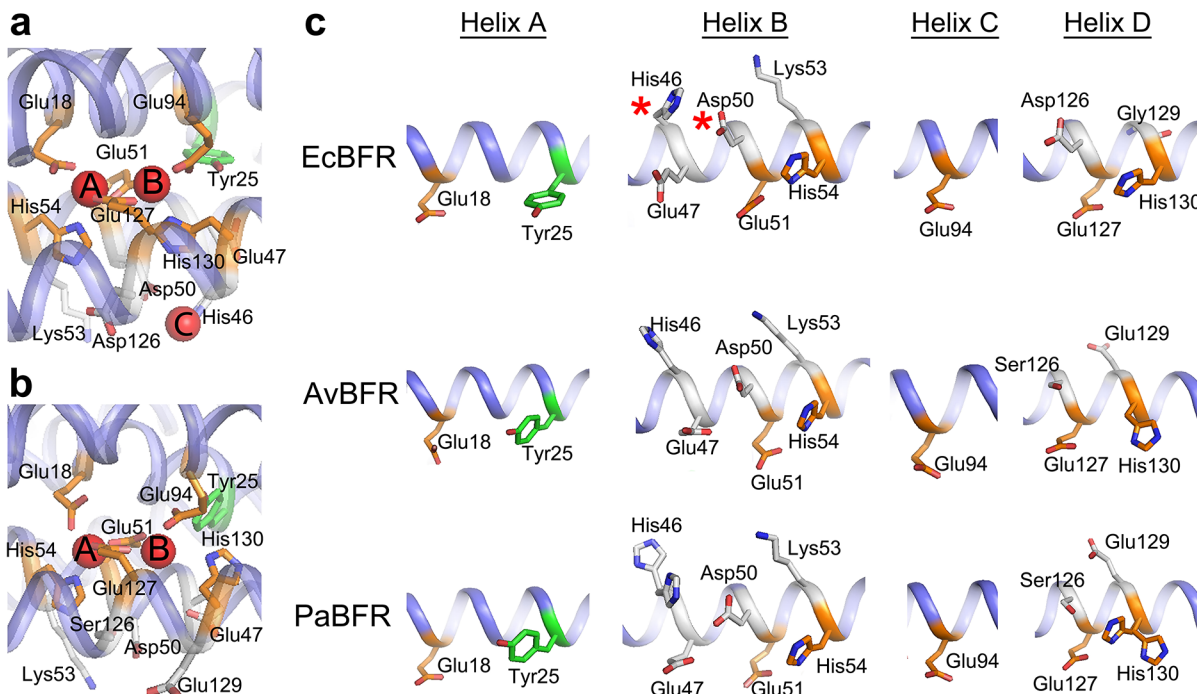


Figure 5. Metal coordination environment of bacterioferritins is conserved. (a) The ferroxidase center of *E. coli* bacterioferritin (EcBFR) (PDB 3E1M) shows two Fe(III) binding sites, and there is a third iron binding site, site C, in the vicinity of the ferroxidase center. Site C in the crystal structure of EcBFR is observed with 40% occupancy, and it can be compared to site C in ferritins. (b) Diiron binding site of *A. vinelandii* bacterioferritin (AvBFR) occupied with Fe(III) ions (PDB 2FL0). (c) Comparison of the amino acid motif of the ferroxidase center of three bacterioferritins (from top to bottom): EcBFR, AvBFR, and *P. aeruginosa* bacterioferritin (PaBFR, PDB 4E6K). Asterisk marks the residues that participate in binding of metal ion to site C of EcBFR. Conserved residues of the ferroxidase center are shown in orange. Residues of site C are shown in light gray, and a highly conserved tyrosine within 4–5 Å of the ferroxidase center is shown in green.

HuHF, and the association constants have a more than 10-fold difference in these ferritins (Table 3).

In Table 3 N (Fe(II) per subunit) is the stoichiometry of binding, K (M^{-1}) is the association constant, and ΔH (kJ/mol) is the enthalpy of binding. Apo-PfFtn or Apo-HuHF contain less than 1 Fe(III) per protein. For PfFtn a sequential binding model with three Fe(II) binding sites gave the best fit. For each site $N = 1$ was assumed. For HuHF a model with two binding sites gave the best fit. The stoichiometry of the second site that was obtained from the fit was 1.8 Fe(II) per subunit. In EcFtnA, at dilute protein concentration the thermodynamic parameters of the third site could not be determined separately. The thermodynamic parameters for PfFtn and HuHF were measured under strictly anaerobic conditions in the absence of any reducing agent to prevent any side effects. The thermodynamic parameters for EcFtnA were measured under anaerobic condition in the presence of sodium dithionite. The presence of sodium dithionite might have an effect on the measurements.

3.2. Bacterioferritin Catalytic Site

The presence of three Fe(II) binding sites and their importance for catalysis of Fe(II) oxidation has also been reported for bacterioferritins. The X-ray crystal structure of several bacterioferritins has been solved in the presence of different metal ions including Fe(II)/Fe(III) (Table 2 and Figure 5). In all these structures two metal ions have been found in the ferroxidase center located in the middle of each subunit just like in ferritins; however, the coordination environment of sites A and B is different from that of sites A and B in ferritins. In bacterioferritins two glutamate residues act as bridging ligand for the metal ions in sites A and B (Figure 5a); in ferritins one

of the glutamate residues is replaced by a glutamine (Figure 4). The second difference in coordination environment is a residue of site B of the ferroxidase center. In ferritins one of the residues of site B is highly variable (Figure 4), i.e., Glu130 in PfFtn or Ala141 in HuHF, while this residue in bacterioferritin appears to always be a histidine (Figure 5). The coordinating amino acid residues to the iron in the ferroxidase center of bacterioferritins are identical to those of the diiron catalytic site in dioxygen-activating enzymes such as methane monooxygenase. However, unlike dioxygen-activating enzymes, bacterioferritins appear to have the coordinating amino acid residues of a highly conserved site C (Figure 5). The presence of Fe(II)/Fe(III) in this site has been reported in the X-ray crystal structure of *E. coli* bacterioferritin (EcBFR).⁹⁸ The coordinating ligands were observed to be His54 and Asp50 (Figure 5). These residues align with those of site C of ferritin (Figure 4). Site C was observed with only 40% occupancy when apo-EcBFR crystals were prepared at pH 5.0, and subsequently, apo-crystals were soaked in Fe(II) solution at pH 7.0. Similar to ferritins, mutation of the conserved coordinating residues of this site, i.e., His54 or Asp50, reduced the rate of Fe(II) oxidation in the ferroxidase center of EcBFR.⁹⁸ The presence of metal ion in the third site has not been observed in the X-ray crystal structures of *A. vinelandii* bacterioferritin (AvBFR)⁹⁹ or *P. aeruginosa* bacterioferritin (PaBFR).¹⁰⁰ In PaBFR the presence of a metal ion binding site near the ferroxidase center is predicted by molecular dynamics (MD) simulation.¹¹⁷ In all structures, except that of EcBFR, the coordinating histidine to Fe(II)/Fe(III) in site B shows different conformations. The dynamics of the coordination environment of the ferroxidase center and the gateway site to the ferroxidase center has also been recently

predicted by MD simulation of PaBFR.¹¹⁷ It thus appears that bacterioferritins also have three metal ion binding sites. The putative site C in bacterioferritin may have a function similar to site C in ferritins (see section 4).

4. HOW DOES Fe(II) SUBSTRATE REACH THE CATALYTIC SITE?

The exact pathway of Fe(II) to the ferroxidase center of ferritin and bacterioferritin is not fully understood. In ferritin and bacterioferritin formation of the 4-3-2 symmetrical structure of the 24-meric protein creates specific areas where the junction of three or four subunits appears to result in formation of channels through the protein shell (Figure 6): (i) A 3-fold channel at the

prediction of these channels in the quaternary structure of ferritins and bacterioferritins have led to the idea that these channels may act as a pathway for Fe(II) entry and translocation to the ferroxidase center. In this section we review the experimental evidence regarding the possible involvement of these channels as a pathway for Fe(II) to reach the ferroxidase center of ferritin and bacterioferritin. We argue that although the 3-fold channels have been proposed as the main entry path of Fe(II) in ferritin, other possible pathways cannot be excluded and that the available data also suggest the presence of the same Fe(II) entry pathways for ferritins and bacterioferritins. We conclude that *in vivo* Fe(II) delivery to ferritin or bacterioferritin and the pathway for Fe(II) translocation from outside protein shell to the ferroxidase site remain elusive.

4.1. Pathway of Fe(II) to Ferroxidase Center in Ferritin

The observation that the catalytic center of ferritin is located in the middle of the four α -helical bundle of each subunit raises the question how Fe(II) reaches this site. It is unclear if *in vivo* Fe(II) is delivered to ferritin by an Fe(II) chaperone protein. Members of the PCBPs family (PCBP is the human poly(rC)-binding protein family that appears to have different functions including mRNA stabilization and translational activation or silencing¹²⁰) have been proposed to be able to act as a chaperone for delivery of Fe(II) to ferritin.^{121–123} This proposal is based on experiments performed using heterologous expression of human ferritin and PCBP in the yeast *Saccharomyces cerevisiae*.^{121–123} A recent study showed that PCBP1 acts as a chaperone for delivery of Fe(II) to ferritin. This suggestion is based on four observations. (i) Heterologous coexpression of human PCBP1 and H and L subunits of human ferritin in yeast *S. cerevisiae* resulted in an increase in the amount of Fe(III) stored in ferritin. Yeast does not have a structural gene for ferritin or PCBP1. (ii) PCBP1 appears to bind ca. 3 Fe(II) with an association constant of $1.1 \times 10^6 \text{ M}^{-1}$ for the first site and $1.72 \times 10^5 \text{ M}^{-1}$ for the remaining sites as measured by ITC. (iii) In human cell lines depletion of PCBP1 decreases iron loading in ferritin. (iv) Human PCBP1 and ferritin coexpressed in yeast interact as measured by immunoprecipitation. Interaction of human PCBP1 and ferritin, however, was not observed in human cell lines. Therefore, we conclude that the role of PCBP1 or other members of this family as a chaperone for delivery of Fe(II) to ferritin requires further investigation. A protein similar to members of the PCBP family has not been identified in microbial cells. In analogy to the mechanism that has recently been reported for delivery of methane and dioxygen to the diiron catalytic site of soluble methane monooxygenase (MMO),¹²⁴ one can envision that a putative Fe(II) chaperone may induce local conformational changes in each subunit of ferritin to induce formation of channels from the surface to the ferroxidase center to facilitate transfer of Fe(II) substrate. In the case of MMO one of the three components of the soluble MMO complex induces conformational changes in the catalytic subunit to facilitate access of methane and molecular oxygen to the catalytic site.¹²⁴

Alternatively, specific channels have been suggested as a route of Fe(II) to the ferroxidase center (Figure 6). The presence of channels in ferritin was suggested after solving the X-ray crystal structure of ferritins and the observation that assembly of 24 subunits results in specific holes between subunits, i.e., 3-fold and 4-fold channels and B pores (Figure 6).

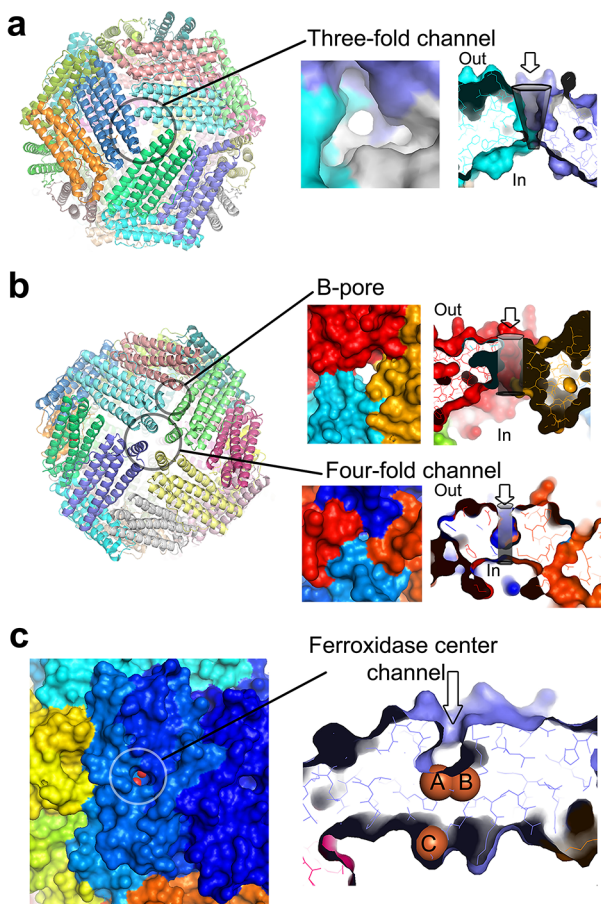


Figure 6. Fe(II) entry pathways of ferritin and bacterioferritin. (a) Funnel-shaped structure of the 3-fold channel of ferritins, and cross-section view of the 3-fold channel showing a possible path of metal ion entry. (b) 4-fold and B-pore channels. (c) Ferroxidase channel showing a pathway directly connecting the outside environment to the ferroxidase center. This channel is observed in the X-ray structure of bacterioferritin and predicted for ferritins by MD simulation studies (see text).

3-fold symmetry axis, (ii) a 4-fold channel at the 4-fold symmetry axis, and (iii) a channel at a specific junction between three subunits named B pore in bacterioferritin. The presence of the L subunit in heteropolymeric eukaryotic ferritin does not affect formation of these channels.¹¹⁸ In ferritin and bacterioferritin, besides the above-described channels, the existence of a fourth channel at 1-fold symmetry (1-fold channel or ferroxidase channel) directly from the surface to the ferroxidase center has been suggested.¹¹⁹ Observation and

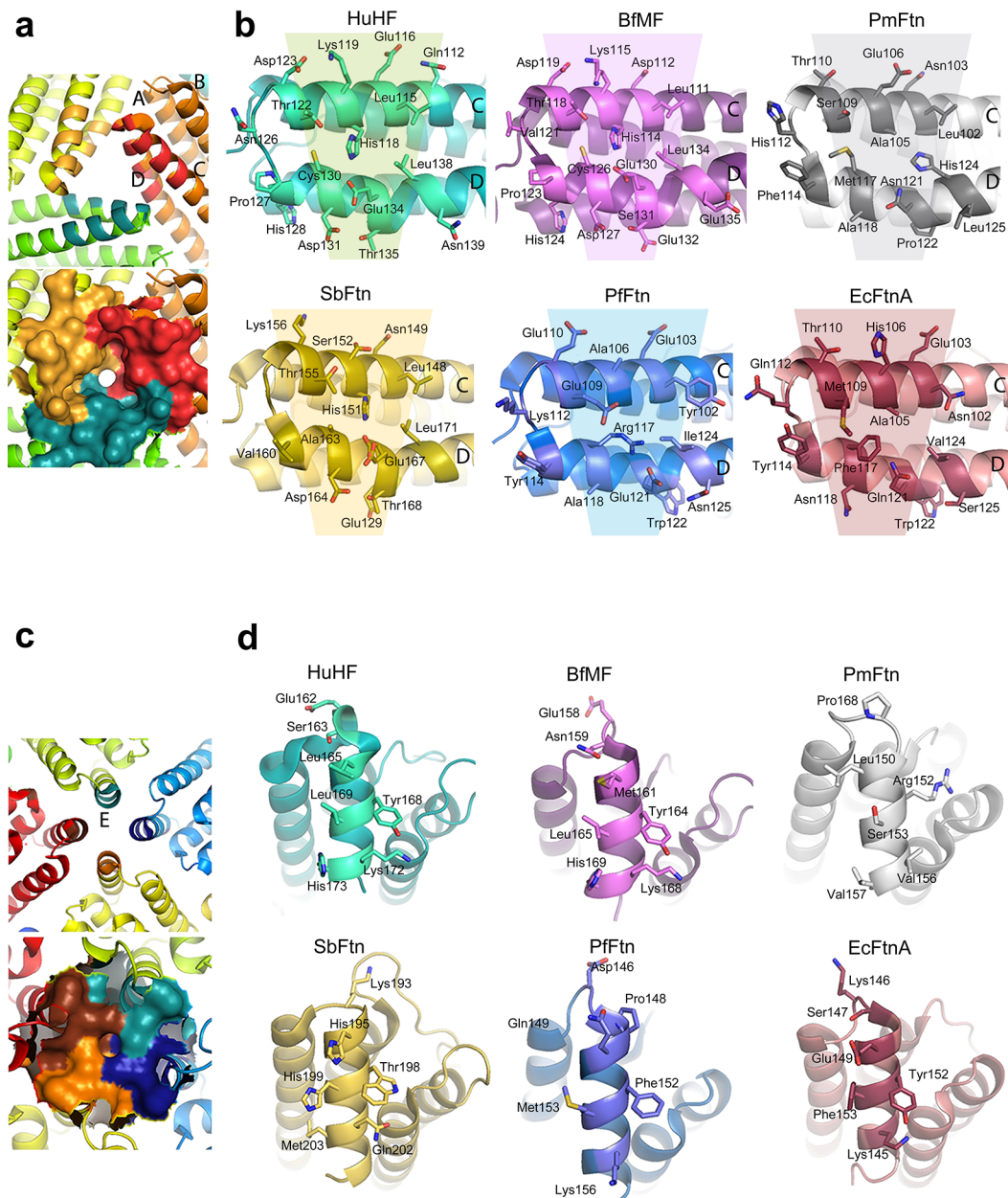


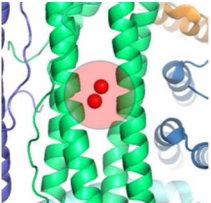
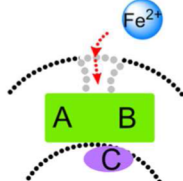
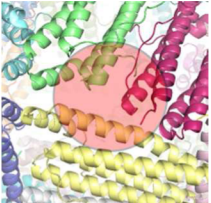
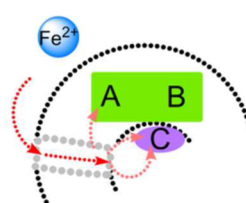
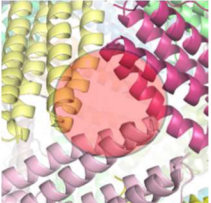
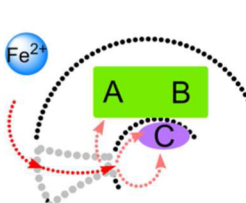
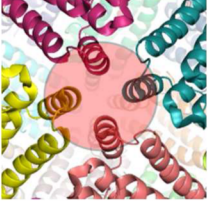
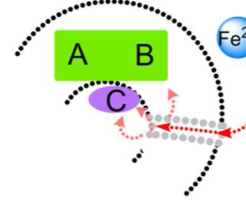
Figure 7. Alignment of the amino acid residues that form the 3-fold or 4-fold channels in ferritin. (a) Junction of three subunits at a 3-fold symmetry axis that forms the 3-fold channel and funnel-shaped structure of this channel from outside are shown. The part of the C and D helices of each subunit that participate in formation of 3-fold channel is highlighted. (b) Amino acid residues of the C and D helices of one subunit that are present at the 3-fold channel are compared for six ferritins: HuHF, BfMF, PmFtn, SbFtn, PfFtn, and EcFtn. Amino acids whose side chains are exposed to the empty space in the 3-fold channel are covered with a funnel. (c) The surface of short C-terminal E-helix of four subunits that form the 4-fold channels is shown. (d) Alignment of the amino acid residues of the E-helix that are present at the 4-fold channels. Exactly the same amino acids from four subunits participate in formation of 4-fold channels.

In heteropolymeric eukaryotic ferritin the same channels are observed in the presence of the L subunit.^{91,118} Moreover, a direct channel to the ferroxidase center, 1-fold channel or the feroxidase channel, was predicted for subunits with the feroxidase center by MD simulation studies.¹¹⁹ From the available data in the literature it is not clear which of these channels is the route of Fe(II) entry. Comparison of the amino acid residues forming 3-fold and 4-fold channels in eukaryotic, bacterial, and archaeal ferritins shows that these amino acids are not conserved among ferritins (Figure 7).

Data obtained from ¹¹³Cd NMR spectroscopy were interpreted as Cd(II) binding in 3-fold channels and inhibiting

Fe(II) oxidation in HoSF (which is a heteropolymer of the L and H subunits).¹²⁵ Chemical modification of Cys126 present in the 3-fold channel of HoSF decreased the Fe(II) oxidation rate.¹²⁵ This observation together with the NMR data led to the suggestion that the 3-fold channels in HoSF are the entry path of Fe(II).¹²⁵ Mutational analysis of the residues of the 3-fold channels in HuHF resulted in the conclusion that the roles of these channels in Fe(II) entry is not clear.⁴² Spin labeling of Cys126 at the 3-fold channel of HoSF and EPR spectroscopy was used to identify initial Fe(II) and VO²⁺ binding sites.¹²⁶ On the basis of these experiments it has been concluded that Fe(II) binds in 3-fold channels and is oxidized there and that

Table 4. Summary of Putative Fe(II) Entry Pathways to the Ferroxidase Center^a

Channel	Location	Ferritin	Bacterioferrin	Pathway
One fold channel or the Ferroxidase channel		Predicted ¹¹⁹	Predicted ^{99,100,117}	
B-pore		Observed in the X-ray structure, not predicted	Predicted ¹¹⁷	
Threefold channel		Predicted, Metal ion (including Fe(III)) binding observed	Not predicted,	
Fourfold channel		Predicted, Fe(III) binding observed ^{85,95*}	Predicted, Metal ion (including Fe(III)) binding observed	

^aThe asterisk indicates Fe(III) was found in the 4-fold channels of BfMF and HpFtn. In HpFtn Fe(III) is observed only when more than 500 Fe(II) was added aerobically to the protein, while Fe(II)/Fe(III) binding in 4-fold channels was not observed when a stoichiometric amount of Fe(II) was added. There is no experimental evidence that 4-fold channels in eukaryotic, bacterial, or archaeal ferritin may act as Fe(II) entry to ferritin and its subsequent catalysis in the ferroxidase center. If Fe(II) enters the protein shell via B pores, 3-fold channels, or 4-fold channels three possible routes can be considered for its translocation to the ferroxidase center. Present data favors a route that involves amino acids residues of site C. The access of Fe(II) to the ferroxidase center and site C via a ferroxidase channel can obviously only occur in those subunits of ferritins that have the catalytically active ferroxidase center. The presence of other pathways is the result of the quaternary structure of ferritin, and it is not affected by the presence of L subunits in heteropolymeric ferritins of eukaryotes.

the 3-fold channel is the path of Fe(II)/Fe(III) entry.¹²⁶ However, the early conclusion that Fe(II) binds to the 3-fold channels and is oxidized at this site can be ruled out, because the ferroxidase center is the site of Fe(II) binding and oxidation (see section 3). Calculating an electrostatic potential map of HuHF led to the conclusion that in this ferritin there is an electrostatic gradient in the 3-fold channel due to the presence of positively charged residues in the outer surface near these sites and negatively charged amino acid residues inside the channel.¹²⁷ This electrostatic gradient was proposed to guide Fe(II) ions into the ferritin cavity through the 3-fold channels.

MD simulation studies of HuHF in the presence of Fe(II) led to the suggestion of two Fe(II) entry pathways:¹¹⁹ 3-fold channel and ferroxidase center channel. It was predicted that if only one Fe(II) is present in a 3-fold channel it cannot enter ferritin. ITC measurements of Zn(II) binding to apo-HuHF led to the observation of a binding site with a stoichiometry of ca. 7.2 Zn(II) per 24-mer.¹²⁸ On the basis of this stoichiometry and because of the observation of Zn(II) in 3-fold channels in the X-ray crystal structure of HuHF it was concluded that Zn(II) initially binds to eight 3-fold channels present in the 24-meric shell.⁸² In the presence of Zn(II), oxidation of Fe(II) at

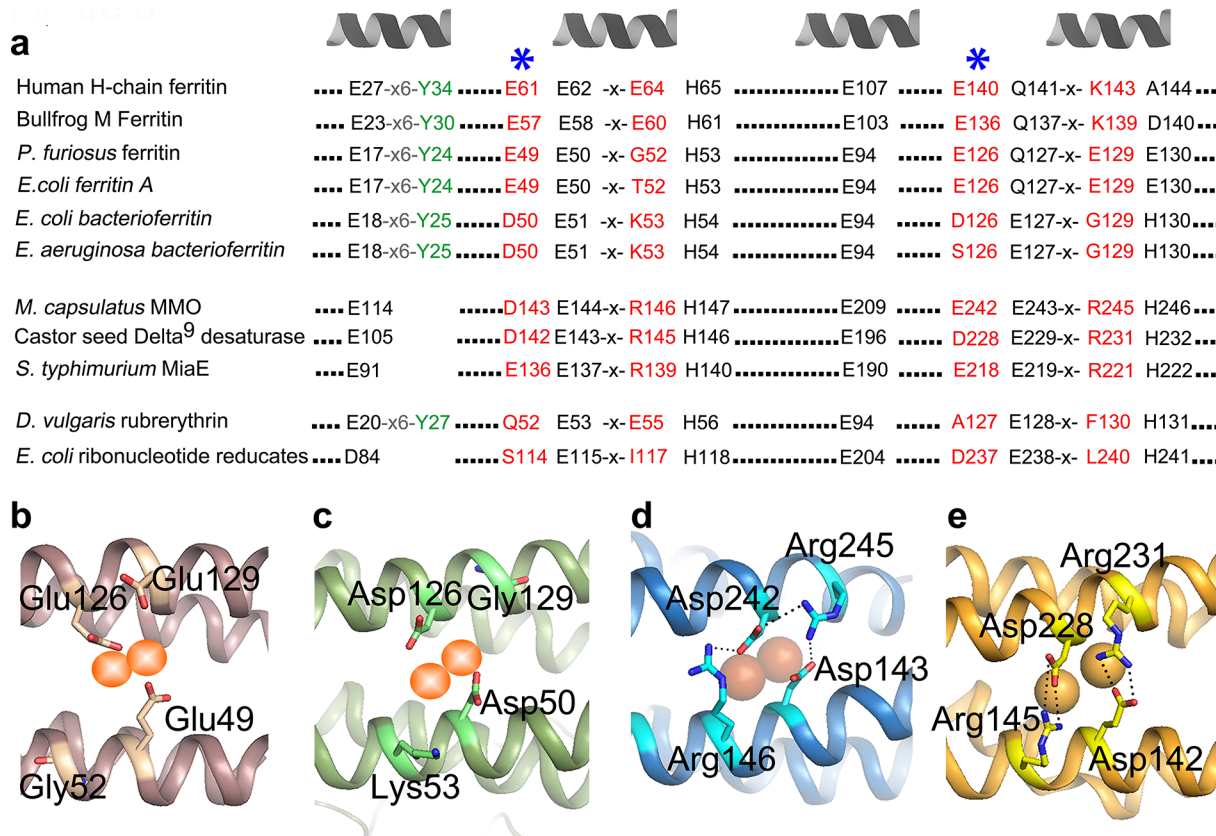


Figure 8. Ferroxidase center gateway. (a) Alignment of the amino acid residues of the ferroxidase center motif with the diiron cofactor motif of other members of the ferritin superfamily shows that the coordinating residues of site C are only present in (bacterio)ferritin and can only participate in a metal ion binding site in ferritin or bacterioferritin. Amino acid residues in the coordination environment of site C are shown in red. The alignment shows that two of the amino acid residues of site C with carboxylate side chain are highly conserved among ferritins, bacterioferritin, and dioxygen-activating enzymes (*). These two residues in ferritins (b) and bacterioferritins (c) participate in metal ion binding to site C, while in dioxygen-activating enzymes such as soluble MMO (d) or delta⁹ desaturase (e) they participate in hydrogen bonding.

the ferroxidase center diminishes.¹²⁸ Accordingly, it was concluded that 3-fold channels are the entry path of Fe(II) and translocation to the ferroxidase center.^{128,129} Assuming that 3-fold channels are the only pathway of Fe(II) ions from outside to the protein cavity where they will have access to the ferroxidase center, the Possion–Nernst–Planck model for ion diffusion was used to estimate the transit time of Fe(II) ions through the HuHF protein shell.¹³⁰ Inputs to the model were obtained from all-atom molecular dynamics (MD) simulations. It was calculated that the average transit time is in the range of milliseconds. 3-fold channels have been suggested as the main entry path of Fe(II) to the protein cavity of bullfrog M ferritin (BfMF) and its subsequent binding to the ferroxidase center. This suggestion is based on the observation of Co(II) or Mg(II)⁸⁶ in 3-fold channels in the X-ray structure of BfMF. In the presence of large amounts of Co(II) or Mg(II) it was observed that these metal ions are present in the 3-fold channel.⁸⁶ Only one Co(II) or Mg(II) ion was found in the narrowest part of the funnel-shaped 3-fold channel, suggesting that one Fe(II) ion at a time can enter ferritin. However, when crystals of BfMF were soaked aerobically in large amounts of Fe(II) and crystals were flash frozen using liquid nitrogen Fe(II)/Fe(III) was found in both the 3-fold and the 4-fold channels by X-ray crystallography.⁸⁵ This data suggests that both channels may act as Fe(III) entry pathway. Fe(II) was not found in the 3-fold or 4-fold channels when anaerobically prepared crystals of PmFtn were soaked anaerobically in 2 mM

ferrous sulfate solution and crystals were frozen in liquid nitrogen.¹³¹

In bacterial and archaeal ferritins similar channels as those present in eukaryotic ferritin exist (Figure 6). However, experimental evidence regarding involvement of these channels in Fe(II) entry to bacterial and archaeal ferritin is limited. Only for *H. pylori* ferritin (HpFtn) a role of 4-fold channels has been suggested.⁹⁵ This was based on alignment of the amino acid residues that are present in 3-fold and 4-fold channels of bacterial and archaeal ferritins (Figure 7) with those of eukaryotic ferritins. It was concluded that, unlike 3-fold channels in eukaryotic ferritin, 3-fold channels in bacterial and archaeal ferritins are hydrophobic while 4-fold channels are hydrophilic. On the contrary, we find that in all ferritins 3-fold channels have predominantly hydrophilic residues (Figure 7). From the observation of an Fe(III) ion in the 4-fold channel of HpFtn when large amounts of Fe(II) per 24-mer were added aerobically, i.e., >500 Fe(II) per 24-mer, it was concluded that the 4-fold channels are the path of Fe(II) entry to bacterial or archaeal ferritins.⁹⁵ The observation of an Fe(III) in the 4-fold channels of HpFtn only when large amounts of Fe(II) were aerobically added does not necessarily bear on involvement of Fe(II) uptake when small amounts of Fe(II) are added.

On the basis of the available data we summarize possible pathways of Fe(II) from outside the protein shell to the ferroxidase center in Table 4. If Fe(II) enters a ferroxidase channel it directly reaches the ferroxidase site. However, if

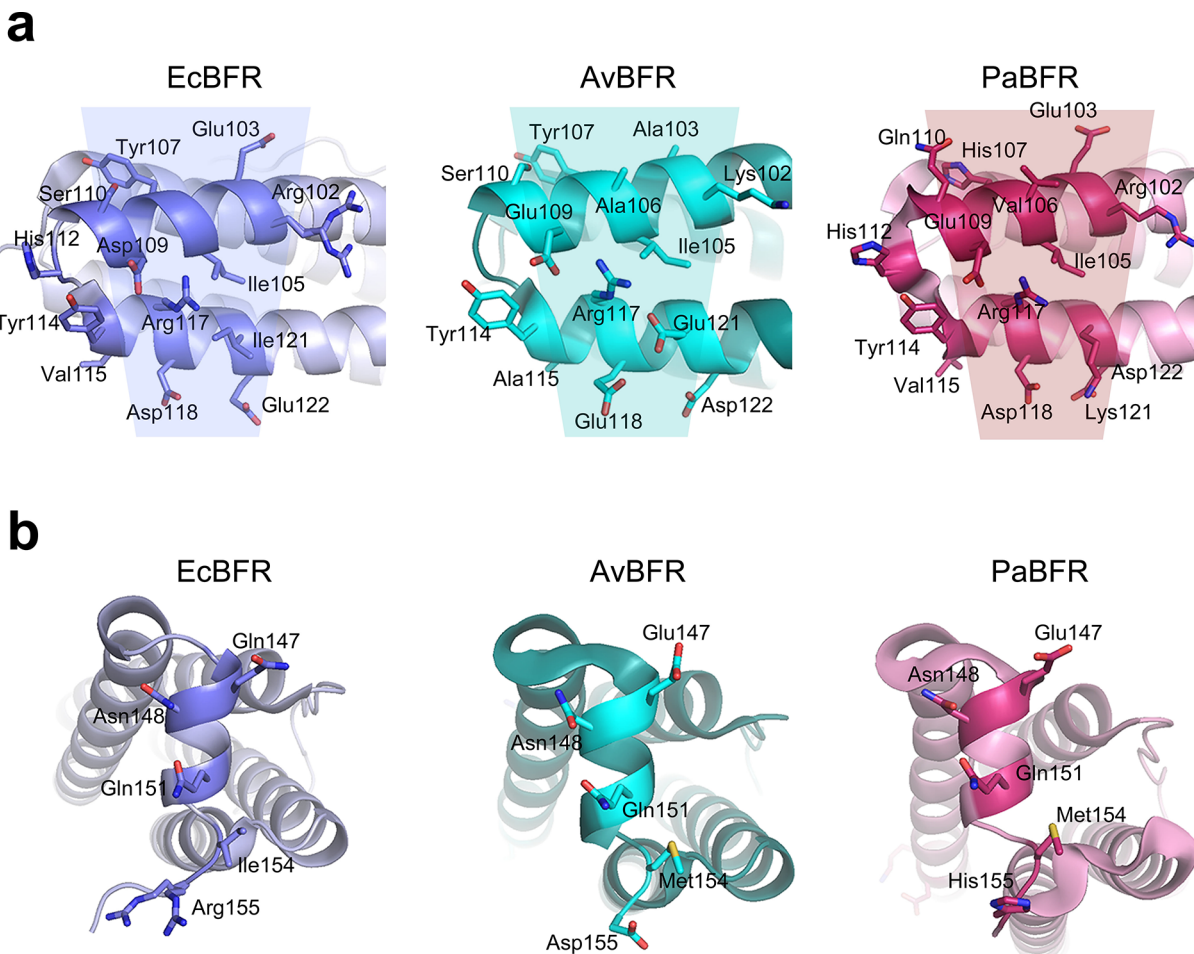


Figure 9. Alignment of the amino acid residues that form the 3-fold and 4-fold channels in bacterioferritin. (a) Amino acid residues at the 3-fold channel of one subunit are compared for three bacterioferritins: EcBFR, AvBFR, and PaBFR. Exactly the same amino acids from three subunits together form the 3-fold channels. Amino acids whose side chains are exposed to the empty space in the 3-fold channel are covered with a funnel. (b) Alignment of the amino acid residues of the E-helix that are present at 4-fold channels. Exactly the same amino acids from four subunits participate in formation of 4-fold channels.

Fe(II) enters via other channels it will not directly reach the ferroxidase center and three different routes can be predicted (Table 4): Fe(II) may reach the ferroxidase center through the protein shell via the inner surface of the 24-meric shell and subsequently site C or directly via site C. It has been suggested that after entry of Fe(II) through 3-fold channels into the protein cavity the rate-limiting step for Fe(II) to reach the ferroxidase center is diffusion.¹²⁹ Coordinating residues of site C have been proposed to be involved in translocation of Fe(II) to the ferroxidase center. This proposal is based on the observation of metal ion binding to these residues in Soybean ferritin (SbFtn)⁹⁰ and HuHF⁷⁹ and on the observation that mutation of these residues decreases the rate of Fe(II) oxidation in the ferroxidase center. Mutation of a residue of site C, i.e., Glu140Gln (Figure 4a), in HuHF has been shown to significantly decrease the rate of Fe(II) oxidation.⁸³ However, in HuHF a controversy exists regarding the importance of two other residues of site C, i.e., Glu61 and Glu64, in catalysis of Fe(II) oxidation in sites A and B of the ferroxidase center. Early studies suggested that mutation of these residues affects catalysis of Fe(II) oxidation and formation of Fe(III),¹³² but a later study reported that mutation of these residues does not affect Fe(II) oxidation in the ferroxidase center.¹³³ MD simulation studies also predicted that coordinating residues of

site C are present in an Fe(II) pathway to the ferroxidase center in HuHF.¹¹⁹ A pathway was suggested based on the X-ray crystal structure of human mitochondrial ferritin (HMFT) in the presence Zn(II).⁸⁹ We aligned the residues of the coordination environment of the ferroxidase center in ferritins and bacterioferritins with those of the diiron cofactor site of other members of ferritin superfamily and found that the amino acid residues of site C are only present in ferritins (Figure 8) and bacterioferritins (see section 4.2).²⁶ Mutation of the highly conserved residues of this site diminishes Fe(II) oxidation in the ferroxidase center of PfFtn, and thus, we suggested that site C is present in the conserved gateway of the ferroxidase center, which may be involved in translocation of Fe(II)/Fe(III) into/out of the ferroxidase center.²⁶ Involvement of site C in translocation of Fe(III) out of the ferroxidase center and into the ferritin cavity was proposed for AfFtn based on the rearrangement of the side chain of two of the coordinating residues of site C, i.e., Glu51 and Glu131, upon Fe(III) binding.⁴⁵ The X-ray crystal structure of BfMF in the presence of Co(II), Cu(II), or Fe(III) (see section 3.1) also provided a picture that suggest involvement of site C in translocation of Fe(II)/Fe(III) in/out of the ferroxidase center. In BfMF mutation of the highly conserved residues of site C in the gateway site to the ferroxidase center was shown to diminish

Fe(II) oxidation rate, and it was concluded that site C is involved in translocation of Fe(II) to the ferroxidase center.¹¹⁰ The effect of mutation of residues of site C on the fast rate of Fe(II) oxidation in the ferroxidase center has also been observed in EcFtnA, although a controversy exists regarding the reported rates for catalysis of Fe(II) oxidation and Fe(III) formation. An early study using stopped flow spectroscopy to measure formation of Fe(III) species at 330 nm showed that mutation of any of the three residues of site C in EcFtnA, Glu49Ala, Glu126Ala, or Glu130Ala decreased the rate of Fe(II) oxidation between 3-fold and 4-fold.¹¹³ On the contrary, in a recent study Glu49Ala mutation was found to have a limited effect and G126Ala was found to decrease the fast rate of Fe(II) oxidation in the ferroxidase center between 4-fold and 10-fold. One possible conclusion from the results obtained with different ferritins is that if 3-fold, 4-fold, or B-pore channels act as Fe(II) entry path to the protein, the coordinating residues of site C may act as a transient site in grabbing the Fe(II) and its subsequent delivery to the ferroxidase center. In summary, we conclude that although the present literature is in favor of an Fe(II) entry pathway that involves 3-fold channels and site C, direct evidence for involvement of this pathway does not exist and we cannot define a bucket brigade as proposed by Theil et al.^{86,110} There are other channels such as the ferroxidase channel at 1-fold symmetry which may act as a route for Fe(II) translocation to the ferroxidase center, and it is possible that Fe(II) entry occurs via different channels simultaneously.

4.2. Pathway of Fe(II) to the Ferroxidase Center in Bacterioferritin

The quaternary structure of bacterioferritin is equivalent to that of ferritin, and channels similar to those of ferritin are observed in bacterioferritin. In addition, in bacterioferritins the residues of the 3-fold channels are predominantly hydrophilic (Figure 9a). In ferritin both hydrophilic and hydrophobic residues are present at 4-fold channels (Figure 7b), but in bacterioferritin the amino acid residues that form the 4-fold channel are mainly hydrophilic (Figure 9b). In bacterioferritin 3-fold channels have not been proposed as a Fe(II) entry pathway. In PaBFR residual electron density was observed in the 3-fold channel that was assigned to SO_4^{2-} ions.¹⁰⁰ Three different channels have been proposed as possible pathways of Fe(II) to the ferroxidase center of bacterioferritin:¹⁰⁰ 4-fold channels, B pore, and ferroxidase center channel (Figure 6). The Fe(II) that enters the ferroxidase channel directly reaches the ferroxidase center where it is oxidized, and the resulting Fe(III) somehow enters the protein cavity (Figure 6c). The proposal that the ferroxidase channel is involved in Fe(II) access to the ferroxidase center is based on the observation of conformational changes of a histidine in the ferroxidase center of three bacterioferritins AvBFR,⁹⁹ PaBFR,¹⁰⁰ or DdBFR.¹⁰² These changes were observed in the X-ray crystal structures, and they appeared to be dependent on the oxidation state of iron. The involvement of the ferroxidase channel in Fe(II) access to the ferroxidase center was also predicted by MD simulations studies of PaBFR.¹¹⁷ Another pathway that has been suggested as the Fe(II) entry route in bacterioferritins is via the 4-fold channel. This proposal is based on the observation of different metal ions at the 4-fold channel in the X-ray crystal structure of some bacterioferritins. In the crystal structure of AvBFR a Ba(II)¹³⁴ or an Fe(III)⁹⁹ ion was present at the 4-fold channels, and in the crystal structure of PaBFR a K(I) was present.¹⁰⁰ MD simulations of PaBFR¹¹⁷ also predicted the importance of

the 4-fold channels for entry of cations to the bacterioferritin cavity and subsequent access to the ferroxidase center. Besides 4-fold channels MD simulations of PaBFR predicted protein dynamics at the B pores and their involvement in Fe(II) entry into the bacterioferritin cavity.¹¹⁷ If the B pores or 4-fold channels act as the main entry pathway for Fe(II), the Fe(II) that enters these channels should somehow reach the ferroxidase center. How Fe(II) reaches the ferroxidase center after entry via B pores or 4-fold channels is not known. Similar to ferritin three routes might be possible (Table 4). MD simulation predicts a pathway that appears to involve the amino acid residues of site C in bacterioferritin.¹¹⁷ Alignment of the coordination environment of the ferroxidase center in bacterioferritin with those of the ferroxidase center in ferritin suggests that site C in the gateway of the ferroxidase center is present in bacterioferritin (Figure 8). The exact role of this site in bacterioferritin is not known. In summary, a specific Fe(II) entry pathway for bacterioferritins has not been identified: possible pathways are summarized in Table 4. Although the available data suggests that the Fe(II) uptake pathways in bacterioferritin are different from ferritin, the data also point to possible similar pathways such as the ferroxidase channel or involvement of the coordinating residues of site C in Fe(II) translocation to the ferroxidase center.

5. HOW IS FE(II) OXIDIZED?

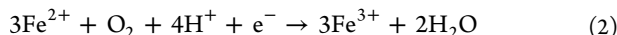
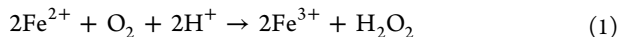
Three different aspects of the catalytic oxidation of Fe(II) in the ferroxidase center have been addressed using eukaryotic, bacterial, and archaeal ferritins: (i) what is the stoichiometry of the ferroxidase reaction, (ii) what are the intermediates that are formed during the ferroxidase reaction, and (iii) what are the final Fe(III) species that are formed as products of oxidation of Fe(II)? In this section we evaluate the studies that have been conducted to answer each of these questions. Our evaluation of the available data together with the observation of the same three metal ion binding sites in all catalytically active ferritins (see section 3) lead us to conclude that the data support a common mechanism of Fe(II) oxidation by the ferroxidase center of eukaryotic, archaeal, and bacterial ferritins. Bacterioferritin studies on this aspect have been limited to determination of the stoichiometry of the ferroxidase reaction in EcBFR.

5.1. What Is the Stoichiometry of the Ferroxidase Reaction?

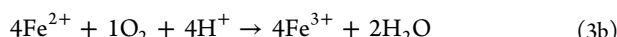
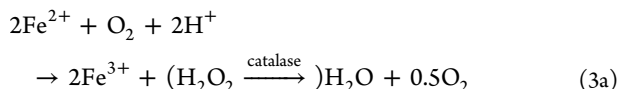
5.1.1. Ferritin Ferroxidase Reaction Stoichiometry. It has been shown for eukaryotic, bacterial, and archaeal ferritins that catalysis of Fe(II) oxidation in the ferroxidase center occurs at least via two pathways: (i) In some subunits only two Fe(II) ions are present in the ferroxidase center, and oxidation of Fe(II) by molecular oxygen results in formation of hydrogen peroxide. (ii) In some subunits two Fe(II) ions are present in the ferroxidase center and a third Fe(II) is present in site C. Fe(II) in site C is oxidized together with Fe(II) in the ferroxidase center, and water is produced. The origin of the fourth electron for reduction of molecular oxygen to water is under debate. For PfFtn and HuHF evidence suggests that this electron is provided by the highly conserved tyrosine in the vicinity of the ferroxidase center (see section 5.2.2).

To determine the stoichiometry of the ferroxidase reaction consumption of molecular oxygen has been measured after aerobic addition of different aliquots of Fe(II) to ferritin. Aerobic addition of two Fe(II) per ferroxidase center to apo-

HuHF results in oxidation of 2.2 Fe(II) per molecular oxygen at pH 7.0. This observation was initially interpreted as oxidation of approximately two Fe(II) per molecular oxygen and release of hydrogen peroxide according to reaction 1.^{135,136} Similarly, addition of one or two Fe(II) per ferroxidase center to PfFtn resulted in a stoichiometry of 2.3–2.8 Fe(II) oxidized per molecular oxygen.^{27,137} For PfFtn also the initial conclusion was that two Fe(II) are oxidized in the ferroxidase center and hydrogen peroxidase is produced (reaction 1).¹³⁷ In EcFtnA a stoichiometry of 3.3 Fe(II) per ferroxidase center was observed, and this stoichiometry was interpreted as oxidation of three Fe(II) in the ferroxidase center and site C (reaction 2).¹¹³ In reaction 2 the origin of the fourth electron for catalysis of Fe(II) oxidation by EcFtnA remained unknown.



To detect formation of hydrogen peroxide based on reaction 1, consumption of molecular oxygen because of the ferroxidase reaction has been measured in the presence of catalase or horseradish peroxidase.¹³⁵ Addition of catalase to the reaction mixture before addition of Fe(II) results in instantaneous conversion of any produced hydrogen peroxide to water and molecular oxygen, and it minimizes the reaction of hydrogen peroxide with any components in the mixture. In the presence of catalase if in each ferroxidase center two Fe(II) are oxidized (reaction 1) by molecular oxygen the produced hydrogen peroxide will be converted to one water molecule and 0.5 dioxygen molecule (reaction 3a). As a result, an overall stoichiometry of 4 Fe(II) per molecular oxygen would have been expected (reaction 3b).



When one Fe(II) per ferroxidase center was added in the presence of catalase a stoichiometry close to 4 Fe(II) per molecular oxygen was observed for PfFtn and HuHF.²⁷ However, when the amount of added Fe(II) was increased to two Fe(II) per ferroxidase center and the overall amount of consumed molecular oxygen was measured in the presence of catalase; the stoichiometry decreased from 4.0 to 3.0 Fe(II) oxidized per molecular oxygen.²⁷ In other words, only 30–50% of hydrogen peroxide that is expected based on reaction 3a was found. Therefore, in PfFtn and HuHF as the amount of Fe(II) increases from one to two Fe(II) per ferroxidase center it appears that either hydrogen peroxide oxidized some of the Fe(II) in ferritin or some Fe(II) was oxidized in a reaction that did not produce hydrogen peroxide. This observation has been interpreted as follows: for addition of 2 Fe(II) per ferroxidase center 50% of the Fe(II) added is oxidized via reaction 1 and 50% of the Fe(II) added is oxidized via a reaction that does not produce hydrogen peroxide, i.e., reaction 2.²⁷ The third Fe(II) in reaction 2 has been suggested to be oxidized in site C via a redox reaction together with two Fe(II) in the ferroxidase center or by the hydrogen peroxide that is produced in the ferroxidase center.²⁷ Thus, a general function of site C might be to increase the capacity of Fe(II) oxidation in one turnover when more than two Fe(II) are present per ferroxidase site. It has also been proposed by us that in PfFtn and HuHF the

fourth electron for reduction of molecular oxygen to water in reaction 2 is provided by the highly conserved tyrosine in the vicinity of site B of the ferroxidase center (see section 5.2.2).²⁷ Recently, the same reaction mechanism has also been proposed by Chasteen et al. for EcFtnA.¹³⁸ It was suggested that when site C in EcFtnA is filled with Fe(II) some of the hydrogen peroxide that is released from oxidation of two Fe(II) in the ferroxidase center reacts with the Fe(II) in site C, and as a result water is produced.¹³⁸ The origin of the fourth electron for reduction of molecular oxygen to water in EcFtnA is unknown. Remarkably, although this model is the same as the model previously proposed for PfFtn and HuHF,²⁷ the authors conclude that EcFtnA works differently than PfFtn and HuHF: in EcFtnA the residues of site C and the conserved tyrosine are not essential for rapid oxidation of Fe(II) in the ferroxidase center.¹³⁸ This conclusion is rather inconsistent with the experimental data reported by Chasteen et al. or by other researchers.^{113,138} In EcFtnA, mutation of the amino acid residues of site C decreased the rate of Fe(II) oxidation at the ferroxidase center at least 3-fold and mutation of the conserved tyrosine, i.e., Tyr24Phe, decreased the rate of Fe(II) oxidation between 2-fold and 26-fold depending on the amount of Fe(II) added. In our view the data show that with Fe(II) distributed among three binding sites the ferroxidase reaction in eukaryotic, archaeal, and bacterial ferritins occurs via a common mechanism that consists of at least two pathways: reaction 1 and reaction 2.²⁷

It should be noted that the presence of the L subunit in heteropolymeric eukaryotic ferritin does not change the stoichiometry of Fe(II) oxidized per ferroxidase center.¹³⁶ Moreover, as the amount of Fe(II) substrate added to HuHF,¹³⁶ PfFtn,¹³⁷ or EcFtnA¹³⁸ increases from 48 Fe(II)/24-mer to more than 200, the stoichiometry of Fe(II) oxidized per molecular oxygen increases gradually and reaches a value between 3.4 and 3.8. This stoichiometry in HuHF and EcFtnA has been attributed to catalysis of Fe(II) oxidation by the Fe(III) mineral core.^{136,138} It was suggested that as the Fe(III) mineral core forms the catalysis of Fe(II) oxidation occurs preferably on the surface of the mineral core with a stoichiometry of 4 Fe(II) per molecular oxygen. In contrast, we suggest that under the condition that the amount of Fe(II) is more than enough to saturate all three Fe(II) binding sites (i.e., >72 Fe(II) per 24-mer) more Fe(II) is oxidized in site C (reaction 2) and also some Fe(II) will be oxidized via a side reaction by hydrogen peroxide produced in reaction 1, resulting in an overall stoichiometry close to 4 Fe(II) per molecular oxygen. Consistent with this conclusion is the observation that the Fe(III) mineral core in PfFtn does not catalyze Fe(II) oxidation.¹³⁷ When we aerobically added 48 or 300 Fe(II) per 24-mer to apo-PfFtn or PfFtn samples that contained different Fe(III) core sizes, we always observed the same stoichiometry.¹³⁷

5.1.2. Bacterioferritin Ferroxidase Reaction Stoichiometry. Studies into the stoichiometry of the ferroxidase reaction in bacterioferritin have been limited to that of EcBFR, and a stoichiometry different from that of ferritin has been observed. Whether the presence of a heme group in EcBFR is essential for oxidation of Fe(II) has remained a matter of debate. Le Brun's group initially suggested that heme does not significantly affect the overall oxidation rate of Fe(II) in EcBFR.³¹ In a more recent study they suggested that the heme group facilitates iron core mineralization in EcBFR via an electron transfer mechanism whose details remain unknown.¹³⁹

In EcBFR, regardless of the concentration of Fe(II) substrate added, a stoichiometry of 4 Fe(II) per molecular oxygen has been found in the absence of catalase (reaction 3b).¹⁴⁰

The reason for the observation of a stoichiometry of 4 Fe(II) oxidized per molecular oxygen is not clear. At least three possible explanations can be envisioned. (i) In analogy to the disproportionation of hydrogen peroxide by ferritin, e.g., PfFtn as discussed above, it is possible that hydrogen peroxide disproportionates very fast to molecular oxygen and water because of a reaction with EcBFR, which results in an overall stoichiometry of 4 Fe(II) per molecular oxygen and formation of water. (ii) Alternatively, hydrogen peroxide may oxidize a third Fe(II) in site C of EcBFR just as proposed for ferritin (see section 5.1.1). (iii) The hydrogen peroxide produced in one ferroxidase center may oxidize two other Fe(II) ions bound to another nearby ferroxidase center. In EcBFR, formation of hydrogen peroxide has not been observed and only the latter possibility has been considered.¹⁴⁰ Chasteen's group suggested that hydrogen peroxide is a better oxidant for bacterioferritin compared to ferritin.¹⁴⁰ This proposal was based on the observation that when Fe(II) was added to EcBFR in the presence of H₂O₂ and O₂ only 25% of molecular oxygen was consumed relative to a control experiment conducted in the absence of H₂O₂. The results were compared to the observation that in ferritin after oxidation of Fe(II) by molecular oxygen hydrogen peroxide is detected by catalase activity (discussed above). In our view the experiment done by Chasteen et al. is not conclusive since H₂O₂ might have reacted with bacterioferritin or with the Fe(III) that is formed because of the ferroxidase reaction, which would result in formation of water and molecular oxygen and observation of less O₂ consumed compared to the control experiment. Moreover, one cannot compare the results obtained from oxidation of Fe(II) by EcBFR in the presence of O₂ and H₂O₂ with the results obtained from oxidation of Fe(II) by ferritin in the presence of only O₂. It is possible that in ferritins also addition of Fe(II) in the presence of H₂O₂ and O₂ leads to the observation of less O₂ consumed compared to a control experiment which is done only in the presence of O₂. The available data appear to be insufficient to work out the mechanism of Fe(II) oxidation in the ferroxidase center of bacterioferritin. It is not clear whether hydrogen peroxide is a product of oxidation of Fe(II) by molecular oxygen in the ferroxidase center of bacterioferritins. Further experiments are required to understand the mechanism of Fe(II) oxidation in the ferroxidase center of bacterioferritin using molecular oxygen as oxidant.

5.2. What Are the Intermediates of the Ferroxidase Reaction?

Two intermediate species have been observed during catalysis of Fe(II) oxidation in the ferroxidase center of catalytically active ferritins: (i) a blue (sometimes: purple) intermediate with UV-vis absorbance between 500 and 800 nm whose color varies slightly among ferritins (Figure 10) and (ii) a radical intermediate. The blue intermediate has been observed in eukaryotic, archaeal, and bacterial ferritins, and it has been studied using different spectroscopic techniques. We review the available data for this intermediate, and we conclude that its formation in the ferroxidase center of ferritins from all three Kingdoms of life suggests a common mechanism of Fe(II) oxidation. The molecular structure of this intermediate has not

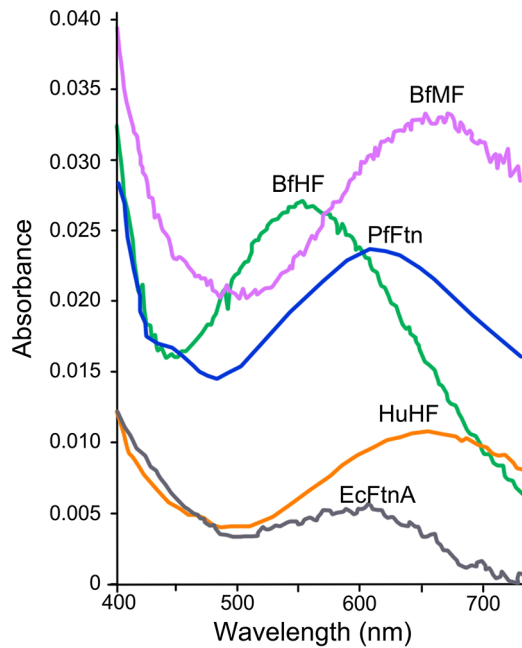


Figure 10. UV-vis absorbance spectra of the blue intermediate for eukaryotic, bacterial, and archaeal ferritins. Data for BfMF and BfHF are extracted from ref 143, those of PfFtn and HuHF are extracted from ref 26, and data for EcFtnA are extracted from ref 138. Concentration of BfMF and BfHF was 2.09 μM (24-mer), that of PfFtn was 2.0 μM (24-mer), that of HuHF was 0.93 μM (24-mer), and that of EcFtnA was 1.0 μM (24-mer).

been unequivocally determined, and the literature is flawed with interpretational inconsistencies.

A radical intermediate has been reported for eukaryotic and archaeal ferritins upon reduction of the highly conserved tyrosine in the vicinity of the ferroxidase center. Mutation of this tyrosine diminishes formation of the blue intermediate in several ferritins and decreases the rate of catalysis of Fe(II) oxidation in all ferritins tested. Therefore, we propose that the conserved tyrosine is involved in the catalysis of Fe(II) oxidation via the blue intermediate.

We argue that the presence of these intermediates in the ferroxidase center of H subunit is not affected by the presence of the L subunit. These intermediates have not been reported for EcBFR¹⁴¹ or other bacterioferritins which, however, do have the ferroxidase center and can catalyze oxidation of Fe(II). Hence, either the decay rate of the intermediates in the ferroxidase reaction of bacterioferritins is much faster than the formation rate or the mechanism of the ferroxidase reaction is different in bacterioferritin compared to ferritin. Further investigation is required to distinguish between these possibilities.

5.2.1. Blue Intermediate. The first evidence regarding the presence of an intermediate during catalysis of Fe(II) oxidation by H-type ferritin came from studies performed by Harrison's group.¹⁴² When formation of Fe(III) from Fe(II) by HuHF was recorded using stopped-flow spectroscopy, a blue intermediate was observed. Site-directed mutagenesis showed that this intermediate is formed upon Fe(II) oxidation in the ferroxidase center and that the conserved tyrosine in the vicinity of site B, i.e., Tyr34 in HuHF, is essential for its formation and for fast catalysis of Fe(II) oxidation.¹⁴² The maximum UV-vis absorbance of this intermediate in HuHF was observed to be at 650 nm.^{26,129} This intermediate was reported in two other

recombinant homopolymeric eukaryotic ferritins, namely, bullfrog H- and M-type ferritins,¹⁴³ which show more than 80% amino acid sequence identity, in heteropolymeric horse spleen ferritin (HoSF)¹⁴⁴ that consists of 20–22 L subunits and 4–2 H subunits, in archaeal PfFtn,²⁶ and in bacterial EcFtnA.¹³⁸ Because the blue intermediate is observed in the H subunit of heteropolymeric HoSF, the presence of the L subunit in eukaryotic ferritin does not appear to affect catalysis of Fe(II) oxidation in the ferroxidase center of the H subunit via the blue intermediate. In BfHF, BfMF, PfFtn, and EcFtnA the blue intermediate has a UV-vis maximum at 550, 650, 625, and 600 nm, respectively (Figure 10), and its rate of formation or its spectrum is affected by mutation of the conserved tyrosine in the vicinity of site B of the ferroxidase center (Figure 4). A plot of the rate of formation of the blue intermediate in PfFtn,²⁶ HuHF,²⁶ or BfMF¹⁴⁵ as a function of the amount of Fe(II) added to these ferritins showed positive cooperativity (apparent degree of cooperativity (n) between 1.5 and 2.3) with an unknown origin. In BfMF site-directed mutagenesis studies showed that, like in HuHF, the blue intermediate is formed in the ferroxidase center.¹⁴⁵ In BfHF mutation of the conserved tyrosine in the vicinity of the ferroxidase center, i.e., Tyr30, decreased the rate of formation of the blue intermediate and catalysis of Fe(II) oxidation more than 10-fold.¹⁴³ In PfFtn mutation of the conserved tyrosine,²⁷ i.e., Tyr24, abolished formation of the blue intermediate and the rate of Fe(II) oxidation. Similarly, in EcFtnA mutation of the conserved tyrosine, i.e., Tyr24, decreased the rate of Fe(II) oxidation ca. 2–26-fold depending on the amount of Fe(II) added.¹³⁸ Because the presence of phosphate accelerates rate of Fe(II) oxidation⁶⁴ and it incorporates into the Fe(III) mineral core,⁶² it was tested if phosphate changes the mechanism of Fe(II) oxidation in PfFtn and HuHF.⁶³ In none of these proteins was the spectrum of the blue intermediate affected by the presence of phosphate; thus, phosphate does not affect the mechanism of Fe(II) oxidation at the ferroxidase center.⁶³ Titration of PfFtn and HuHF with different amounts of Fe(II) and recording formation of Fe(III) species parallel to the formation and decay of the blue intermediate using UV-vis stopped-flow spectroscopy showed that the intensity of the blue color increased linearly with the Fe(II) added up to one Fe(II) per ferroxidase center.²⁷ If more than one Fe(II) per ferroxidase center was added the intensity of the blue color did not change significantly. On the basis of these observations several models have been tested to understand the mechanism of Fe(II) oxidation.²⁷ Only the dual-way model in Figure 11 could successfully be used to simulate the progress curves of the blue intermediate and Fe(III) formation.²⁷ In this model Fe(II) is distributed among three binding sites, i.e., sites A, B, and C. Site C in the ferroxidase center gateway is empty in some subunits, while in other subunits it is filled with Fe(II). If site C is empty two Fe(II) are oxidized in the ferroxidase center via the blue intermediate and hydrogen peroxide is released. If an Fe(II) is present in site C it may react either with the blue intermediate or with the hydrogen peroxide that is released because of the decay of this intermediate. In this reaction water is formed instead of hydrogen peroxide (Figure 11). The fourth electron for reduction of molecular oxygen to water is proposed to be provided by the highly conserved tyrosine in the vicinity of the ferroxidase center (see section 5.2.2). Because site C in bacterial and archaeal ferritin has a higher affinity for Fe(II) than site C in eukaryotic ferritin (Table 3), slightly more Fe(II)

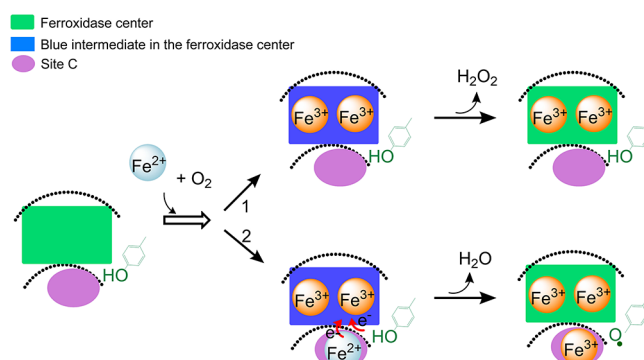


Figure 11. Mechanism of Fe(II) oxidation by ferritin. Because of the distribution of Fe(II) among three binding sites, oxidation of Fe(II) occurs at least via two pathways: (Path 1) Two Fe(II) ions bind to the ferroxidase center, and there is no Fe(II) present in site C of the ferroxidase center gateway. In this case, two Fe(II) are oxidized simultaneously via an intermediate with blue color and molecular oxygen is reduced to hydrogen peroxide. (Path 2) Two Fe(II) ions bind to the ferroxidase center, and an Fe(II) ion binds to site C in the ferroxidase center gateway. In this situation the two Fe(II) in the ferroxidase center are simultaneously oxidized to form a blue intermediate. The third Fe(II) either reacts with this intermediate or it is oxidized by the peroxide that is released as the blue intermediate decays. The fourth electron for complete reduction of molecular oxygen to water is proposed to be provided by the conserved tyrosine in the vicinity of the ferroxidase center.

may be oxidized at this site in archaeal or bacterial ferritins compared to eukaryotic ferritin.

To determine the molecular structure of the blue intermediate two spectroscopic methods have been used: Mössbauer and resonance Raman spectroscopy. Three ferritins have been studied using these methods: HuHF,¹⁴⁶ BfMF,¹⁴⁷ and BfHF.¹⁴⁸ Complexity and confusion prevail in the reported data analysis for these ferritins, suggesting to us that the origin and molecular structure of the blue intermediate are not understood. The groups of Theil and Huynh used Mössbauer spectroscopy to study the molecular structure of the blue intermediate in BfMF.¹⁴⁷ Measurements of the Mössbauer spectra when the blue intermediate was at its maximum suggested formation of ca. 70% Fe(III) species, while 30% of Fe(II) remained unoxidized. Chasteen's group reported similar results for HuHF.¹⁴⁶ For BfMF the Mössbauer spectra were originally simulated as a single Fe(III) dimeric species,¹⁴⁷ but in a later study these spectra were simulated as a sum of two Fe(III) dimeric species.¹⁴⁹ A justification for this doubling of simulation parameters was not given. In addition, for HuHF the Fe(III) species were simulated as the sum of two Fe(III) dimeric species without proper justification that should have been obtained by recording variable-temperature, high-applied field Mössbauer spectra.¹⁴⁸ The reported Mössbauer isomer shift (δ) and quadrupole splitting (ΔE_Q) for Fe(III) species in BfMF and HuHF (Table 5) were compared with those of the blue intermediate in dioxygen-activating enzymes such as soluble MMO. On the basis of these comparisons it has been concluded that the blue intermediate in BfMF and HuHF is a Fe(III) dimeric species with a μ -1,2-O₂ bonding mode similar to a blue intermediate in soluble MMO. A similar conclusion was obtained from the results of resonance Raman spectroscopy measurements of the blue intermediate in BfMF.¹⁵⁰ Raman excitation of the blue intermediate species in BfMF at 650 nm was performed to record Fe–O and O–O stretching

Table 5. Comparison of the Spectroscopic Properties of the Fe(III) Species That Are Formed during Ferroxidase Reaction with Those of Blue Intermediate in Dioxygen-Activating Enzymes, and with Different Fe(III)-Peroxo Complexes^a

name	λ_{\max} ($M^{-1}cm^{-1}$)	δ (mms $^{-1}$)	ΔE_Q (mms $^{-1}$)	ν (Fe–O) (cm $^{-1}$)	ν (O–O) (cm $^{-1}$)	Fe–Fe Å	bonding mode	ref
ferritin								
BfMF	650 ^(a)	0.62	1.08	485	851	2.53	?	147,149,150,152
BfMF	650 ^(a)	0.65	1.05					
		0.55	1.06					
HuHF	650	0.58	1.07				?	146
		0.55	1.11					
BfHF	550	0.53	0.69				?	148
		0.50	1.23					
		0.51	1.68					
PfFtn	625							26
EcFtnA	600							138
intermediate P in dioxygen-activating enzymes								
MMO	625 (1500)	0.66	1.51		905		?(^b)	153,154
RNR ^(c)	700 (1500)	0.63	1.58	458	870		μ -1,2-O ₂	155,156
Δ^9 desaturase ^(d)	700 (1100)	0.68	1.9	442	898		μ -1,2-O ₂	157,158
		0.64	1.06					
core structure (Fe ₂ (O ₂))								
1	694 (2650)	0.66	1.4	415	888		μ -1,2-O ₂	159
2	588 (1500)			476	900	3.43	μ -1,2-O ₂	160
3^(e)	500–800 (1700)	0.58	0.74			3.327	μ -1,2-O ₂	161
		0.65	1.7					
4^(f)	500 (1000)	0.65	1.27		822		η^2 -O ₂	162
		0.52	0.71					
core structure (Fe ₂ (O)(O ₂))								
5	648 (1200)	0.54	1.68	462	848	3.14	(μ -O)(μ -1,2-O ₂)	163
6	510 (1300)	0.53	1.67	472	816		(μ -O)(μ -1,2-O ₂)	164
core structure (Fe ₂ (O) ₂)								
7		0.5	1.93			2.7	(μ -O) ₂	165
core structure (Fe(O ₂))								
8	520 (520)	0.65	0.72	459	816		side-on (η^2 -O ₂)	166,167
9	755 (450)	0.63	1.12	470	817		side-on (η^2 -O ₂)	168,169

^a **1**, Fe₂(O₂)(μ -O₂CCH₂Ph)₂-[HB(pz')₂]₂; **2**, Fe₂(O₂)(N-Et-HPTB)OBZ(BF₄)₂; **3**, [Fe₂(O₂)(Ph-bimp)(C₆H₅COO)]²⁺; **4**, Fe₂(O₂)(Py)₂(μ -dxlCO₂)₄; **5**, [Fe₂(O)(O₂)(6-Me₃-TPA)]²⁺; **6**, [Fe₂(O)(O₂)₂(OAc)(L)]²⁺; **7**, [Fe₂(μ -O)₂(6TLA)]₂(COL₄)₂; **8**, (Fe–O₂)(EDTA); **9**, (Fe–O₂)(tpen). (a) The molar extinction coefficient in reference¹⁴⁷ was incorrectly calculated to be 1000 cm $^{-1}$ M $^{-1}$. On the basis of the data in this reference we calculate a molar extinction coefficient of ca. 640 M $^{-1}$ cm $^{-1}$. (b) Several different molecular structures have been proposed for the blue intermediate in soluble methane monooxygenase (sMMO). (c) The Mössbauer parameters are for *E. coli* ribonucleotide reductase RNR-R2-D84E¹⁵⁶ and the resonance Raman data are for *E. coli* RNR-R2-W48D/D84E.¹⁵⁵ (d,e,f) The ratio of the two doublets observed by Mössbauer spectroscopy is 1.

frequencies (Table 5). The resulting Fe–O and O–O stretching frequencies were compared with those of model compounds with Fe₂(O₂) core structure and μ -1,2-O₂ bonding mode. This conclusion is based on the assumption that the molecular structure of the blue intermediate in MMO or other dioxygen-activating enzymes is well established, i.e., a μ -1,2-peroxodifferic species. This assumption appears to be premature because recently several possible molecular structures have been proposed for the blue intermediate in soluble MMO.¹⁵¹ When we compare Mössbauer isomer shifts and quadrupole splittings of the blue intermediate in BfMF and HuHF with those of model compounds (Table 5) we find that the parameters in ferritins are rather close to those reported for η^2 -O₂ bonding in model compounds with an Fe₂(O₂) core structure or side-on (η^2 -O₂) bonding in model compounds with an Fe(O₂) core structure. On the other hand, comparison of the resonance Raman Fe–O and O–O stretching frequencies (Table 5) of the blue intermediate in BfMF with those of model compounds shows that these values are very close to those reported for (μ -O)(μ -1,2-O₂) bonding in model compounds with Fe₂(O)(O₂) core structure. We conclude

that the molecular structure of the blue intermediate in ferritin remains undetermined.

In addition to the results for BfMF and HuHF the groups of Theil and Huynh also reported Mössbauer data for bullfrog H-type ferritin (BfHF).¹⁴⁸ The amino acid sequence of BfHF has more than 80% identity with that of BfMF. Mössbauer spectra of the Fe(II)/Fe(III) species in BfHF were recorded a few milliseconds after aerobic addition of Fe(II) when the blue intermediate formed (Figure 12). The spectrum of Fe(III) species in BfHF (Figure 12) when the blue intermediate in this ferritin was at its maxima¹⁴³ was simulated as the sum of three distinct Fe(III) dimers (Table 5) plus an Fe(III) trimer. However, the resulting fit to the Mössbauer spectrum was not shown (Figure 12), and a justification for simulating the spectra using these Fe(III) species was not given.¹⁴⁸ Contrary to the analysis for HuHF and BfMF in which the dimers were assigned to the blue intermediate, in BfHF the dimers were assigned to Fe(III) final products, i.e., Fe(III) oxodimer, which were formed because of the decay of the blue intermediate. Theil et al. previously proposed that in BfHF the blue intermediate is a Tyr → Fe(III) charge transfer complex.¹⁷⁰

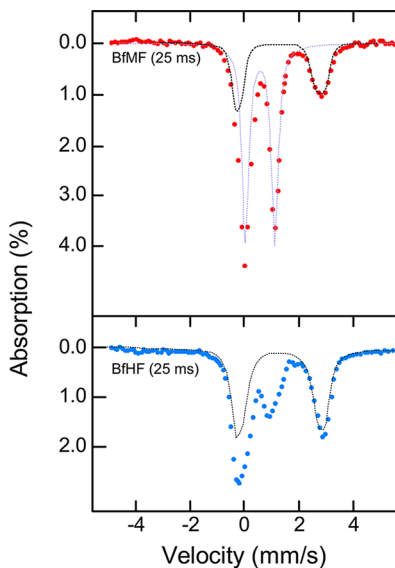


Figure 12. Low-field Mössbauer spectra of the Fe(II)/Fe(III) species in ferritins when the blue intermediate is at its maximum concentration. Comparison of the Mössbauer spectra of the blue intermediate in BfHF and BfMF. Spectra for BfHF are from ref 148, and those for BfMF are from ref 147. The Mössbauer spectrum of both proteins 25 ms after aerobic addition of Fe(II) shows Fe(II) and Fe(III) species. Black dashed lines show simulations of the Fe(II) species. The purple dashed line in the spectrum of BfMF shows the simulation of Fe(III) species. A simulation of Fe(III) species in BfHF was not given in ref 148. In BfHF ca. 55% of Fe(II) remains unreacted, and in BfMF ca. 30% of Fe(II) remains unreacted. This amount of Fe(II) disappears slowly as the blue intermediate decays.

This latter conclusion is inconsistent with a report by the same group in which mutation of the highly conserved tyrosine in the vicinity of the ferroxidase center, i.e., Tyr30 in BfHF, does not abolish formation of the blue intermediate.¹⁴³ Thus, the blue intermediate in BfHF appears to be neither due to formation of an Fe(III) intermediate species nor due to Tyr → Fe(III) charge transfer. By comparing the Mössbauer isomer shift (δ) and quadrupole splitting (ΔE_Q) of the Fe(III) dimeric species in BfHF (Table 5) with those of model compounds we observe that just like BfMF and HuHF (see above) these values are close to those reported for η^2 -O₂ bonding in model compounds with an Fe₂(O₂) core structure or for side-on (η^2 -O₂) bonding mode in model compounds with an Fe(O₂) core structure.

With the interpretational inconsistencies of the data for BfHF, BfMF, and HuHF discussed above we conclude that the nature of the blue intermediate is not known. Whether the blue intermediate represents Tyr → Fe(III) charge transfer or an Fe(III) dimeric species should be investigated. In Figure 13 we discuss possible molecular structures for an Fe(III) dimeric species that may form in the ferroxidase center.

5.2.2. Radical Intermediate. A radical intermediate of unknown origin was observed in HoSF using electron paramagnetic resonance (EPR) spectroscopy.¹⁷¹ More recently, a radical intermediate was also observed during catalysis of Fe(II) oxidation by PfFtn and HuHF.²⁷ In PfFtn this intermediate radical has two peaks in the absorption spectra at 408 and 412 nm, which are the same as those observed for tyrosine radical in α -ketoglutarate dioxygenase (TauD).¹⁷² EPR spectroscopy has confirmed the presence of a radical during catalysis of Fe(II) oxidation both in PfFtn and in HuHF.²⁷ On the basis of the spectroscopic properties of this intermediate

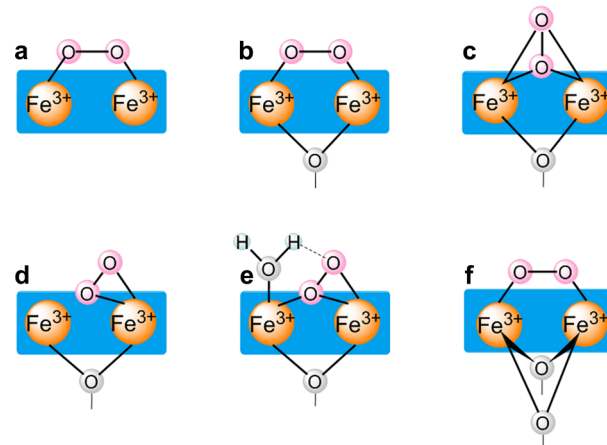


Figure 13. Possible molecular structures of the blue intermediate in ferritin. Comparison of the spectroscopic properties of the diamagnetic Fe(III) intermediate in ferritin with those of different model compounds (Table 5) suggests several different possible molecular structures for the Fe(III) species with blue color. (a) Structure is less likely because of the long Fe–Fe distance that is observed for similar structures with model compounds. Mössbauer and resonance Raman parameters of the blue intermediate in different ferritins can be compared with those of (μ -O)(μ -1,2-O₂) bonding in model compounds with Fe₂(O)(O₂) core structure (b), with those of η^2 -O₂ bonding in model compounds with Fe₂(O₂) core structure (c), or with side-on (η^2 -O₂) bonding mode in the Fe(O₂) core structure (d, e). (e) Structure has been proposed for the intermediate P with blue color in soluble methane monooxygenase. (f) Structure has been suggested for BfMF because of an unusually short Fe–Fe distance of 2.54 Å for the blue intermediate. A short Fe(III)–Fe(III) distance (2.7 Å) has been reported for (μ -O)₂ bonding in a model compound (see Table 5).

and mutagenesis studies it has been suggested that the radical is formed by one-electron oxidation of the conserved tyrosine in the vicinity of site B of the ferroxidase center, i.e., Tyr 24 in PfFtn or Tyr34 in HuHF (Figure 4). Simulation of kinetic progress curves of the blue intermediate (see section 5.2.1) and the tyrosine radical together suggested a common mechanism of Fe(II) oxidation for HuHF and PfFtn. It has been proposed that because of the distribution of Fe(II) among three binding sites,²⁶ when 48 Fe(II) per 24-mer are added, ca. 17% of Fe(II) may oxidize in the C site by the blue intermediate that is formed in the ferroxidase center or by the peroxide that is produced in the ferroxidase site (Figure 11).²⁷ In this reaction the conserved tyrosine has been suggested to provide a fourth electron for complete reduction of molecular oxygen to water and thus prevent formation of ROS. The cationic tyrosine radical then is reduced via reaction with an Fe(II) ion or by a yet to be identified redox partner of ferritin, resulting in substoichiometric concentration of tyrosine radical. Thus, besides the possible role of the highly conserved tyrosine in formation of the blue intermediate (see section 5.2.1), this tyrosine may also act as a molecular single-electron capacitor. In a recent study a similar mechanism for Fe(II) oxidation was suggested for EcFtnA,¹³⁸ but it was also concluded that the conserved tyrosine does not have any role in catalysis of Fe(II) oxidation in the ferroxidase center. However, this conclusion appears to be inconsistent with the reported kinetics of Fe(II) oxidation by the WT and Tyr24Phe mutant EcFtnA measured using UV-vis spectroscopy.¹³⁸ When EcFtnA did not contain Fe(III) the rate of Fe(II) oxidation and formation of Fe(III) by

WT was ca. 2-fold faster than that of the Tyr24Phe mutant, and when EcFtnA contained Fe(III) the rate of catalysis of Fe(II) oxidation and Fe(III) formation by WT was between 4-fold and 26-fold faster than that of Tyr24Phe mutant. Therefore, we conclude that also in EcFtnA similar to PfFtn and HuHF the conserved tyrosine in the vicinity of the ferroxidase center site B is essential for rapid catalysis of Fe(II) oxidation in the ferroxidase center. As proposed for PfFtn and HuHF this tyrosine might be important for formation of the blue intermediate and/or act as a molecular single-electron capacitor.

5.3. What Are the Fe(III) Species That Are Formed Because of Fe(II) Oxidation?

The third aspect of the catalytic oxidation of Fe(II) in the ferroxidase center that has been studied to understand the mechanism of Fe(II) oxidation is the nature of the Fe(III) species that are produced after complete oxidation of Fe(II). These species have been studied using ^{57}Fe Mössbauer spectroscopy. In our view two general conclusions can be drawn from the available data: (i) typically 60–80% of the Fe(II) added per ferroxidase center is oxidized via the blue intermediate in the ferroxidase center to form the Fe(III)–O(H)–Fe(III) product and (ii) the remaining 20–40% of the Fe(II) added per ferroxidase center is presumably oxidized in site C.

Mössbauer spectroscopy has been used to study the Fe(III) products in three eukaryotic ferritins, HuHF,^{146,173} BfMF,¹⁴⁹ and BfHF,¹⁴⁹ and in bacterial ferritin, EcFtnA.^{174,175} In HuHF the Mössbauer spectra of Fe(III) species were recorded at low magnetic field only, i.e., in the milliTesla range. The resulting data were simulated either as the sum of three distinct species,¹⁷³ i.e., Fe(III) monomer, Fe(III) dimers, and Fe(III) cluster ($\geq 3\text{Fe(III)}$), or as the sum of two species,¹⁴⁶ i.e., Fe(III) dimer and Fe(III) cluster. Typically 60–80% of Fe(II) added per ferroxidase center was observed as Fe(III) dimer, and the Mössbauer spectra of the remaining iron could be simulated as Fe(III) monomer and/or cluster. These simulations have limited value because Mössbauer spectra of Fe(III) species in HuHF were not recorded at high applied fields. Mössbauer spectra of different Fe(III) species in ferritin overlap, and to characterize various Fe(III) species it is necessary to record spectra at various temperatures and at high applied fields. For BfMF¹⁴⁹ and BfHF¹⁴⁸ high-field, low-temperature Mössbauer spectra of Fe(III) species that are formed immediately after oxidation of Fe(II) are quite similar (Figure 14). However, these two spectra have been interpreted with different models. In BfMF the spectra were simulated as a sum of four Fe(III) dimers and an Fe(III) cluster.¹⁴⁹ This simulation did not give a good fit to the data (Figure 14); however, simulation of Mössbauer spectra of Fe(III) species in BfHF as a sum of three Fe(III) dimers (Table 6) and a trimer did give a good fit. The Fe(III) dimers in BfMF and BfHF account for 60–80% of the total Fe(II) added (Table 6). Our conclusion is that in all eukaryotic ferritins ca. 60–80% of the Fe(II) is oxidized in the ferroxidase center to form Fe(III) dimer and the remaining 20–40% of Fe(II) oxidized via another mechanism. Studies of Fe(III) products of bacterial or archaeal ferritin ferroxidase reaction have been limited to EcFtnA. In EcFtnA the Mössbauer spectra were simulated using two Fe(III) species (Table 6): 60–70% Fe(III) dimer and 30–40% Fe(III) monomer.^{174,175}

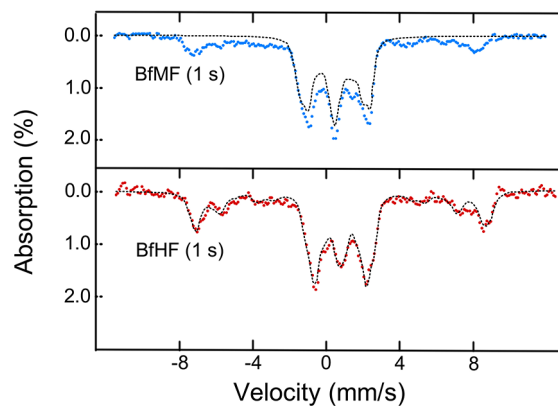


Figure 14. Comparison of high-field Mössbauer spectra of BfHF and BfMF and their simulations. Data for BfHF are from ref 148, and data for BfMF are from ref 149. Spectra were collected at 4.2 K with an applied field of 8 T. Dashed lines show simulations of the spectra. Although the spectra are quite similar, a different model was used to obtain a fit to spectra of BfHF compared to those of BfMF. For BfMF the spectra were simulated as a sum of four dimeric species and the simulation did not provide a proper fit. For BfHF the spectra were simulated as the sum of three dimers and a trimer and a good fit was obtained.

Table 6. Mössbauer Parameters of the Fe(III) Products Formed after Complete Oxidation of Fe(II) by Ferritins^a

ferritin name	time (s)	Fe(III) species	% of the Fe(II) added	δ (mms ⁻¹)	ΔE_Q^0 (mms ⁻¹)	ref
HuHF	600	dimer	60	0.48	1.26	146
		cluster	40	0.48	0.74	
HuHF	60	dimer 1	43	0.50	1.23	173
		dimer 2	25	0.53	1.61	
		monomer	7	0.51		
		clusters	26	0.49	0.75	
BfMF	1	dimer 1	63	0.48	1.95	149
		dimer 2		0.55	1.63	
		dimer 3		0.48	1.17	
		dimer 4		0.52	0.63	
		cluster	32	0.63	1.20	
BfHF	1	dimer 1	26	0.53	0.69	148
		dimer 2	9	0.50	1.23	
		dimer 3	16	0.51	1.68	
		trimer	42	0.51	0.7	
EcFtnA	60	dimer 1	26	0.52	1.56	174
		dimer 2	44	0.49	0.75	
		monomer	30			

^aMössbauer parameters of Fe(III) species obtained from simulation of spectra that were recorded at low applied field. For HuHF Mössbauer spectra were not recorded at high applied field to test if the parameters obtained from the simulation of spectra at low applied field can be used to simulate the spectra recorded at higher applied field.

In conclusion, the Mössbauer data reported for eukaryotic and bacterial ferritin consistently show formation of 60–80% of the Fe(II) added per ferroxidase center as Fe(III) dimer. Because typically 60–80% of the Fe(II) added per ferroxidase center was observed to be oxidized in the ferroxidase center via the blue intermediate,¹⁴⁷ it can be concluded that the Fe(III) dimer is formed in the ferroxidase center. Mössbauer spectra of the remaining 20–40% of Fe(II) added per ferroxidase center disappear slowly. We suggest that this amount of Fe(II) must

have been oxidized in a different way to form Fe(III) species whose Mössbauer spectra can possibly be simulated as different Fe(III) species, e.g., Fe(III) monomer, trimer, or cluster. This analysis of Mössbauer data is consistent with the proposal of a common mechanism for catalysis of Fe(II) oxidation by eukaryotic, archaeal, and bacterial ferritin. On the basis of the mechanism depicted in Figure 11 and explained in previous sections we suggest that 20–40% of Fe(II) is oxidized in site C. Mössbauer spectra of the Fe(III) product of oxidation of Fe(II) in site C may be observed as Fe(III) monomer or Fe(III) trimer if coupled to the Fe(III) dimer in the ferroxidase center or as Fe(III) multimer if the Fe(III) leaves site C to form Fe(III) multimers inside the ferritin cavity. This suggestion requires further investigation, and it would be particularly valuable to test different models for the various Fe(III) species that are formed to justify the simplest model that can be used to simulate the Mössbauer spectra of Fe(III) products. This analysis will possibly give a clear picture of the type of Fe(III) species that are formed.

6. HOW IS THE FE(III) PRODUCT STORED AFTER ITS FORMATION IN THE CATALYTIC SITE?

The mechanism of Fe(II) storage in ferritin and bacterioferritin has been the subject of debate for many years. Recent studies however have provided significant new insight into this step. These data suggest a common mechanism of Fe(III) storage for ferritins of all three Kingdoms of life: after oxidation of Fe(II), the Fe(III) stays metastably in the ferroxidase center until it is pushed to the ferritin cavity by Fe(II).²⁶ This Fe(III)–Fe(II) displacement model is different from the hitherto widely accepted substrate site model which states that after oxidation of Fe(II) the Fe(III) immediately leaves the ferroxidase center, leaving behind an empty site. Therefore, we review previous studies based on which the substrate model was suggested for ferritin and discuss the fact that these data do not support the substrate site model. Moreover, based on the available data for bacterioferritins we propose that the mechanism of Fe(III) storage in bacterioferritins could well be similar to the displacement model of ferritin.

6.1. Mechanism of Fe(III) Storage in Ferritin

For the Fe(III) mineral core to be formed the Fe(III) product of the ferroxidase reaction should somehow leave the ferroxidase center and migrate to the cavity of ferritin where Fe(III) core nucleation can start. Recent studies have provided significant insight in this stage of ferritin functioning. It has been shown that Fe(III) stays metastably in the ferroxidase center until Fe(II) displaces the Fe(III), which is subsequently stored in the internal cavity via a yet unknown pathway. Initial evidence for this model came from studies with PfFtn. After oxidation of Fe(II) in the ferroxidase center of PfFtn and formation of Fe(III), reductive titration monitored by EPR spectroscopy showed formation of a mixed-valence [Fe(II)–Fe(III)] cluster in the ferroxidase center.¹⁷⁶ Because phosphate increases the rate of Fe(II) oxidation, it was tested if in the presence of phosphate the Fe(III) spontaneously leaves the ferroxidase center.⁶³ The presence of phosphate did not affect formation of the mixed-valence [Fe(II)–Fe(III)] cluster.⁶³ Thus, Fe(III) remains in the ferroxidase center even in the presence of phosphate. Subsequently, X-ray crystallography also showed that Fe(III) is present in the ferroxidase center and does not leave this site spontaneously.⁹² The X-ray crystal structure of BfMF⁸⁵ or bacterial ferritins PaFtn⁹⁷ and CtFtn⁹⁶

also provided direct evidence that Fe(III) remains in the ferroxidase center of eukaryotic and bacterial ferritins and does not spontaneously leave this site. With apo-PfFtn it was found that oxidation of Fe(II) is significantly faster than with PfFtn, which contains Fe(III).¹³⁷ Also, the presence of Fe(III) impedes binding of Zn(II) to the ferroxidase center as determined by ITC and fluorescence spectrofluorometry.¹⁷⁷ These initial observations were interpreted to mean either that the Fe(III) in the ferroxidase site acts as a stable cofactor center or alternatively that metastable Fe(III) in the ferroxidase center is only displaceable by Fe(II) and thus that the rate of Fe(II) oxidation decreases in ferritins when Fe(III) is present in the ferroxidase center.¹³⁷ Consistent with the latter suggestion, it has been shown for HuHF and PfFtn that the Fe(III) is displaced from the ferroxidase center by Fe(II).²⁶ This conclusion is based on two different observations: (1) Oxidation of Fe(II) by ferritin fills the ferroxidase centers and Fe(III) decreases the binding affinity of Fe(II) to the ferroxidase center as measured by ITC (Table 7) and (2) ⁵⁷Fe(III) in the ferroxidase center is displaced by natural abundance Fe(II) as measured by Mössbauer spectroscopy.²⁶

Table 7. Thermodynamic Parameters for Anaerobic Fe(II) Binding to Ferritin That Contains Fe(III)^a

parameters	PfFtn + 2Fe(III) per subunit 50 °C pH 7.0	HuHF + 2Fe(III) per subunit at 25 °C pH 7.0
N_1	0.8 ± 0.03	0.9 ± 0.2
K_1	$(5.2 \pm 0.3) \times 10^4$	$(3.2 \pm 0.3) \times 10^4$
ΔH_1	15.3 ± 0.8	6.7 ± 1.1
N_2	0.85 ± 0.05	1.0 ± 0.2
K_2	$(1.1 \pm 0.1) \times 10^3$	840 ± 90
ΔH_2	79.0 ± 5.4	35.9 ± 0.9
ref	²⁶	²⁶

^a N (Fe(II) per subunit) is the stoichiometry of binding, K (M^{-1}) is the association constant, and ΔH (kJ/mol) is the enthalpy of binding. The overall enthalpy of Fe(II) binding to ferritin that has Fe(III) has increased compared to that of Fe(II) binding to apo-ferritin (Table 3).

To understand how Fe(III) is displaced by Fe(II), EPR spectroscopy was used to follow the Fe(III)/Fe(II) species that are formed after titration of Fe(II) to ferritin that contains Fe(III) in the ferroxidase center.²⁶ After addition of Fe(II) a mixed-valence [Fe(II)–Fe(III)] species was formed in the ferroxidase center. The maximum intensity of the mixed-valence species was observed after addition of one Fe(II) per ferroxidase site. When more than one Fe(II) per ferroxidase site was added anaerobically the amount of mixed-valence species decreased. A distribution model (Figure 15) was derived based on different possibilities for binding of Fe(II) to the three sites.²⁶ Data from EPR spectroscopy were then fitted using this model. It was concluded that Fe(II) displaces the Fe(III) in the ferroxidase center sequentially (Figure 16a). An alternative explanation for the observation of a mixed-valence [Fe(III)–Fe(II)] cluster in the ferroxidase center would be displacement of an Fe(III)–O(H)–Fe(III) unit from the ferroxidase center by Fe(II) and subsequent internal electron transfer from the Fe(III)–O(H)–Fe(III) unit to the Fe(II) in the ferroxidase center, producing an equilibrium situation (Figure 16b).¹⁷⁸ This model, however, is less probable since it would have been expected that the amount of mixed-valence Fe(II)–Fe(III) species in the ferroxidase center reaches a maximum after addition of two Fe(II) per ferroxidase center.

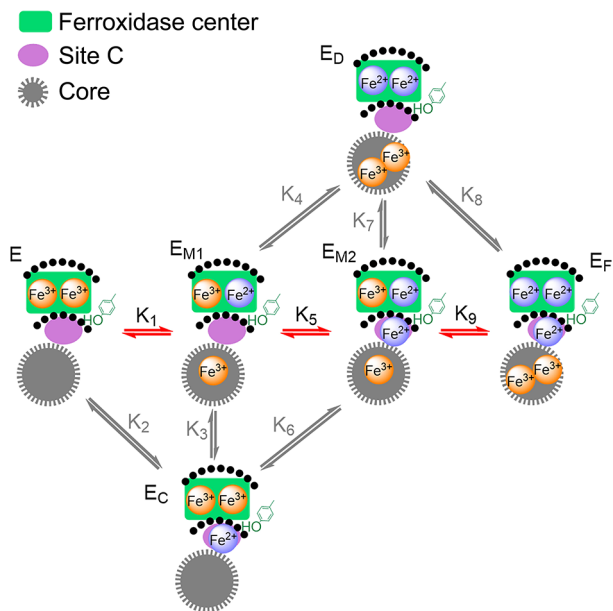


Figure 15. Model describing the distribution of Fe(II) among three binding sites. In this model K_1 , K_2 , K_4 , K_5 , K_6 , K_8 , and K_9 are binding constants and K_3 and K_7 are equilibrium constants. This distribution model was used to fit the data obtained with EPR spectroscopy for monitoring formation of mixed-valence [Fe(II)-Fe(III)] species upon titration of Fe(II) to Fe(III)-loaded HuHf or PffTn. On the basis of the values obtained for the binding constants it was concluded that Fe(II) displaces the Fe(III) sequentially and that the main path of displacement of Fe(III) in the ferroxidase center by Fe(II) consists of K_1 , K_5 , and K_9 (shown by red arrows). In this model K_7 , which is the concentration ratio between the E_D state and the E_{M2} state, was found to be 0.5. Thus, the main species that are formed during displacement of Fe(III) by Fe(II) and distribution of Fe(II) among three binding sites are E_{M1} , E_{M2} , E_F , and E_D . The model does not suggest what the entry path of Fe(II) to ferritin is, it is only a distribution model for Fe(II) binding to three sites, and it is valid independent of what the entry path of Fe(II) ion is. If the Fe(II) entry occurs only via the 3-fold channel the model suggests that site C is a gateway for Fe(II) entry to the ferroxidase center.

The Fe(III)-Fe(II) displacement model described above is in contrast with the earlier substrate site model (Figure 16c). Therefore, we re-evaluate the previous data based on which the substrate site model was proposed. The substrate site model was initially drawn based on an EXAFS study to measure the Fe(III)-Fe(III) distance in the blue intermediate during catalysis of Fe(II) oxidation in the ferroxidase center of BfMF.¹⁵² It was observed that the Fe(III)-Fe(III) distance in the blue intermediate is unusually small (Table 5). From this study it was suggested that as the blue intermediate in BfMF decays hydrogen peroxide is released. The authors went further and proposed that the Fe(III)-O(H)-Fe(III) product of decay of the blue intermediate spontaneously leaves the ferroxidase center and that the empty ferroxidase center then can oxidize more Fe(II) (the substrate site model in Figure 16c).¹⁵² This was rather a far-fetched speculation because EXAFS was only used to measure the intermediate species and not the Fe(III) products. This proposal has subsequently been used as the framework to interpret data obtained by other methods, for example, by MCD¹¹ or NMR spectroscopy.¹⁷⁹ However, a recent X-ray crystal structure of BfMF by Bertini's group showed that after oxidation of Fe(II), the Fe(III) remains in the ferroxidase center and does not leave this site

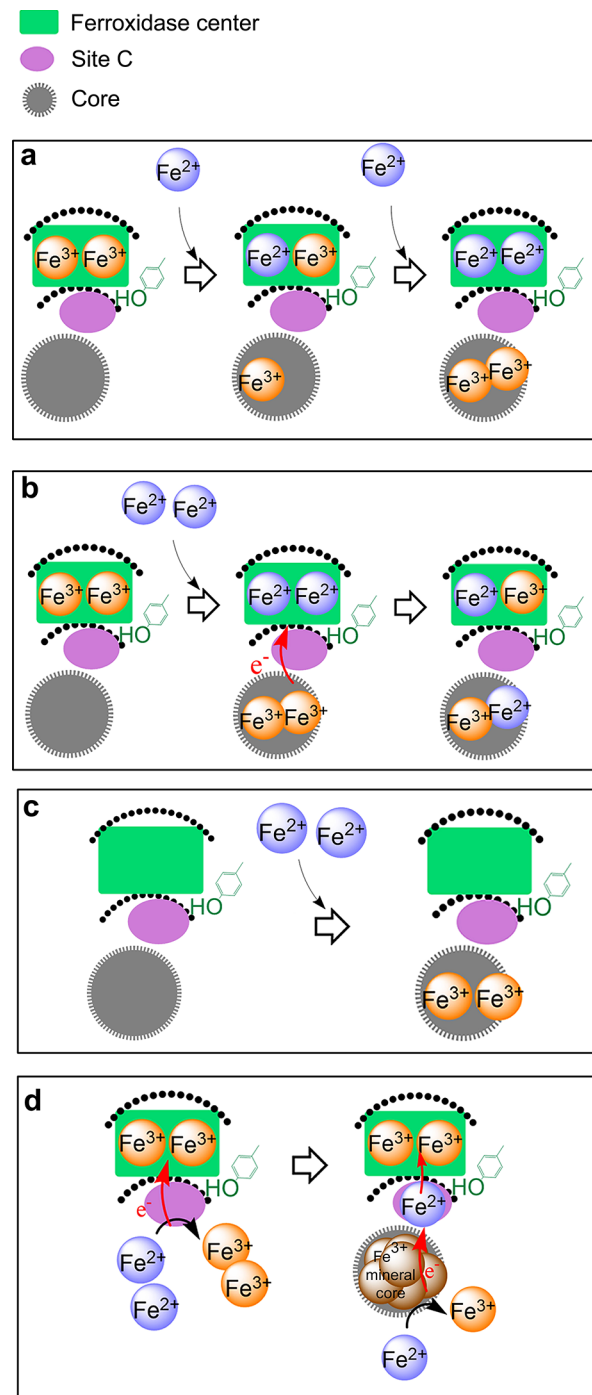


Figure 16. Models for the mechanism of iron storage by ferritin and bacterioferritin. (a, b) Fe(III) displacement model for ferritin. On the basis of this model, after oxidation of Fe(II) in the ferroxidase center the Fe(III) stays metastably in the ferroxidase center. Movement of Fe(III) from the ferroxidase center requires the presence of Fe(II). (a) Fe(II) either sequentially displaces the two Fe(III) in the ferroxidase center or (b) it displaces both Fe(III) simultaneously. (c) Substrate site model for ferritin. On the basis of this model two Fe(II) simultaneously bind to the ferroxidase center and after oxidation Fe(III) spontaneously leave the center to form the Fe(III) mineral core. As a result the ferroxidase center is left empty. There is no direct experimental evidence to support this model, and all data on which this model was proposed are consistent with Fe(III)-Fe(II) displacement model (see text). (d) Complex cofactor site model proposed for EcBFR. In this model the Fe(III) in the ferroxidase center acts as a cofactor. When there is no core present, Fe(II) ions

Figure 16. continued

bind to a third binding site and are oxidized at this site via an electron transfer mechanism to the Fe(III) in the ferroxidase center where molecular oxygen is reduced to hydrogen peroxide. When enough Fe(III)–mineral core is formed, the Fe(II) ions are oxidized on the surface of a core and the electrons are transferred to the Fe(III) in the ferroxidase center via the proposed Fe(II) binding site. Subsequently, molecular oxygen is reduced in the ferroxidase center to water. Experimental data based on which this complex model was proposed can be interpreted in the frame of the simplified Fe(III)–Fe(II) displacement model.

spontaneously.⁸⁵ When two Fe(II) per subunit were added aerobically, the metal–metal distance between the Fe(III) in sites A and B of the ferroxidase center was 3.1 Å. This distance has increased from the distance that was reported for Fe(III)–Fe(III) in the blue intermediate (2.53 Å).¹⁵² Therefore, we now re-evaluate other studies that used the substrate site model for data analysis.

Mössbauer spectroscopy shows that typically 60–80% of the Fe(II) substrate added to apo-ferritin is oxidized with a fast rate in the ferroxidase center. The remaining 20–40% of the Fe(II) substrate disappears with a slow rate (see discussion in section 5.3).^{147,149} Besides the Fe(III)–O(H)–Fe(III) that is formed in the ferroxidase center, 30–40% of the Fe(II) initially added was observed as other Fe(III) species such as monomer, trimer, and cluster. In the frame of the substrate site model these data were interpreted to mean that the Fe(III)–O(H)–Fe(III) unit in the ferroxidase center spontaneously leaves this site, moves toward the nucleation site, and forms the Fe(III) mineral core.¹⁴⁸ As a result the ferroxidase center becomes empty (Figure 16c). As discussed above, because X-ray crystallography shows that Fe(III) remains in the ferroxidase center, we suggest that the Fe(III) species that were assigned to the Fe(III) mineral core resulted from slow oxidation of 20–40% of the Fe(II) substrate in site C as explained in the model of Figure 11 (see section 5.3). From 60% to 80% of the Fe(II) is oxidized in the ferroxidase center to form the Fe(III) dimer. The amount of Fe(III) dimer does not change significantly over time, and thus, the Fe(III) dimer stays in the ferroxidase center.

NMR spectroscopy was used in an attempt to measure the movement of Fe(III) product of the ferroxidase reaction of BfMF.¹⁷⁹ After oxidation of Fe(II) in the ferroxidase center paramagnetic broadening of ¹³C resonances from amino acid side chains due to the close proximity to Fe(III) species (less than 5 Å) was interpreted as reflecting spontaneous movement of Fe(III)–O(H)–Fe(III) product from the ferroxidase center into a possible channel. As more Fe(III) dimers would move into the channel they would cluster together into tetramers until they arrive as octamer at the channel exit near the 4-fold symmetry axis ca. 20 Å away from the ferroxidase center. This detailed mechanistic description is in our view untenable for the following reasons. (i) As mentioned above, X-ray crystal structure analysis of BfMF⁸⁵ after oxidation of two Fe(II) per ferroxidase center shows that the Fe(III)–O(H)–Fe(III) unit remains in the ferroxidase center and that Fe(III) does not coordinate to His54 and Tyr30 in the proposed nucleation channel in contrast to what was deduced from NMR spectroscopy.¹⁷⁹ (ii) The ¹³C–¹³C NMR cross peaks of Ile144 but not Ile141 were broadened. In the 2.8 Å crystal structure of Mg(II)-loaded BfMF the distance of Ile141 to the Mg(II) in the ferroxidase center site B is shorter than that of

Ile144 to the Mg(II). Therefore, NMR data were interpreted to indicate that Fe(III)–O(H)–Fe(III) spontaneously leaves the ferroxidase center and moves toward Ile144 away from the ferroxidase center in a putative nucleation channel. However, two later, higher resolution X-ray crystal structures of BfMF solved in the presence of Fe(III) and Co(II) (Table 2) showed that Ile144 and not Ile141 is closer to Fe(III) or Co(II) in the ferroxidase center site B, which would be consistent with the Fe(III)–O(H)–Fe(III) unit not leaving the ferroxidase site at all.⁸⁵ (iii) The final nuclearity of 8Fe(III) was deduced from bulk magnetic susceptibility measurements at ambient temperature. Such determinations are rarely done on biological systems because purification of proteins generally leads to some contamination of iron typically in the form of mononuclear high-spin Fe(III) (detectable as the *g* = 4.3 “dirty iron” signal in EPR) with strong paramagnetism that even in small quantities may swamp the susceptibility of antiferromagnetically coupled irons in clusters. The apo-BfMF that was used for NMR study was prepared in such a way that the protein contained up to 8Fe(III) per molecule.¹⁴³ This amount of Fe(III) could significantly interfere with the magnetic susceptibility measurements. Furthermore, results from the NMR shift method are particularly difficult to interpret because they only afford data at ambient temperature and therefore provide no information on the spin ladder of a cluster. It was reported¹⁷⁹ that the susceptibility of 8Fe(III)/subunit ferritin preparation is comparable to the room-temperature value of a group of synthetic 8Fe(III) clusters.¹⁸⁰ Why the two values should be similar is not a priori obvious; the model compounds consist of an inner Fe₄O₄ with four additional Fe linked to the μ -O bridges forming an Fe₈(μ^4 -O)₄ structure with very weak antiferromagnetic coupling within the cube (*J* ≈ -2 cm⁻¹) and very strong coupling between the cube and the external Fe's (*J* ≈ -50 cm⁻¹).¹⁸⁰ If this would be a model for ferritin then the susceptibility as a function of Fe loading would have to show a steep step function between 4 and 8 Fe added per subunit. On the contrary, a smooth increase of susceptibility between 0 and 20 Fe added per subunit was found. The present reviewers suggest the following alternative interpretation of the susceptibility data: addition of Fe beyond 2 Fe per subunit directly leads to ferrihydrite-like superparamagnetic core formation without defined intermediate coordination complexes within the protein shell. This would be consistent with a smoothly increasing total susceptibility and a smoothly decreasing susceptibility per Fe atom. It would also be consistent with the crystallographic study of BfMF preloaded with 2 Fe in each ferroxidase center and—after crystallization—loaded with another 45 Fe per subunit in which the second loading of 1080 Fe in total did not lead to a single identifiable Fe(III) coordination site in the putative nucleation channel.⁸⁵ It would furthermore obviate the need to model the two ferroxidase irons as a magnetically integral part of a 4 or an 8 Fe cluster in 4–8 Fe/subunit loaded ferritin, where indeed no spectroscopic evidence to support such a model has ever been reported.

Thus, as we discussed previously²⁶ the NMR data should be reinterpreted as to strongly suggest that Fe(III)–O(H)–Fe(III) remains metastably in the ferroxidase center and does not enter a putative nucleation channel under the conditions used. This reinterpretation with our data regarding displacement of Fe(III) by Fe(II) in the ferroxidase center of HuHF and PfFtn²⁶ was used by Turano et al. to reinterpret their NMR data to mean that Fe(III) stays stable in the ferroxidase center

of BfMF and that the displacement model is valid for this ferritin.¹⁸¹ In the X-ray crystal structure of BfMF solved in the presence of large amounts of Fe(III)⁸⁵ no Fe(III) was observed in the proposed nucleation channel; therefore, further investigation is required to determine the validity of the proposal of a nucleation channel based on NMR spectroscopy.

It should be noted that the NMR experiments were performed with homopolymeric BfMF which was obtained via heterologous expression and not with hetropolymeric naturally occurring bullfrog ferritin.¹⁷⁹ In eukaryotic ferritin it appears that the presence of the L subunit is required for storage of Fe(III) and proper core formation.¹⁸² Mutation of the L chain abolishes Fe(III) mineralization in humans¹⁸³ and causes neuroferritinopathy.¹⁸⁴ These data suggest that the L subunit may have a specific role in Fe(III) mineralization. The exact role of the L subunit is not known. The L subunit can only oxidize Fe(II) at a rate that is slightly above the background oxidation. However, the L subunit appears to induce Fe(III) core nucleation more efficiently than the H subunit;¹⁸⁵ therefore, the L subunit in eukaryotes may have emerged to provide a means to control the overall capacity of iron storage. Because the number of L and H subunits in heteropolymeric eukaryotic ferritin varies over different tissues,¹³ the presence of the L subunit in eukaryotes appears to control the tissue-dependent specific need for Fe(III) storage or Fe(II) oxidation capacities. After displacement of Fe(III) from the ferroxidase center by Fe(II) the L subunit might be important for nucleation of Fe(III) mineral core via a yet to be identified mechanism.

As discussed in section 3.1, the ferroxidase center sites A and B in PmFtn were found unoccupied or partially occupied with Fe(III)^{87,131} (Table 2) because X-ray structures were prepared at a low pH value which is known to disrupt binding of Fe(II) to the ferroxidase center and its subsequent oxidation. Thus, the observation that in PmFtn some ferroxidase centers were occupied with Fe(III) and some sites were empty is a consequence of the crystallographic conditions and does not reflect a complex iron-storage mechanism as suggested by the authors.¹³¹ On the other hand, the displacement model proposed for PfFtn and HuHF would be consistent with the measurement of Fe(II) oxidation by PmFtn at neutral pH values. In apo-PmFtn oxidation of Fe(II) is faster than in PmFtn, which contains Fe(III),¹³¹ suggesting that in the presence of Fe(III) the Fe(II) first should displace the Fe(III) from the ferroxidase center and only then it can be oxidized.

In summary, all of the present experimental data for several ferritins are consistent with the displacement model:²⁶ after oxidation of Fe(II) in the ferroxidase center the Fe(III) remains in this site. The Fe(III) in the ferroxidase center is displaced by Fe(II), and Fe(III) moves to the internal cavity where it starts to accumulate and form the ferrihydrite-like mineral core. The path of Fe(III) after its displacement from the ferroxidase center to the core is not known, and there is no defined bucket brigade. This path in eukaryotic ferritin may be different than bacterial or archaeal ferritins due to the presence of the L subunit in eukaryotic ferritins.

6.2. Mechanism of Fe(III) Storage in Bacterioferritin

Studies regarding the mechanism of iron storage by bacterioferritins are limited compared to those of ferritin, and details of the mechanism have only been worked out in a few cases. Furthermore, a debate is ongoing on how different bacterioferritins store Fe(III). For three bacterioferritins,

namely, *P. aeruginosa* bacterioferritin (PaBFR),¹⁰⁰ *A. vinelandii* bacterioferritin (AvBFR),⁹⁹ and *D. desulfuricans* bacterioferritin (DdBFR),¹⁰² a common mechanism has been suggested, but in *E. coli* bacterioferritin (EcBFR) a different mechanism has been proposed.²⁵ For PaBFR, AvBFR, and DdBFR it has been proposed that Fe(II) may reach the ferroxidase center through a ferroxidase channel. Because of the conformational changes observed in one of the histidines in the coordinating environment of the ferroxidase center it is proposed that the ferroxidase center acts as a gateway from where the Fe(III) product of oxidation of Fe(II) somehow enters the protein cavity. Details of this mechanism remain to be explored. It is possible that in these bacterioferritins the presence of Fe(II) displaces the Fe(III) from the ferroxidase center (Figure 16a and 16b). This suggestion requires further experimental evidence.

For EcBFR a different model has been proposed, namely, that the ferroxidase center is a cofactor site (Figure 16d):^{25,98} Two Fe(III) in this center catalyze oxidation of Fe(II) that is present in the internal cavity of protein. Unlike in the model proposed for PaBFR, AvBFR, and DdBFR, in the cofactor site model proposed for EcBFR the Fe(II) does not enter via the ferroxidase center channel and the ferroxidase center does not act as a gateway. We suggest that the experimental data for EcBFR can be reinterpreted in the frame of the Fe(III)–Fe(II) displacement model proposed for ferritins. First, similar to ferritins, in EcBFR oxidation of Fe(II) by apoprotein is faster than oxidation of Fe(II) by protein that contains Fe(III).¹⁴⁰ This observation has been interpreted to mean that Fe(III) stays stably in the ferroxidase center and can act as a cofactor site. Alternatively, we interpret these data to mean that when the ferroxidase center is empty Fe(II) can bind immediately to this site and be oxidized, while when Fe(III) is present in the ferroxidase center the Fe(II) first should displace the Fe(III) and only then Fe(II) can be oxidized. Thus, the rate of Fe(II) oxidation decreases when Fe(III) is present in the ferroxidase center. Second, fluorescence spectrophotometry¹⁸⁶ and X-ray crystallography⁹⁸ show that in EcBFR Fe(III) stays in the ferroxidase center and does not leave this site spontaneously; these results have been interpreted to further support the cofactor site model in EcBFR. In PfFtn and HuHF experiments to test whether Fe(III) remains permanently in the ferroxidase center showed that it is metastable and displaced by Fe(II).²⁶ Analogous to PfFtn and HuHF we suggest that Fe(III) in the ferroxidase center of EcBFR can also be displaced by Fe(II). Finally, in the X-ray crystal structure of EcBFR a third Fe(II) binding site with partial occupancy (40%) has been observed in the vicinity of the ferroxidase center. Mutation of the coordinating residues of the third site affects oxidation of Fe(II) in the ferroxidase center. On the basis of these data and the assumption that Fe(III) remains permanently stable in the ferroxidase center a complicated model has been proposed for EcBFR.^{25,98} Site C is supposedly involved in oxidation of Fe(II) directly or an Fe(II) in this site facilitates transfer of electrons from the Fe(II) that is oxidizing on the surface of Fe(III) mineral core (Figure 16d).^{25,98} Unlike this complicated picture (Figure 16d) by comparison of the coordinating residues of the ferroxidase center in ferritin and bacterioferritin we suggest that site C in EcBFR is identical to site C in ferritins, and it might well have similar functions as discussed in section 4.2. In conclusion, we propose to substitute the complex model previously proposed for EcBFR (Figure 16d) by the simple Fe(III)–Fe(II) displacement model (Figure 16a and 16b).

7. HOW IS IRON RECOVERED FROM FERRITIN?

The mechanism of Fe(III) recovery from ferritin is poorly understood. On the basis of the present data, at least three distinct mechanisms can be suggested for Fe(III) release from ferritin:¹⁸⁷ (i) Fe(III) bound to the ferroxidase center is scavenged by Fe(III) chelating agents, (ii) Fe(III) in the ferroxidase center or in the mineral core is first reduced to Fe(II) and only then is scavenged by chelating agents, or (iii) partial or complete degradation of ferritin results in direct release of Fe(III). Only the second mechanism has been considered for bacterioferritins, and the heme group, which is absent in ferritin, appears to be essential for reduction of Fe(III). In this section we discuss evidence in support of each hypothesis.

7.1. Iron release in Ferritin

7.1.1. Spontaneous Dissolution of Fe(III). Fe(III) present in the ferroxidase center or stored as mineral core can be scavenged by Fe(III) binding proteins such as transferrin. The rate of Fe(III) uptake by transferrin from the ferroxidase center is in the range of minutes, but the rate of Fe(III) uptake from the mineral core is in the range of days. Spontaneous dissolution of the Fe(III) mineral core of ferritin has been measured using dialysis of HoSF (HoSF consists of 2–4 H subunits and 20–22 L subunits) containing 2000 Fe(III) per 24-meric protein against apotransferrin.¹⁸⁸ The holoferritin was prescrubbed from nonbound iron, and dialysis experiments were performed in the dark to prevent possible photoreduction. Steady formation of Fe(III)–transferrin was observed with a slow rate, suggesting that Fe(III) may be spontaneously released from ferritin. After 4 days only ca. 10% of the Fe(III) present initially in HoSF was scavenged by transferrin. In contrast, transferrin is able to scavenge the Fe(III) from the ferroxidase center with a much higher rate than the rate of scavenging the Fe(III) from the core.²⁶ Transferrin could completely scavenge the Fe(III) from the ferroxidase center within 20 min. This observation was obtained after addition of transferrin to Fe(III)-loaded ferritin. Fe(III)-loaded ferritin was prepared by addition of at least two Fe(II) per ferroxidase center and incubated at room temperature for at least 10–20 min. The experiment was done with different ferritins: apo-HuHF (only H subunit), apo-HoSF, apo-PfFtn (wild type), or apo-PfFtn mutant disabled in ferroxidase activity. Addition of apo-transferrin to Fe(III)-loaded ferritin resulted in formation of Fe(III)–transferrin complex (maximum absorbance at 470 nm).²⁶ It was observed that the initial rate of Fe(III)–transferrin complex formation is 5–6-fold higher in HuHF or WT-PfFtn, which only consist of catalytically active subunits compared, respectively, with HoSF which has 2–4 H subunits or with PfFtn mutants which did not have an active ferroxidase center. Whether scavenging the Fe(III) directly from the ferroxidase center by transferrin is a physiologically relevant mechanism requires further investigation. In humans this mechanism may play a role in scavenging the Fe(III) from the serum ferritin that appears to be released mainly from damaged cells.¹⁸⁹

7.1.2. Reduction of Fe(III) and Release of Fe(II). Iron can be released from ferritin in vitro after chemical reduction followed by complexation with a chelating agent for Fe(II) such as bipyridyl.^{190,191} Many different reducing agents have been found to be effective, e.g., relatively small molecules such as dithionite, thiols, dihydroflavin, ascorbate, and methyl viologen¹⁹² or large molecules such as flavoproteins.¹⁹³ A study of

Fe(II) release by bulk reduction of the Fe(III) mineral core using dithionite and a series of redox mediators showed that at least in the case of PfFtn the highest reduction potential for iron release activity is −47 mV vs the standard hydrogen electrode.¹⁹⁴ On the basis of this finding a role of the ferroxidase center (E_m [Fe(III)–Fe(III)/Fe(III)–Fe(II)] = +210 mV and E_m [Fe(III)–Fe(II)/Fe(II)–Fe(II)] = +50 mV) in the mechanism of iron release was proposed: the metastable Fe(III) in the ferroxidase center acts as mediator to pass the electrons from an external reducing agent to the Fe(III) in the mineral core. Dihydroflavins¹⁹⁵ or flavoproteins¹⁹³ are the only biologically relevant reductants that have been found to mediate reduction of Fe(III) and complete iron release at a physiologically relevant rate (within few minutes). Localized unfolding around 3-fold channels of BfMF achieved under in vitro conditions in the presence of mild denaturing conditions (1–10 mM urea or 0.1 mM guanidine)¹⁹⁶ or mutation of 3-fold channel amino acid residues was found to increase the rate of the dissolution of the mineral after addition of a reducing agent.¹⁹⁷ All of these studies have been performed in vitro and in most cases using nonphysiological reducing agents or chelators. Whether reduction of Fe(III) mineral core is a physiologically relevant mechanism and whether localized unfolding at 3-fold channels is required for reduction of Fe(III) mineral core in vivo remains to be investigated.

7.1.3. Release of Fe(III) Because of Ferritin Degradation. Fe(III) release due to degradation of ferritin is the only mechanism that has been claimed from in vivo studies. In eukaryotes degradation of ferritin occurs in the lysosome where Fe(III) is released.¹⁹⁸ When cultured rat hepatoma cells were treated with an Fe(III) chelating agent to remove the free Fe(II)/Fe(III), the rate of ferritin degradation and Fe(III) release increased, while treatment of the cells with ferric ammonium citrate prevented ferritin degradation and release of Fe(III). The results suggest that Fe(III) release from ferritin is dependent on the rate of ferritin turnover.¹⁹⁹ Inhibitors of lysosome function and lysosomal protease activity decreased the Fe(III) release from ferritin.¹⁹⁹ Degradation of ferritin by the proteasome has also been observed in the cytosol; however, in that case release of Fe(III) from ferritin occurs before degradation of ferritin and is induced by expression of the iron-export protein ferroportin.²⁰⁰ Whether Fe(III) release by protein degradation is relevant for bacterial or archaeal ferritins has not been investigated.

7.2. Iron Release in Bacterioferritin

Among the three mechanisms outlined above for ferritins only one has been considered for bacterioferritins: the Fe(III) mineral core is reduced, and subsequently Fe(II) is released. It has been proposed that the heme group in bacterioferritin is essential for reduction of the Fe(III) mineral core via an electron transfer mechanism. The reduction rate of the Fe(III) mineral core of WT-EcBFR with a heme content of 1 heme/24-mer is ca. 2-fold higher than reduction of the Fe(III) mineral core of heme-free EcBFR (a mutant of EcBFR which is deficient in heme binding).²⁰¹ Upstream of the heme-containing bacterioferritin gene there is a gene which encodes bacterioferritin-associated ferredoxin (Bfd).²⁰² Bfd has a [2Fe-2S] cluster with a midpoint potential of −254 mV, and this cluster was suggested to be able to reduce the Fe(III) mineral core in bacterioferritin via the heme group.²⁰² A recent X-ray crystallography study using *Pseudomonas aeruginosa* bacterioferritin (PaBFR) showed that PaBfd associates with the

bacterioferritin surface at the 2-fold symmetry axis on the top of the heme group (Figure 17).²⁰³ As a result, the edge-to-edge

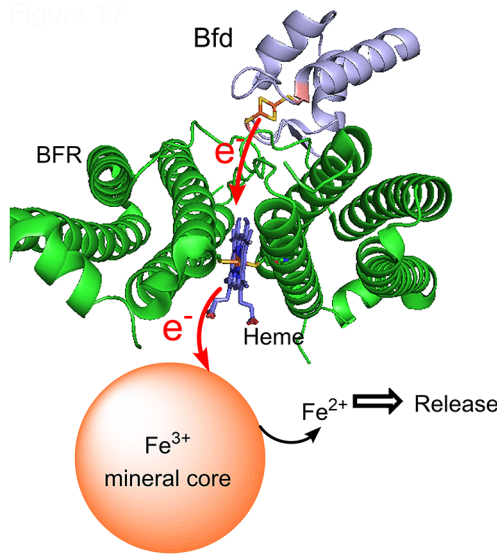


Figure 17. Mechanism of Fe(III) release from bacterioferritin. Bacterioferritin-associated ferredoxin (Bfd) binds at the 2-fold symmetry axis. The [2Fe-2S] cluster of Bfd facilitates reduction of the Fe(III) mineral core via an electron transfer mechanism that involves the heme group of bacterioferritin. Produced Fe(II) is released. This figure was prepared using the crystal structure of PaBfd associated with PaBFR (PDB 4E6K).

distance between the [2Fe-2S] cluster in PaBfd and the heme group in PaBFR is ca. 18 Å, suggesting long distance electron transfer²⁰⁴ (Figure 17). Indeed, biochemical studies showed that PaBfd binds to the PaBFR and facilitates electron transfer to the heme group in PaBfd²⁰⁵ and as a result increases the rate of reduction of Fe(III) mineral core to Fe(II) which is subsequently released.²⁰³

8. CONCLUDING REMARKS AND PERSPECTIVES

It was the Dutch microbiologist Albert Jan Kluyver who first introduced the concept of unity in biochemistry in 1926²⁰⁶ which he summarized in the statement “from elephant to butyric acid bacterium—it is all the same”.²⁰⁷ We take the liberty to paraphrase Kluyver’s statement with reference to the biochemistry of (bacterio)ferritin: “what is true for iron-storage mechanism of *P. furiosus* ferritin (PfFtn) is also true for that of human H-chain ferritin (HuHF) (and for that matter for any catalytically active ferritin on this planet be it eukaryotic, bacterial, or archaeal). This concept suggests that although in the course of evolution the amino acid sequence of (bacterio)ferritins has changed or modifications have emerged to satisfy a special need of an organism, the basic principles of Fe(II) oxidation and storage mechanism in (bacterio)ferritin have remained the same: self-assembly of 24-meric ferritin and bacterioferritin starts with a dimeric species and in eukaryotic ferritin the presence of L subunit does not change the mechanism of self-assembly. Self-assembly of dimers results in a 4-3-2 symmetry structure and formation of channels that appear to connect the outside environment to the (bacterio)ferritin internal cavity. The present data suggests that the exact pathway of Fe(II) entry to ferritin and bacterioferritin remains to be determined and that the same potential pathways for Fe(II) entry such as the ferroxidase channel or B pores are

present in ferritin and bacterioferritin. It is also possible that Fe(II) entry into (bacterio)ferritin occurs via different pathways simultaneously. After entry into the protein cavity or shell, Fe(II) reaches the catalytic site, the ferroxidase center, which is highly conserved among (bacterio)ferritins with three Fe(II) binding sites, two Fe(II) binding sites in the middle of the four α -helical bundle of each subunit where Fe(II) is oxidized to Fe(III) by molecular oxygen and a third site in the vicinity of the ferroxidase center whose presence is required for fast catalysis of Fe(II) oxidation in the ferroxidase center of all ferritins tested. The third site appears to act as a gateway for the ferroxidase center as an Fe(II) entry or possibly Fe(III) exit path. In ferritins of all three Kingdoms of life a blue intermediate is observed during catalysis of Fe(II) oxidation in the ferroxidase center, and in heteropolymeric ferritin of eukaryotes the amount of blue intermediate is dependent on the amount of H subunit, i.e., the presence of the L subunit does not affect formation of the blue intermediate in the H subunit. A highly conserved tyrosine in the vicinity of the ferroxidase is important for fast catalysis of Fe(II) oxidation via this blue intermediate. This tyrosine appears to be able to also act as a single-electron molecular capacitor to prevent formation of ROS if an Fe(II) in the third site, i.e., site C, reacts with the blue intermediate or with the hydrogen peroxide that is produced by oxidation of Fe(II) in the ferroxidase center. Thus, a general role of site C in catalysis of Fe(II) oxidation might be to increase the capacity of oxidation of Fe(II) by ferritin in case large amounts of Fe(II), e.g., more than two Fe(II) per ferroxidase center, are needed to be oxidized. In (bacterio)ferritin the Fe(III) product of the ferroxidase reaction stays metastably in the ferroxidase center and is only displaced from this site by Fe(II). How Fe(III) after its displacement is transferred to the interior and stored there remains unknown. Little is known about how Fe(III) inside ferritin is released, while the mechanism of Fe(III) release in bacterioferritin appears to be dependent on the heme group which is not present in ferritin.

Several key questions still remain to be answered. (1) How is Fe(II) delivered to ferritin or bacterioferritin *in vivo*? (2) Does the heme group in bacterioferritin have any role in oxidation of Fe(II)? (3) What is the role of site C in the mechanism of functioning of ferritin or bacterioferritin? (4) What is the pathway of Fe(II) to the ferroxidase center in (bacterio)ferritin? (5) What is the molecular structure of the blue intermediate that is formed in the ferroxidase center? (6) Does molecular oxygen reach the ferroxidase center via a specific channel or via more or less random diffusion? (7) What is the path of Fe(III) from the ferroxidase center to the internal cavity? (8) Is there a nucleation site from which the Fe(III) mineral core starts to grow? (9) What is the exact role of the L subunit in iron storage by eukaryotic ferritin? (10) What is the physiological mechanism of Fe(III) release from ferritin? Finally, (11) what happens to the iron *in vivo* directly after it is released from ferritin or bacterioferritin? Studies to answer each of these questions can contribute significantly to our understanding of cellular iron homeostasis and will help us to understand how these amazing proteins work in detail. This knowledge can be applied to develop treatments for iron metabolism disorders or new industrial applications such as to convert the catalytic center of ferritin to a cofactor center that can activate dioxygen for performing biocatalytic reactions such as oxidation of alkanes to their corresponding alcohols.

AUTHOR INFORMATION**Corresponding Authors**

*Phone: 0031(0)152782347. E-mail: k.h.ebrahimi@tudelft.nl.

*Phone: 0031(0)152785051. E-mail: w.r.hagen@tudelft.nl.

Notes

The authors declare no competing financial interest.

Biographies

Kourosh Honarmand Ebrahimi (1979 Kerman, Iran) earned his undergraduate degree in Chemical Engineering in 2002, and then he worked for 5 years in the petrochemical industry in Iran. In 2007 he found the opportunity to pursue his dreams and started his M.Sc. studies in Biochemical Engineering at Delft University of Technology. He obtained his M.Sc. degree with cum laude under the supervision of Professor W. R. Hagen with whom he continued his Ph.D. work to study the iron-storage mechanism of ferritin. In 2013 he received his doctorate degree with cum laude, and subsequently, he worked in the Infectious Disease Department of the Scripps Research Institute (Florida, USA) with Professor M. Farzan on the glycobiology of HIV-1 envelope glycoprotein. In 2014 he decided to return to TU Delft to work as a researcher with Professor W. R. Hagen. His current research interests include metalloproteins, biocatalysis, and development of label-free methods for studying enzyme kinetics.



Peter-Leon Hagedoorn studied molecular sciences at the Wageningen University. He completed his Ph.D. work on metalloproteins containing iron and tungsten in 2002 with W. R. Hagen at the Delft University of Technology. He then worked as a research scientist at the University of Leiden with H. Y. Steensma and at the Delft University of Technology with W. R. Hagen. In 2007 he became an assistant professor in biocatalysis at the Delft University of Technology. His research is focused on metalloproteomics, directed

evolution of (metallo)enzymes, and calorimetry of enzyme-catalyzed reactions.



Wilfred (Fred) R. Hagen studied chemistry at the University of Amsterdam, where he also completed his Ph.D. work on EPR of metalloproteins in 1982 with S. P. J. Albracht and E. C. Slater. He then worked as a research scientist in the Biophysics Research Division of The University of Michigan in Ann Arbor, MI, with W. R. Dunham and R. H. Sands. In 1984 he returned to The Netherlands to join the Biochemistry Department of C. Veeger at Wageningen University and to set up a group on metalloproteins. In 1995 he was appointed to Chair of Physical Chemistry at the University of Nijmegen, where he headed the high-frequency EPR spectroscopy group. In 1998 he was also appointed Professor of Bioinorganic Chemistry in Wageningen. In 2000 he moved to Delft University of Technology to take the Chair of Enzymology in the Department of Biotechnology. His research is focused on the roles of metal ions in biocatalysis and methodological development in EPR spectroscopy.

REFERENCES

- (1) Boukhalfa, H.; Crumbliss, A. L. *Biometals* **2002**, *15*, 325.
- (2) Andrews, S. C.; Robinson, A. K.; Rodríguez-Quiñones, F. *FEMS Microbiol. Rev.* **2003**, *27*, 215.
- (3) Aisen, P.; Enns, C.; Wessling-Resnick, M. *Int. J. Biochem. Cell Biol.* **2001**, *33*, 940.
- (4) Edison, E. S.; Bajel, A.; Chandy, M. *Eur. J. Haematol.* **2008**, *81*, 411.
- (5) Andrews, S. C. *Biochim. Biophys. Acta* **2010**, *1800*, 691.
- (6) Honarmand Ebrahimi, K.; Hagedoorn, P.-L.; van der Weel, L.; Verhaert, P. D.; Hagen, W. R. *J. Biol. Inorg. Chem.* **2012**, *17*, 975.
- (7) Carrondo, M. A. *EMBO J.* **2003**, *22*, 1959.
- (8) Haikarainen, T.; Papageorgiou, A. *Cell. Mol. Life Sci.* **2010**, *67*, 341.
- (9) Calhoun, L. N.; Kwon, Y. M. *J. Appl. Microb.* **2011**, *110*, 375.
- (10) Wiedenheft, B.; Mosolf, J.; Willits, D.; Yeager, M.; Dryden, K. A.; Young, M.; Douglas, T. *Proc. Natl. Acad. Sci. U.S.A.* **2005**, *102*, 10551.
- (11) Grant, R.; Filman, D.; Finkel, S.; Kolter, R.; Hogle, J. *Nat. Struct. Mol. Biol.* **1998**, *5*, 294.
- (12) Dickey, L. F.; Sreedharan, S.; Theil, E. C.; Didsbury, J. R.; Wang, Y. H.; Kaufman, R. E. *J. Biol. Chem.* **1987**, *262*, 7901.
- (13) Arosio, P.; Adelman, T. G.; Drysdale, J. W. *J. Biol. Chem.* **1978**, *253*, 4451.
- (14) Harrison, P. M.; Arosio, P. *Biochim. Biophys. Acta* **1996**, *1275*, 161.
- (15) Ferreira, C.; Buccini, D.; Martin, M.-E.; Levi, S.; Arosio, P.; Grandchamp, B.; Beaumont, C. *J. Biol. Chem.* **2000**, *275*, 3021.
- (16) Curtis, A. R.; Fey, C.; Morris, C. M.; Bindoff, L. A.; Ince, P. G.; Chinnery, P. F.; Coulthard, A.; Jackson, M. J.; Jackson, A. P.; McHale, D. P. *Nat. Genet.* **2001**, *28*, 350.

- (17) Jellinger, K.; Paulus, W.; Grundke-Iqbali, I.; Riederer, P.; Youdim, M. *J. Neural Transm.* **1990**, *2*, 327.
- (18) Drakesmith, H.; Chen, N.; Ledermann, H.; Scream, G.; Townsend, A.; Xu, X.-N. *Proc. Natl. Acad. Sci. U.S.A.* **2005**, *102*, 11017.
- (19) Watt, R. K. *Biometals* **2011**, *24*, 489.
- (20) Recalcati, S.; Invernizzi, P.; Arosio, P.; Cairo, G. *J. Autoimmun.* **2008**, *30*, 84.
- (21) Bu, W.; Liu, R.; Cheung-Lau, J. C.; Dmochowski, I. J.; Loll, P. J.; Eckenhoff, R. G. *FASEB J.* **2012**, *26*, 2394.
- (22) Le Brun, N. E.; Crow, A.; Murphy, M. E. P.; Mauk, A. G.; Moore, G. R. *Biochim. Biophys. Acta* **2010**, *1800*, 732.
- (23) Bou-Abdallah, F. *Biochim. Biophys. Acta* **2010**, *1800*, 719.
- (24) Theil, E. C.; Behera, R. K.; Toshia, T. *Coord. Chem. Rev.* **2013**, *257*, 579.
- (25) Bradley, J. M.; Moore, G. R.; Le Brun, N. E. *J. Biol. Inorg. Chem.* **2014**, *19*, 775.
- (26) Honarmand Ebrahimi, K.; Bill, E.; Hagedoorn, P.-L.; Hagen, W. *R. Nat. Chem. Biol.* **2012**, *8*, 941.
- (27) Honarmand Ebrahimi, K.; Hagedoorn, P. L.; Hagen, W. R. *ChemBioChem* **2013**, *14*, 1123.
- (28) Theil, E. C. *Nanoscopic Materials: Size-Dependent Phenomena and Growth Principles*; Royal Society of Chemistry: London, 2014; p 358.
- (29) Finazzi, D.; Arosio, P. *Arch. Toxicol.* **2014**, *88*, 1787.
- (30) George, G. N.; Richards, T.; Bare, R. E.; Gea, Y.; Prince, R. C.; Stiefel, E. I.; Watt, G. D. *J. Am. Chem. Soc.* **1993**, *115*, 7716.
- (31) Andrews, S. C.; Le Brun, N. E.; Barynin, V.; Thomson, A. J.; Moore, G. R.; Guest, J. R.; Harrison, P. M. *J. Biol. Chem.* **1995**, *270*, 23268.
- (32) Yamashita, I.; Iwahori, K.; Kumagai, S. *Biochim. Biophys. Acta* **2010**, *1800*, 846.
- (33) Douglas, T.; Allen, M.; Young, M. *Biopolymers Online*; Wiley-VCH Verlag GmbH & Co. KGaA: New York, 2005.
- (34) Uchida, M.; Kang, S.; Reichhardt, C.; Harlen, K.; Douglas, T. *Biochim. Biophys. Acta* **2010**, *1800*, 834.
- (35) Thomas, C. M.; Ward, T. R. *Chem. Soc. Rev.* **2005**, *34*, 337.
- (36) Stefanini, S.; Vecchini, P.; Chiancone, E. *Biochemistry* **1987**, *26*, 1831.
- (37) Gerl, M.; Jaenicke, R.; Smith, J. M.; Harrison, P. M. *Biochemistry* **1988**, *27*, 4089.
- (38) Zhang, Y.; Raudah, S.; Teo, H.; Teo, G. W.; Fan, R.; Sun, X.; Orner, B. P. *J. Biol. Chem.* **2010**, *285*, 12078.
- (39) Huard, D. J.; Kane, K. M.; Tezcan, F. A. *Nat. Chem. Biol.* **2013**, *9*, 169.
- (40) Salgado, E. N.; Lewis, R. A.; Faraone-Mennella, J.; Tezcan, F. A. *J. Am. Chem. Soc.* **2008**, *130*, 6082.
- (41) Salgado, E. N.; Faraone-Mennella, J.; Tezcan, F. A. *J. Am. Chem. Soc.* **2007**, *129*, 13374.
- (42) Levi, S.; Luzzago, A.; Franceschinelli, F.; Santambrogio, P.; Cesareni, G.; Arosio, P. *Biochem. J.* **1989**, *264*, 381.
- (43) Bernacchioni, C.; Ghini, V.; Pozzi, C.; Di Pisa, F.; Theil, E. C.; Turano, P. *ACS Chem. Biol.* **2014**, DOI: 10.1021/cb500431r.
- (44) Swift, J.; Butts, C. A.; Cheung-Lau, J.; Yerubandi, V.; Dmochowski, I. J. *Langmuir* **2009**, *25*, 5219.
- (45) Johnson, E.; Cascio, D.; Sawaya, M. R.; Gingery, M.; Schröder, I. *Structure* **2005**, *13*, 637.
- (46) Sana, B.; Johnson, E.; Le Magueres, P.; Criswell, A.; Cascio, D.; Lim, S. *J. Biol. Chem.* **2013**, *288*, 32663.
- (47) MaHam, A.; Tang, Z.; Wu, H.; Wang, J.; Lin, Y. *Small* **2009**, *5*, 1706.
- (48) Kanbak-Aksu, S.; Hasan, M. N.; Hagen, W.; Hollmann, F.; Sordi, D.; Sheldon, R.; Arends, I. *Chem. Commun.* **2012**, *48*, 5745.
- (49) Kasyutich, O.; Ilari, A.; Fiorillo, A.; Tatchev, D.; Hoell, A.; Ceci, P. *J. Am. Chem. Soc.* **2010**, *132*, 3621.
- (50) Suzuki, M.; Abe, M.; Ueno, T.; Abe, S.; Goto, T.; Toda, Y.; Akita, T.; Yamada, Y.; Watanabe, Y. *Chem. Commun.* **2009**, 4871.
- (51) Webb, B.; Frame, J.; Zhao, Z.; Lee, M.; Watt, G. *Arch. Biochem. Biophys.* **1994**, *309*, 178.
- (52) Aime, S.; Frullano, L.; Geninatti Crich, S. *Angew. Chem., Int. Ed.* **2002**, *41*, 1017.
- (53) Makino, A.; Harada, H.; Okada, T.; Kimura, H.; Amano, H.; Saji, H.; Hiraoka, M.; Kimura, S. *Nanomed. Nanotechnol.* **2011**, *7*, 638.
- (54) Simsek, E.; Akif Kilic, M. *J. Magn. Magn. Mater.* **2005**, *293*, 509.
- (55) Kilic, M. A.; Ozlu, E.; Calis, S. *J. Biomed. Nanotechnol.* **2012**, *8*, 508.
- (56) Liang, M.; Fan, K.; Zhou, M.; Duan, D.; Zheng, J.; Yang, D.; Feng, J.; Yan, X. *Proc. Natl. Acad. Sci. U.S.A.* **2014**, *111*, 14900.
- (57) Kanekiyo, M.; Wei, C.-J.; Yassine, H. M.; McTamney, P. M.; Boyington, J. C.; Whittle, J. R.; Rao, S. S.; Kong, W.-P.; Wang, L.; Nabel, G. J. *Nature* **2013**, *499*, 102.
- (58) Abe, S.; Niemeyer, J.; Abe, M.; Takezawa, Y.; Ueno, T.; Hikage, T.; Erker, G.; Watanabe, Y. *J. Am. Chem. Soc.* **2008**, *130*, 10512.
- (59) Takezawa, Y.; Böckmann, P.; Sugi, N.; Wang, Z.; Abe, S.; Murakami, T.; Hikage, T.; Erker, G.; Watanabe, Y.; Kitagawa, S. *Dalton Trans.* **2011**, *40*, 2190.
- (60) Abe, S.; Hirata, K.; Ueno, T.; Morino, K.; Shimizu, N.; Yamamoto, M.; Takata, M.; Yashima, E.; Watanabe, Y. *J. Am. Chem. Soc.* **2009**, *131*, 6958.
- (61) Jacobs, J. F.; Hasan, M. N.; Paik, K. H.; Hagen, W. R.; van Loosdrecht, M. *Biotechnol. Bioeng.* **2010**, *105*, 918.
- (62) Polanams, J.; Ray, A. D.; Watt, R. K. *Inorg. Chem.* **2005**, *44*, 3203.
- (63) Honarmand Ebrahimi, K.; Hagedoorn, P.-L.; Hagen, W. R. *FEBS Lett.* **2013**, *587*, 220.
- (64) Cutler, C.; Bravo, A.; Ray, A. D.; Watt, R. K. *J. Inorg. Biochem.* **2005**, *99*, 2270.
- (65) Johnson, J. L.; Cannon, M.; Watt, R. K.; Frankel, R. B.; Watt, G. D. *Biochemistry* **1999**, *38*, 6706.
- (66) Watt, G. D.; Frankel, R. B.; Jacobs, D.; Huang, H.; Papaefthymiou, G. C. *Biochemistry* **1992**, *31*, 5672.
- (67) Tatur, J.; Hagedoorn, P.-L.; Overeijnder, M. L.; Hagen, W. R. *Extremophiles* **2006**, *10*, 139.
- (68) Cowley, J. M.; Janney, D. E.; Gerkin, R. C.; Buseck, P. R. *J. Struct. Biol.* **2000**, *131*, 210.
- (69) Papaefthymiou, G. C. *Biochim. Biophys. Acta* **2010**, *1800*, 886.
- (70) Mann, S.; Williams, J. M.; Treffry, A.; Harrison, P. M. *J. Mol. Biol.* **1987**, *198*, 405.
- (71) Mahmoudi, M.; Sant, S.; Wang, B.; Laurent, S.; Sen, T. *Adv. Drug Delivery Rev.* **2011**, *63*, 24.
- (72) Qiao, R.; Yang, C.; Gao, M. *J. Mater. Chem.* **2009**, *19*, 6274.
- (73) Genove, G.; DeMarco, U.; Xu, H.; Goins, W. F.; Ahrens, E. T. *Nat. Med.* **2005**, *11*, 450.
- (74) Cohen, B.; Dafni, H.; Meir, G.; Harmelin, A.; Neeman, M. *Neoplasia* **2005**, *7*, 109.
- (75) Campan, M.; Lionetti, V.; Aquaro, G. D.; Forini, F.; Matteucci, M.; Vannucci, L.; Chiuppesi, F.; Di Cristofano, C.; Faggioni, M.; Maioli, M. *Am. J. Physiol.-Heart C* **2011**, *300*, H2238.
- (76) Earls, J. P.; Ho, V. B.; Foo, T. K.; Castillo, E.; Flamm, S. D. *J. Magn. Reson. Imaging* **2002**, *16*, 111.
- (77) Nikandrov, V.; Grätzel, C.; Moser, J.-E.; Grätzel, M. *J. Photochem. Photobiol. B* **1997**, *41*, 83.
- (78) Keyes, J.; Hilton, R.; Farrer, J.; Watt, R. *J. Nanopart. Res.* **2011**, *13*, 2563.
- (79) Ensign, D.; Young, M.; Douglas, T. *Inorg. Chem.* **2004**, *43*, 3441.
- (80) Kim, I.; Hosein, H.-A.; Strongin, D. R.; Douglas, T. *Chem. Mater.* **2002**, *14*, 4874.
- (81) Lawson, D. M.; Artymiuk, P. J.; Yewdall, S. J.; Smith, J. M. A.; Livingstone, J. C.; Treffry, A.; Luzzago, A.; Levi, S.; Arosio, P.; Cesareni, G.; Thomas, C. D.; Shaw, W. V.; Harrison, P. M. *Nature* **1991**, *349*, 541.
- (82) Toussaint, L.; Bertrand, L.; Hue, L.; Crichton, R. R.; Declercq, J.-P. *J. Mol. Biol.* **2007**, *365*, 440.
- (83) Masuda, T.; Goto, F.; Yoshihara, T.; Mikami, B. *Biochem. Biophys. Res. Commun.* **2010**, *400*, 94.
- (84) Ha, Y.; Shi, D.; Small, G. W.; Theil, E. C.; Allewell, N. M. *J. Biol. Inorg. Chem.* **1999**, *4*, 243.
- (85) Bertini, I.; Lalli, D.; Mangani, S.; Pozzi, C.; Rosa, C.; Theil, E. C.; Turano, P. *J. Am. Chem. Soc.* **2012**, *134*, 6169.

- (86) Toshia, T.; Ng, H.-L.; Bhattachari, O.; Alber, T.; Theil, E. C. *J. Am. Chem. Soc.* **2010**, *132*, 14562.
- (87) Marchetti, A.; Parker, M. S.; Moccia, L. P.; Lin, E. O.; Arrieta, A. L.; Ribalet, F.; Murphy, M. E. P.; Maldonado, M. T.; Armbrust, E. V. *Nature* **2009**, *457*, 467.
- (88) Pfaffen, S.; Abdulqadir, R.; Le Brun, N. E.; Murphy, M. E. P. *J. Biol. Chem.* **2013**, *288*, 14917.
- (89) Langlois d'Estaintot, B.; Santambrogio, P.; Granier, T.; Gallois, B.; Chevalier, J. M.; Précigoux, G.; Levi, S.; Arosio, P. *J. Mol. Biol.* **2004**, *340*, 277.
- (90) Masuda, T.; Goto, F.; Yoshihara, T.; Mikami, B. *J. Biol. Chem.* **2010**, *285*, 4049.
- (91) Hamburger, A. E.; West, A. P., Jr; Hamburger, Z. A.; Hamburger, P.; Bjorkman, P. *J. J. Mol. Biol.* **2005**, *349*, 558.
- (92) Tatur, J.; Hagen, W.; Matias, P. *J. Biol. Inorg. Chem.* **2007**, *12*, 615.
- (93) Hempstead, P. D.; Hudson, A. J.; Artymiuk, P. J.; Andrews, S. C.; Banfield, M. J.; Guest, J. R.; Harrison, P. M. *FEBS Lett.* **1994**, *350*, 258.
- (94) Stillman, T. J.; Hempstead, P. D.; Artymiuk, P. J.; Andrews, S. C.; Hudson, A. J.; Treffry, A.; Guest, J. R.; Harrison, P. M. *J. Mol. Biol.* **2001**, *307*, 587.
- (95) Cho, K. J.; Shin, H. J.; Lee, J.-H.; Kim, K.-J.; Park, S. S.; Lee, Y.; Lee, C.; Park, S. S.; Kim, K. H. *J. Mol. Biol.* **2009**, *390*, 83.
- (96) Arenas-Salinas, M.; Townsend, P. D.; Brito, C.; Marquez, V.; Maraboli, V.; Gonzalez-Nilo, F.; Matias, C.; Watt, R. K.; López-Castro, J. D.; Domínguez-vera, J. *Biochimie* **2014**, *106*, 39.
- (97) Yao, H.; Jepkorir, G.; Lovell, S.; Nama, P. V.; Weeratunga, S.; Battaile, K. P.; Rivera, M. *Biochemistry* **2011**, *50*, 5236.
- (98) Crow, A.; Lawson, T. L.; Lewin, A.; Moore, G. R.; Brun, N. E. L. *J. Am. Chem. Soc.* **2009**, *131*, 6808.
- (99) Swartz, L.; Kuchinskas, M.; Li, H.; Poulos, T. L.; Lanzilotta, W. N. *Biochemistry* **2006**, *45*, 4421.
- (100) Weeratunga, S. K.; Lovell, S.; Yao, H.; Battaile, K. P.; Fischer, C. J.; Gee, C. E.; Rivera, M. *Biochemistry* **2010**, *49*, 1160.
- (101) Janowski, R.; Auerbach-Nevo, T.; Weiss, M. S. *Protein Sci.* **2008**, *17*, 1138.
- (102) Macedo, S.; Romão, C. V.; Mitchell, E.; Matias, P. M.; Liu, M. Y.; Xavier, A. V.; LeGall, J.; Teixeira, M.; Lindley, P.; Carrondo, M. A. *Nat. Struct. Mol. Biol.* **2003**, *10*, 285.
- (103) Coelho, A. V.; Macedo, S.; Matias, P. M.; Thompson, A. W.; LeGall, J.; Carrondo, M. A. *Acta Crystallogr., Sect. D* **2001**, *57*, 326.
- (104) Levi, S.; Luzzago, A.; Cesareni, G.; Cozzi, A.; Franceschinelli, F.; Albertini, A.; Arosio, P. *J. Biol. Chem.* **1988**, *263*, 18086.
- (105) Levi, S.; Salfeld, J.; Franceschinelli, F.; Cozzi, A.; Dorner, M. H.; Arosio, P. *Biochemistry* **1989**, *28*, 5179.
- (106) Boyd, D.; Vecoli, C.; Belcher, D. M.; Jain, S. K.; Drysdale, J. W. *J. Biol. Chem.* **1985**, *260*, 11755.
- (107) Sun, S.; Arosio, P.; Levi, S.; Chasteen, N. D. *Biochemistry* **1993**, *32*, 9362.
- (108) Lawson, D. M.; Treffry, A.; Artymiuk, P. J.; Harrison, P. M.; Yewdall, S. J.; Luzzago, A.; Cesareni, G.; Levi, S.; Arosio, P. *FEBS Lett.* **1989**, *254*, 207.
- (109) Toshia, T.; Hasan, M. R.; Theil, E. C. *Proc. Natl. Acad. Sci. U.S.A.* **2008**, *105*, 18182.
- (110) Behera, R. K.; Theil, E. C. *Proc. Natl. Acad. Sci. U.S.A.* **2014**, *111*, 7925.
- (111) Schwartz, J. K.; Liu, X. S.; Toshia, T.; Theil, E. C.; Solomon, E. I. *J. Am. Chem. Soc.* **2008**, *130*, 9441.
- (112) Kwak, Y.; Schwartz, J. K.; Haldar, S.; Behera, R. K.; Toshia, T.; Theil, E. C.; Solomon, E. I. *Biochemistry* **2014**, *53*, 473.
- (113) Treffry, A.; Zhao, Z.; Quail, M. A.; Guest, J. R.; Harrison, P. M. *FEBS Lett.* **1998**, *432*, 213.
- (114) Bou-Abdallah, F.; Arosio, P.; Santambrogio, P.; Yang, X.; Janus-Chandler, C.; Chasteen, N. D. *Biochemistry* **2002**, *41*, 11184.
- (115) Edgcomb, S. P.; Murphy, K. P. *Proteins* **2002**, *49*, 1.
- (116) Bou-Abdallah, F.; Woodhall, M. R.; Velázquez-Campoy, A.; Andrews, S. C.; Chasteen, N. D. *Biochemistry* **2005**, *44*, 13837.
- (117) Rui, H.; Rivera, M.; Im, W. *Biochemistry* **2012**, *51*, 9900.
- (118) de Val, N.; Declercq, J.-P.; Lim, C. K.; Crichton, R. R. *J. Inorg. Biochem.* **2012**, *112*, 77.
- (119) Laghaei, R.; Evans, D. G.; Coalson, R. D. *Proteins* **2013**, *81*, 1042.
- (120) Makeyev, A. V.; Liebhaber, S. A. *Rna* **2002**, *8*, 265.
- (121) Leidgens, S.; Bullough, K. Z.; Shi, H.; Li, F.; Shakoury-Elizeh, M.; Yabe, T.; Subramanian, P.; Hsu, E.; Natarajan, N.; Nandal, A. *J. Biol. Chem.* **2013**, *288*, 17791.
- (122) Shi, H.; Bencze, K. Z.; Stemmler, T. L.; Philpott, C. C. *Science* **2008**, *320*, 1207.
- (123) Izumi, Y.; Yumiko, Y.; Mitsuaki, T.; Fumio, K. *Biochem. J.* **2014**, *462*, 25.
- (124) Lee, S. J.; McCormick, M. S.; Lippard, S. J.; Cho, U.-S. *Nature* **2013**, *494*, 380.
- (125) Stefanini, S.; Desideri, A.; Vecchini, P.; Drakenberg, T.; Chiancone, E. *Biochemistry* **1989**, *28*, 378.
- (126) Desideri, A.; Stefanini, S.; Polizzi, F.; Petruzzelli, R.; Chiancone, E. *FEBS Lett.* **1991**, *287*, 10.
- (127) Douglas, T.; Ripoll, D. R. *Protein Sci.* **1998**, *7*, 1083.
- (128) Bou-Abdallah, F.; Arosio, P.; Levi, S.; Janus-Chandler, C.; Chasteen, N. D. *J. Biol. Inorg. Chem.* **2003**, *8*, 489.
- (129) Bou-Abdallah, F.; Zhao, G.; Biasiotto, G.; Poli, M.; Arosio, P.; Chasteen, N. D. *J. Am. Chem. Soc.* **2008**, *130*, 17801.
- (130) Laghaei, R.; Kowallis, W.; Evans, D. G.; Coalson, R. D. *J. Phys. Chem. A* **2014**, *118*, 7442.
- (131) Pfaffen, S.; Abdulqadir, R.; Le Brun, N. E.; Murphy, M. E. *J. Biol. Chem.* **2013**, *288*, 14917.
- (132) Wade, V. J.; Levi, S.; Arosio, P.; Treffry, A.; Harrison, P. M.; Mann, S. *J. Mol. Biol.* **1991**, *221*, 1443.
- (133) Bou-Abdallah, F.; Biasiotto, G.; Arosio, P.; Chasteen, N. D. *Biochemistry* **2004**, *43*, 4332.
- (134) Liu, H.-L.; Zhou, H.-N.; Xing, W.-M.; Zhao, J.-F.; Li, S.-X.; Huang, J.-F.; Bi, R.-C. *FEBS Lett.* **2004**, *573*, 93.
- (135) Zhao, G.; Bou-Abdallah, F.; Yang, X.; Arosio, P.; Chasteen, N. D. *Biochemistry* **2001**, *40*, 10832.
- (136) Yang, X.; Chen-Barrett, Y.; Arosio, P.; Chasteen, N. D. *Biochemistry* **1998**, *37*, 9743.
- (137) Honarmand Ebrahimi, K.; Hagedoorn, P.-L.; Jongejan, J.; Hagen, W. *J. Biol. Inorg. Chem.* **2009**, *14*, 1265.
- (138) Bou-Abdallah, F.; Yang, H.; Awomolo, A.; Cooper, B.; Woodhall, M. R.; Andrews, S. C.; Chasteen, N. D. *Biochemistry* **2013**, *53*, 483.
- (139) Wong, S. G.; Abdulqadir, R.; Le Brun, N. E.; Moore, G. R.; Mauk, A. G. *Biochem. J.* **2012**, *444*, 553.
- (140) Yang, X.; Le Brun, N. E.; Thomson, A. J.; Moore, G. R.; Chasteen, N. D. *Biochemistry* **2000**, *39*, 4915.
- (141) Bou-Abdallah, F.; Lewin, A. C.; Le Brun, N. E.; Moore, G. R.; Chasteen, N. D. *J. Biol. Chem.* **2002**, *277*, 37064.
- (142) Treffry, A.; Zhao, Z.; Quail, M. A.; Guest, J. R.; Harrison, P. M. *Biochemistry* **1995**, *34*, 15204.
- (143) Fetter, J.; Cohen, J.; Danger, D.; Sanders-Loehr, J.; Theil, E. C. *J. Biol. Inorg. Chem.* **1997**, *2*, 652.
- (144) Zhao, G.; Su, M.; Chasteen, N. D. *J. Mol. Biol.* **2005**, *352*, 467.
- (145) Liu, X.; Theil, E. C. *Proc. Natl. Acad. Sci. U.S.A.* **2004**, *101*, 8557.
- (146) Bou-Abdallah, F.; Papaefthymiou, G. C.; Scheswohl, D. M.; Stanga, S. D.; Arosio, P.; Chasteen, N. D. *Biochem. J.* **2002**, *364*, 57.
- (147) Pereira, A. S.; Small, W.; Krebs, C.; Tavares, P.; Edmondson, D. E.; Theil, E. C.; Huynh, B. H. *Biochemistry* **1998**, *37*, 9871.
- (148) Pereira, A. S.; Tavares, P.; Lloyd, S. G.; Danger, D.; Edmondson, D. E.; Theil, E. C.; Huynh, B. H. *Biochemistry* **1997**, *36*, 7917.
- (149) Jameson, G. N. L.; Jin, W.; Krebs, C.; Perreira, A. S.; Tavares, P.; Liu, X.; Theil, E. C.; Huynh, B. H. *Biochemistry* **2002**, *41*, 13435.
- (150) Moënne-Locoz, P.; Krebs, C.; Herlihy, K.; Edmondson, D. E.; Theil, E. C.; Huynh, B. H.; Loehr, T. M. *Biochemistry* **1999**, *38*, 5290.
- (151) Tinberg, C. E.; Lippard, S. J. *Acc. Chem. Res.* **2011**, *44*, 280.
- (152) Hwang, J.; Krebs, C.; Huynh, B. H.; Edmondson, D. E.; Theil, E. C.; Penner-Hahn, J. E. *Science* **2000**, *287*, 122.

- (153) Liu, K. E.; Valentine, A. M.; Qiu, D.; Edmondson, D. E.; Appelman, E. H.; Spiro, T. G.; Lippard, S. J. *J. Am. Chem. Soc.* **1995**, *117*, 4997.
- (154) Liu, K. E.; Valentine, A. M.; Wang, D.; Huynh, B. H.; Edmondson, D. E.; Salifoglou, A.; Lippard, S. J. *J. Am. Chem. Soc.* **1995**, *117*, 10174.
- (155) Moënne-Locozzo, P.; Baldwin, J.; Ley, B. A.; Loehr, T. M.; Bollinger, J. M. *Biochemistry* **1998**, *37*, 14659.
- (156) Bollinger, J. M.; Krebs, C.; Vicol, A.; Chen, S.; Ley, B. A.; Edmondson, D. E.; Huynh, B. H. *J. Am. Chem. Soc.* **1998**, *120*, 1094.
- (157) Broadwater, J. A.; Achim, C.; Müncck, E.; Fox, B. G. *Biochemistry* **1999**, *38*, 12197.
- (158) Broadwater, J. A.; Ai, J.; Loehr, T. M.; Sanders, L.; Fox, B. G. *Biochemistry* **1998**, *37*, 14664.
- (159) Kim, K.; Lippard, S. J. *J. Am. Chem. Soc.* **1996**, *118*, 4914.
- (160) Dong, Y.; Menage, S.; Brennan, B. A.; Elgren, T. E.; Jang, H. G.; Pearce, L. L.; Que, L. *J. Am. Chem. Soc.* **1993**, *115*, 1851.
- (161) Ookubo, T.; Sugimoto, H.; Nagayama, T.; Masuda, H.; Sato, T.; Tanaka, K.; Maeda, Y.; Okawa, H.; Hayashi, Y.; Uehara, A.; Suzuki, M. *J. Am. Chem. Soc.* **1996**, *118*, 701.
- (162) Chavez, F. A.; Ho, R. Y. N.; Pink, M.; Young, J. V. G.; Kryatov, S. V.; Rybak-Akimova, E. V.; Andres, H.; Müncck, E.; Que, J. L.; Tolman, W. B. *Angew. Chem.* **2002**, *114*, 157.
- (163) Dong, Y.; Zang, Y.; Shu, L.; Wilkinson, E. C.; Que, L.; Kauffmann, K.; Müncck, E. J. *Am. Chem. Soc.* **1997**, *119*, 12683.
- (164) Kodera, M.; Taniike, Y.; Itoh, M.; Tanahashi, Y.; Shimakoshi, H.; Kano, K.; Hirota, S.; Iijima, S.; Ohba, M.; Okawa, H. *Inorg. Chem.* **2001**, *40*, 4821.
- (165) Zang, Y.; Dong, Y.; Que, L.; Kauffmann, K.; Muenck, E. *J. Am. Chem. Soc.* **1995**, *117*, 1169.
- (166) Horner, O.; Jeandey, C.; Oddou, J.-L.; Bonville, P.; Latour, J.-M. *Eur. J. Inorg. Chem.* **2002**, *2002*, 1186.
- (167) Ahmad, S.; McCallum, J. D.; Shiemeke, A. K.; Appelman, E. H.; Loehr, T. M.; Sanders-Loehr, J. *Inorg. Chem.* **1988**, *27*, 2230.
- (168) Horner, O.; Jeandey, C.; Oddou, J.-L.; Bonville, P.; McKenzie, C. J.; Latour, J.-M. *Eur. J. Inorg. Chem.* **2002**, *2002*, 3278.
- (169) Simaan, A. J.; Döpner, S.; Banse, F.; Bourcier, S.; Bouchoux, G.; Boussac, A.; Hildebrandt, P.; Girerd, J.-J. *Eur. J. Inorg. Chem.* **2000**, *2000*, 1627.
- (170) Waldo, G. S.; Ling, J.; Sanders-Loehr, J.; Theil, E. C. *Science* **1993**, *259*, 796.
- (171) Sun, S.; Chasteen, N. D. *Biochemistry* **1994**, *33*, 15095.
- (172) Ryle, M. J.; Liu, A.; Muthukumaran, R. B.; Ho, R. Y.; Koehntop, K. D.; McCracken, J.; Que, L.; Hausinger, R. P. *Biochemistry* **2003**, *42*, 1854.
- (173) Bauminger, E. R.; Harrison, P. M.; Hechel, D.; Hodson, N. W.; Nowik, I.; Treffry, A.; Yewdall, S. J. *Biochem. J.* **1993**, *296*, 709.
- (174) Bauminger, E. R.; Treffry, A.; Quail, M. A.; Zhao, Z.; Nowik, I.; Harrison, P. M. *Biochemistry* **1999**, *38*, 7791.
- (175) Bauminger, E. R.; Treffry, A.; Quail, M. A.; Zhao, Z.; Nowik, I.; Harrison, P. M. *Inorg. Chim. Acta* **2000**, *297*, 171.
- (176) Tatur, J.; Hagen, W. R. *FEBS Lett.* **2005**, *579*, 4729.
- (177) Honarmand Ebrahimi, K.; Hagedoorn, P.-L.; Hagen, W. R. *J. Biol. Inorg. Chem.* **2010**, *15*, 1243.
- (178) Watt, R. K. *ChemBioChem* **2013**, *14*, 415.
- (179) Turano, P.; Lalli, D.; Felli, I. C.; Theil, E. C.; Bertini, I. *Proc. Natl. Acad. Sci. U.S.A.* **2010**, *107*, 545.
- (180) Baran, P.; Boca, R.; Chakraborty, I.; Giapintzakis, J.; Herchel, R.; Huang, Q.; McGrady, J. E.; Raptis, R. G.; Sanakis, Y.; Simopoulos, A. *Inorg. Chem.* **2008**, *47*, 645.
- (181) Lalli, D.; Turano, P. *Acc. Chem. Res.* **2013**, *46*, 2676.
- (182) López-Castro, J.; Delgado, J.; Perez-Omil, J.; Gálvez, N.; Cuesta, R.; Watt, R. K.; Domínguez-Vera, J. M. *Dalton Trans.* **2012**, *41*, 1320.
- (183) Lusciati, S.; Santambrogio, P.; d'Estaintot, B. L.; Granier, T.; Cozzi, A.; Poli, M.; Gallois, B.; Finazzi, D.; Cattaneo, A.; Levi, S. *J. Biol. Chem.* **2010**, *285*, 11948.
- (184) Cozzi, A.; Rovelli, E.; Frizzale, G.; Campanella, A.; Amendola, M.; Arosio, P.; Levi, S. *Neurobiol. Dis.* **2010**, *37*, 77.
- (185) Levi, S.; Yewdall, S.; Harrison, P.; Santambrogio, P.; Cozzi, A.; Rovida, E.; Albertini, A.; Arosio, P. *Biochem. J.* **1992**, *288*, 591.
- (186) Lawson, T. L.; Crow, A.; Lewin, A.; Yasmin, S.; Moore, G. R.; Le Brun, N. E. *Biochemistry* **2009**, *48*, 9031.
- (187) Watt, R. K.; Hilton, R. J.; Graff, D. M. *Biochim. Biophys. Acta* **2010**, *1800*, 745.
- (188) Castruita, M.; Elmegreen, L. A.; Shaked, Y.; Stiefel, E. I.; Morel, F. M. *J. Inorg. Biochem.* **2007**, *101*, 1686.
- (189) Kell, D. B.; Pretorius, E. *Metallooms* **2014**, *6*, 748.
- (190) FUNK, F.; LENDERS, J. P.; Crichton, R. R.; Schneider, W. *Eur. J. Biochem.* **1985**, *152*, 167.
- (191) Sirivech, S.; Frieden, E.; Osaki, S. *Biochem. J.* **1974**, *143*, 311.
- (192) Jacobs, D.; Watt, G.; Frankel, R.; Papaefthymiou, G. *Biochemistry* **1989**, *28*, 1650.
- (193) Watt, G. D.; Jacobs, D.; Frankel, R. B. *Proc. Natl. Acad. Sci. U.S.A.* **1988**, *85*, 7457.
- (194) Tatur, J.; Hagen, W. R.; Heering, H. A. *Dalton T.* **2009**, 2837.
- (195) Jones, T.; Spencer, R.; Walsh, C. *Biochemistry* **1978**, *17*, 4011.
- (196) Liu, X.; Jin, W.; Theil, E. C. *Proc. Natl. Acad. Sci. U.S.A.* **2003**, *100*, 3653.
- (197) Tosha, T.; Behera, R. K.; Ng, H.-L.; Bhattachari, O.; Alber, T.; Theil, E. C. *J. Biol. Chem.* **2012**, *287*, 13016.
- (198) Kidane, T. Z.; Sauble, E.; Linder, M. C. *Am. J. Physiol. (Cell Physiol.)* **2006**, *291*, C445.
- (199) Truty, J.; Malpe, R.; Linder, M. C. *J. Biol. Chem.* **2001**, *276*, 48775.
- (200) De Domenico, I.; Vaughn, M. B.; Li, L.; Bagley, D.; Musci, G.; Ward, D. M.; Kaplan, J. *EMBO J.* **2006**, *25*, 5396.
- (201) Yasmin, S.; Andrews, S. C.; Moore, G. R.; Le Brun, N. E. *J. Biol. Chem.* **2011**, *286*, 3473.
- (202) Quail, M. A.; Jordan, P.; Grogan, J. M.; Butt, J. N.; Lutz, M.; Thomson, A. J.; Andrews, S. C.; Guest, J. R. *Biochem. Biophys. Res. Commun.* **1996**, *229*, 635.
- (203) Yao, H.; Wang, Y.; Lovell, S.; Kumar, R.; Ruvinsky, A. M.; Battaile, K. P.; Vakser, I. A.; Rivera, M. *J. Am. Chem. Soc.* **2012**, *134*, 13470.
- (204) McLendon, G. *Acc. Chem. Res.* **1988**, *21*, 160.
- (205) Weeratunga, S. K.; Gee, C. E.; Lovell, S.; Zeng, Y.; Woodin, C. L.; Rivera, M. *Biochemistry* **2009**, *48*, 7420.
- (206) Kluyver, A. J.; Donker, H. *J. Chemie der Zelle und Gewebe* **1926**, *13*, 134.
- (207) Kamp, A. F.; LaRiviere, J. W. M.; Verhoeven, W. *Albert Jan Kluyver: his life and works*; North Holland Publ. Comp.: Amsterdam, 1959.
- (208) Cozzi, A.; Corsi, B.; Levi, S.; Santambrogio, P.; Biasiotto, G.; Arosio, P. *Blood* **2004**, *103*, 2377.